UNIVERSIDAD DE JAÉN

CENTRO DE ESTUDIOS AVANZADOS EN
CIENCIAS DE LA TIERRA, ENERGÍA
Y MEDIO AMBIENTE

FACULTAD DE CIENCIAS EXPERIMENTALES

DEPARTAMENTO DE GEOLOGÍA

TESIS DOCTORAL

INTERACCIÓN DE APORTES HIDROTERMALES EN AGUAS Y SEDIMENTOS LACUSTRES: EL LAGO SOCHAGOTA (BOYACÁ - COLOMBIA)

PRESENTADA POR:

GABRIEL RICARDO CIFUENTES OSORIO

DIRIGIDA POR:

DR. ROSARIO JIMÉNEZ ESPINOSA

DR. JUAN JIMÉNEZ MILLÁN

Jaén, octubre 2021

UNIVERSIDAD DE JAÉN

Interacción de Aportes Hidrotermales en Aguas y Sedimentos Lacustres:

El Lago Sochagota (Boyacá - Colombia)

Tesis Doctoral 2021 / Gabriel Ricardo Cifuentes-Osorio

Zona de estudio: El Lago Sochagota (Boyacá - Colombia)

INTERACCIÓN DE APORTES HIDROTERMALES EN AGUAS Y SEDIMENTOS LACUSTRES: EL LAGO SOCHAGOTA (BOYACÁ - COLOMBIA)

INTERACTION OF HYDROTHERMAL INPUTS IN LAKE WATERS AND SEDIMENTS: THE SOCHAGOTA LAKE (BOYACA – COLOMBIA)

Memoria para optar al grado de Doctor
Jaén, octubre de 2021

Fdo.: Gabriel Ricardo Cifuentes Osorio Aspirante al Grado de Doctor

Los Directores del trabajo:

Fdo: Rosario Jiménez Espinosa

Fdo: Juan Jiménez Millán

Centro de Estudios Avanzados en
Ciencias de la Tierra, Energía y Medio Ambiente
Departamento de Geología.
Facultad de Ciencias Experimentales.
Universidad de Jaén.

Los directores de tesis, **Dª. Rosario Jiménez Espinosa, D. Juan Jiménez Millán** y pertenecientes al Departamento de Geología de la Universidad de Jaén

HACEN CONSTAR: Que el trabajo expuesto en la presente Tesis Doctoral:

"Interacción de aportes hidrotermales en aguas y sedimentos lacustres: el Lago Sochagota (Boyacá - Colombia) presentado por **D. Gabriel Ricardo Cifuentes Osorio** ha sido realizado bajo nuestra dirección y supervisión, cumpliendo todas las exigencias para su presentación y defensa para optar al Grado de Doctor.

Jaén, octubre de 2021

Fdo.: Rosario Jiménez Espinosa

Fdo.: Juan Jiménez Millán

Este trabajo fue financiado por el proyecto de investigación español PGC2018-094573-B-I00 del MCIU-AEI-FEDER, y grupo de investigación RNM- 325 de la Junta de Andalucía (España). A la Asociación Universitaria Iberoamericana de Posgrado (AUIP), a la Universidad de Boyacá y a los grupos de investigación colombianos Gestión Ambiental COL0005468 y Gestión de Recursos Hídricos COL0005477.

Esta tesis se presenta como una recopilación de los siguientes artículos científicos:

Cifuentes, G.R., Jiménez-Millán, J., Quevedo, C.P., Jiménez-Espinosa, R., 2020. Transformation of S-bearing minerals in organic matter-rich sediments from a saline lake with hydrothermal inputs. *Minerals* 10, 525. https://doi.org/10.3390/min10060525.

Cifuentes, G.R., Jiménez-Millán, J., Quevedo, C.P., Gálvez A., Castellanos-Rozo J., Jiménez-Espinosa, R., 2020. Trace element fixation in sediments rich in organic matter from a saline lake in tropical latitude with hydrothermal inputs (Sochagota Lake, Colombia): The role of bacterial communities. *Science of the Total Environment.* https://doi.org/10.1016/j.scitotenv.2020.143113https://doi.org/10.1016/j.scitotenv.2020.143113

Cifuentes, G.R., Jiménez-Millán, J., Quevedo, C.P., Nieto Fernando., Cuadros Javier., Jiménez-Espinosa, R., 2020. Low Temperature Illitization through Illite-Dioctahedral Vermiculite Mixed-Layers in a Tropical Saline Lake rich in Hydrothermal Fluids (Sochagota Lake, Colombia). *Minerals* 2021, 11,523. https://doi.org/10.3390/min 11050523.

Cifuentes, G.R., Jiménez-Espinosa, R, Jiménez-Millán, J., Quevedo, C.P. 2021. Damming induced natural attenuation of hydrothermal waters by runoff freshwater dilution and sediment biogeochemical transformations (Sochagota Lake, Colombia). Enviado a la revista *Water*.

Agradecimientos

E*ste es mi agradecimiento a todas aquellas personas que me han ayudado a poder realizar la tesis.*

Mis más sinceros agradecimientos a mis directores de tesis, a los profesores Dª Rosario Jiménez Espinosa y a D. Juan Jiménez Millán por todo el apoyo, dedicación, paciencia, conocimiento y consejos que me permitieron comprender de una forma precisa el significado de afrontar el proceso investigativo de alto nivel, así como el que me han ayudado con todas las dudas que me han podido surgir sobre el trabajo a lo largo de la tesis. Ha sido un privilegio el haber conocido y trabajado con estos dos grandiosos investigadores y seres humanos, mil gracias

Quiero también expresar mi especial agradecimiento a los coautores de los artículos de los que se compone esta tesis doctoral, a los Doctores Javier Cuadros, Fernando Nieto, Antonio Gálvez del Postigo, José Castellanos Rosso, y Claudia Patricia Quevedo Vargas que han contribuido de manera significativa en mi formación y que generosamente han dedicado su tiempo, conocimiento y esfuerzo para la consecución de estos resultados.

A la Dª. Rosita Cuervo Payeras, Presidenta del Consejo Directivo de la Universidad de Boyacá, quien gestionó y materializó el programa de becas para la formación de doctores en ciencias básicas entre la Universidad de Jaén de España, Universidad de Boyacá y la Universidad de Ciencias Ambientales de Colombia, bajo la gestión administrativa y financiera de la Asociación Universitaria Iberoamericana de Postgrado (AUIP). y quien desde el inicio confió y brindó el apoyo necesario para culminar con éxito este nuevo logró académico.

A todos los técnicos que aportaron a la consecución de los datos pertenecientes al Centro de Instrumentación Científico-Técnico (CICT) de la Universidad de Jaén y al Centro de Instrumentación Científica (CIC) de la Universidad de Granada, que me explicaron y estuvieron conmigo mientras llevaba a cabo la realización de los experimentos. A Antonio Piedra por su gran ayuda, apoyo y colaboración en la preparación de las muestras.

A mis compañeros del programa de la AUIP pertenecientes a la Universidad de Ciencias Ambientales UDCA de Colombia, en especial a Iván Herrera que desde el inicio de estos estudios ha estado apoyando con su amistad y conocimiento para lograr este objetivo tan importante, y a mis compañeros de la Universidad de Boyacá con quienes vivimos esta etapa tan importante académica y personal para cada uno de nosotros María Inés, Patricia, Claudia y José.

Y finalmente, a mi familia por siempre estar ahí apoyándome para conseguir mis sueños. A Marcela que, con su amor incondicional, su tenacidad y ganas de vivir me enseñó a ver la vida diferente, solo palabras y sentimientos de amor y de admiración para la mejor esposa y mamá. A mis hijos Daniel y Andrés quienes también han dado lo mejor en este tiempo que estuve lejos de ellos, que han entendido el valor del estudio y el sacrificio. Gracias

A todos aquellos que de alguna forma hicieron parte de este proyecto.

Índice

ÍNDICE

Resumen

En ambientes lacustres de salinidad elevada e intensa actividad biológica asociada a la descomposición de la materia orgánica se producen transformaciones minerales complejas. El estudio de estas transformaciones es una herramienta esencial para la evaluación de los principales ciclos biogeoquímicos en entornos naturales, la evaluación de su integridad medioambiental y su uso eficiente. Este trabajo plantea el análisis de los procesos que ocurren en el Lago Sochagota (Boyacá, Colombia), formado por aguas sulfatadas sódico-potásicas con sedimentos siliciclásticos ricos en caolinita y materia orgánica. La determinación del comportamiento integral de este sistema lacustre requiere una aproximación multidisciplinar (mineralógica, hidrológica y geomicrobiológica) y multiescala (desde la nanométrica mineral hasta la escala de ciclos locales y globales de elementos).

El estudio, en primer lugar, tiene como propósito examinar el efecto que tiene el Lago Sochagota como represa y su función de atenuación natural de los contaminantes. La construcción de esta puede considerarse una estrategia eficaz para amortiguar las aguas que contengan una alta salinidad. El área volcánica del sistema de Paipa (Boyacá, Colombia) presenta procesos de hidrotermalismo ligado a la fuente de calor endógeno residual de la actividad volcánica de la región. Además, la presencia de un entramado de fracturas profundas ayuda al flujo de aguas termales y altamente mineralizadas ricas en SO_4^{2-}, Na^+-K^+, así como en otros elementos metálicos, en el agua del área de la cuenca del río Salitre y de recarga del lago. Un proceso hidrogeoquímico adicional es la mezcla con agua fría rica en Fe procedente de acuíferos cuaternarios superficiales ligados a sedimentos aluviales adyacentes al lago. De esta forma, esta agua salinizada rica en Fe está siendo incorporada el Lago Sochagota, aunque es importante destacar la influencia de las aguas de lluvia en la composición química del lago. Dentro del Lago

Sochagota tienen lugar una serie de procesos hidrogeoquímicos, biogeoquímicos y mineralógicos significativos que influyen en la dinámica que presenta este cuerpo de agua, pudiéndose observar que las concentraciones de elementos disueltos se atenuaron significativamente debido a una serie de transformaciones. La dilución por escorrentía pluvial y la precipitación de sulfuros de hierro mediada por bacterias reductoras de sulfato en los sedimentos ricos en materia orgánica fueron los principales procesos involucrados en la atenuación de la concentración de SO_4^{2-}, Fe, As Cu y Co en el agua del lago. Los procesos de illitización que se producen en los sedimentos podrían favorecer la disminución de K y Al.

La caracterización mineral sugiere que en la formación de los sedimentos del lago estuvieron implicadas diversas fuentes de aportes (detrítica, hidrotermal y órgano-antropogénica) que propiciaron el desarrollo de transformaciones minerales que afectan a los principales ciclos biogeoquímicos. La formación de minerales en sedimentos superficiales de sistemas lacustres puede producirse como consecuencia de la saturación de la concentración de algunos iones en los fluidos intersticiales, la interacción con los aportes detríticos y procesos asociados a la descomposición de materia orgánica y la actividad microbiana.

Los principales minerales de los materiales depositados en el Lago Sochagota son caolinita y cuarzo detríticos. En las zonas central y norte del lago aparecen sedimentos con alto contenido de materia orgánica y minerales arcillosos neoformados. La mayoría de estos materiales ricos en materia orgánica se caracterizan por la presencia de minerales portadores de azufre como son la mackinawita, pirita, y azufre elemental (S^0). Asimismo, se realizó la identificación de un interestratificado vermiculita ilita-dioctaédrica (I-DV) e illita, los cuales están ausentes en los sedimentos de la entrada sur.

En los sedimentos, las características texturales de pirita, azufre nativo y calcita podrían asociarse a la neoformación de minerales como consecuencia de la interacción entre los fluidos intersticiales y los componentes sólidos del sedimento. Las facies sulfatadas-sódico-potásicas de las aguas hidrotermales que alimentan el Lago Sochagota pueden suponer la fuente de azufre y potasio necesarias para la formación de algunas de estas fases. Los sistemas geotermales pueden ser fuente de cantidades significativas de azufre hidrotermal para las aguas superficiales, incrementando la salinidad y reduciendo las opciones potenciales de uso antrópico.

La alta salinidad promovida por aportes hidrotermales, las condiciones reductoras de los sedimentos ricos en materia orgánica y la presencia de un precursor mineral arcilloso apropiado proporcionaron un marco adecuado para los procesos de illitización a baja temperatura. Las condiciones climáticas húmedas, templadas y frías provocaron la formación de partículas metaestables de pequeño tamaño de I-DV por la meteorización de las rocas sedimentarias y las rocas volcánicas ácidas que drenan el Lago Sochagota. Estas partículas se depositaron en el entorno de baja energía de la parte central y norte del lago. La interacción de estos sedimentos ricos en materia orgánica con las aguas salinas del lago enriquecidas en potasio hidrotermal provocó un ambiente reductor que favoreció los procesos de movilización de hierro y su incorporación al interestratificado I-DV, que actuó como precursor mineral para una illitización rápida a baja temperatura, revelando el importante papel de los minerales arcillosos como sumidero de potasio de origen hidrotermal en lagos de regiones geotermales.

Por otro lado, la presencia de agregados de formaciones celulares de nanopartículas de mackinawita rellenando la parte interna de

fragmentos de plantas indica que los microorganismos estuvieron involucrados en la asimilación de azufre hidrotermal. La alteración de mackinawita en un ambiente con exceso de sulfuro libre produjo la formación de pirita framboidal. La evolución hacia condiciones con la presencia de oxigeno favoreció la formación de morfologías complejas de azufre.

En un último estudio se abordaron las relaciones entre la concentración de los elementos traza en los sedimentos, el contenido de materia orgánica, la composición mineralógica y la actividad de la comunidad bacteriana en los sedimentos del lago. En la entrada sur del lago, caracterizada por la presencia de sedimentos ricos en cuarzo y caolinita y pobres en materia orgánica, se localizan los mayores contenidos en Zr (hasta 603 mg/kg) y elementos mayores detríticos tales como Na, Ti, Al y Si. Por otra parte, en la zona central y norte del lago los sedimentos arcillosos ricos en materia orgánica (hasta 11.10%) que contienen minerales con S, I-DV e illita, están enriquecidos en S, Fe, Zn, Mo, Rb, Co, K, Cr, Sb, Ni, As, Ba, Cu, Mn, Pb, P, Mg y Sr. La presencia de nanopartículas de sulfuro de hierro enriquecidas en metales pesados en las costras de células microbianas y la presencia de una comunidad bacteriana en la que predominan las bacterias sulfatoreductoras (SRB) (*Desulfatiglans, Desulfobacterales y Sva0485*) sugieren que la precipitación del azufre hidrotermal y la acumulación de elementos traza en los sedimentos es regulada por la actividad de dichos microorganismos. La cristalización de azufre, barita y calcita y las buenas correlaciones entre Ba, Sr y Ca indican que el sulfuro previamente precipitado puede ser oxidado por la actividad de una comunidad de bacterias oxidantes del azufre (*Thioalkalimicrobium, Sulfurovum, Arcobacter y Sulfurimonas*), lo que posiblemente propicia procesos de liberación de los metales al medio.

Capítulo 1.

1. Introducción

1.1 Problema de investigación que se aborda: catalizadores de procesos minerales y geoquímicos en condiciones extremas.

El ambiente restringido que puede desarrollarse en algunos sedimentos lacustres condicionados por la acción conjunta de diversos factores, tales como el contexto geológico, climático o biótico, propicia el desarrollo de condiciones favorables para la aceleración de determinados procesos geoquímicos y de transformación mineral.

La composición mineral y química de los sedimentos lacustres es el resultado del balance entre un conjunto de procesos detríticos y autigénicos que ocurren en la cuenca de depósito. Dado que es frecuente que las asociaciones minerales de los sedimentos sean utilizadas como indicadores ambientales y climáticos (Chamley *et al*., 1983; Chamley 1989; Griffin *et al*., 1968), es necesario profundizar en el conocimiento de las variables que controlan el equilibrio químico que determina la conservación de la naturaleza detrítica, su modificación o la formación de nuevas fases minerales en sedimentos superficiales. El avance en este aspecto del conocimiento es especialmente importante en los casos en que las condiciones extremas del medio (salinidad, Eh, pH, actividad microbiológica) actúan como catalizadores de los procesos de neoformación y transformación de minerales en los sedimentos (Andrade *et al*., 2014, 2018; Cuadros *et al*., 2017; Deocampo *et al*., 2009). Dichos procesos pueden afectar significativamente a los principales ciclos elementales y condicionar la interpretación de la asociación mineral como indicadora de condiciones climáticas o ambientales.

En la presente tesis doctoral se ha abordado la integración de la caracterización minuciosa de los sedimentos y aguas de un lago de

elevada salinidad producida por los aportes hidrotermales procedentes del sistema geotérmico en el que se integra: el Lago Sochagota (Colombia). La combinación de la composición mineral y geoquímica de los sedimentos, la hidroquímica de las aguas y la constitución de las principales comunidades microbiológicas de los sedimentos ha permitido: a) identificar algunos de los procesos implicados en la neoformación de arcillas y sulfuros y su papel en la fijación o movilización de metales y b) evaluar las implicaciones ambientales de dichos procesos.

Para ello, este estudio ha pretendido expandir el estado del conocimiento sobre: 1. La atenuación de las condiciones físico-químicas extremas de aguas hidrotermales en embalses lacustres artificiales; 2. La illitización lacustre sedimentaria promovida por el efecto de fluidos de origen hidrotermal; 3. Las transformaciones de minerales con S en dichos ambientes; 4. El efecto de las comunidades bacterianas de los sedimentos en dichas transformaciones y en los ciclos de los principales elementos.

En el siguiente apartado se expone la forma en que se ha planteado el desarrollo de estos temas de investigación y cómo se estructuran en la Tesis

1.2 Introducción a los contenidos del estudio y estructura de la Tesis

La presente tesis doctoral se presenta como un conjunto de trabajos publicados por el doctorando de acuerdo con lo establecido en el artículo 25 del Reglamento de Estudios de Doctorado de la Universidad de Jaén (versión aprobada por el Consejo de Gobierno de la Universidad de Jaén con fecha 18 de febrero de 2019). De este modo, cuatro

capítulos desarrollan los campos en los que la presente tesis ha expandido el conocimiento, indicados en el apartado anterior. Estos capítulos se corresponden con los artículos publicados o en proceso de publicación o revisión redactados en inglés. Se incluyen, además, los siguientes capítulos redactados en castellano: introducción general, objetivos, discusión y conclusiones finales. La descripción de la metodología empleada se realiza en cada uno de los trabajos que constituyen los capítulos de la Tesis.

1.2.1. La atenuación de las condiciones físico-químicas extremas de aguas hidrotermales en embalses lacustres artificiales

Los sistemas hidrotermales activos son fuente de fluidos que introducen y transportan metales y otros elementos. Algunos de los elementos presentes en este tipo de fluidos hidrotermales, por ejemplo: Fe, Pb, Zn, S y As pueden tener efectos negativos sobre el ambiente. Los fluidos hidrotermales pueden ser una fuente importante de hierro y elementos traza en aguas enriquecidas que descargan en ríos y lagos en áreas geotermales activas. Los embalses son considerados como una estrategia efectiva para controlar contaminantes disueltos transportados por ríos; estos pueden ser empleados para controlar la calidad de agua regulando los contaminantes originados por actividades urbanas, industriales y agrícolas (Khadse *et al*., 2019) así como de procesos naturales. Adicionalmente, aquellas que tienen función de almacenamiento de agua son parte importante para el manejo regional de los ríos y sirven como solución para el control y administración de los recursos hídricos (Aghasian *et al*., 2019)

El azufre es un componente importante y muy frecuente en numerosos sistemas hidrotermales. Su presencia controla la geoquímica y la distribución de la mayoría de los elementos traza (Kaasalainen *et*

al., 2011; Kaasalainen *et al*., 2015). En los sistemas geotérmicos, este elemento se encuentra en forma de ácido sulfhídrico (H_2S) en los reservorios hidrotermales y es puesto en la superficie, a menudo, a través de manantiales de aguas termales alcalinas de origen hidrotermal (Björke, *et al*., 2015).

Los reservorios pueden producir fluidos enriquecidos en gases volátiles, como gas carbónico (CO_2) y ácido sulfhídrico (H_2S), en una proporción que puede cambiar dependiendo del grado de ebullición (el contenido en H_2S aumenta con el incremento de la ebullición). La mezcla del fluido hidrotermal con H_2S y el agua superficial no termal da lugar a aguas ricas en sulfatos (SO_4^{2-}) debido a la oxidación del H_2S de origen hidrotermal (Kaasalainen *et al*., 2011; Nordstrom *et al*., 2009) Las descargas de manantiales con flujos ricos en SO_4^{-2} puede alterar la composición de las aguas superficiales produciendo importantes alteraciones ambientales aguas abajo de los manantiales, tales como el incremento de la salinidad, lo cual puede impedir el aprovechamiento de los recursos hídricos para diferentes usos antrópicos. Además, los sistemas hidrotermales activos son una fuente importante de fluidos que transportan metales a los sistemas superficiales. Algunos de esos metales presentes en los fluidos hidrotermales (p.ej., Pb, Zn, y As) pueden tener efecto negativo sobre el ambiente, por lo que es necesario determinar su comportamiento para reconocer los posibles impactos ambientales (p.ej., Kristmannsdóttir *et al*., 2003). Los metales de los fluidos hidrotermales pueden proceder de volátiles ígneos o incorporarse por los procesos de interacción agua-roca, causando fluidos salinos con altas concentraciones de metales (Aiuppa *et al*., 2005). En ocasiones, estas aguas son acumuladas en lagos naturales o embalses artificiales que generan ambientes hidrológicamente restringidos.

Los embalses se consideran, con frecuencia, una estrategia eficaz para controlar los contaminantes disueltos transportados por los ríos. Estos se pueden utilizar para controlar la calidad del agua mediante la regulación de los contaminantes procedentes de las actividades urbanas, industriales y agrícolas, así como de los procesos naturales. Además, los embalses son herramientas importantes para la gestión regional de ríos y proporcionan soluciones para el control y la gestión de los recursos hídricos (Willis *et al*., 2003). Sin embargo, el entorno hidrológicamente restringido causado por los embalses puede aumentar los procesos de eutrofización (p.ej., Aghasian *et al*., 2019; Zhang *et al*., 2019) que producen sedimentos ricos en materia orgánica que pueden interactuar con las aguas almacenadas. En estos sedimentos se desarrollan importantes comunidades de microorganismos asociadas a la descomposición de la materia orgánica (tales como bacterias sulfato-reductoras) que pueden jugar un papel importante en la inmovilización y remoción de azufre y otros elementos relacionados (Niu *et al*., 2018; Cifuentes *et al*., 2020b). El destino de los elementos en estos sistemas acuáticos depende de diversos procesos biogeoquímicos que controlan su precipitación, adsorción, desorción y transporte (Chen *et al*., 2018; Wang *et al*., 2015). Para comprender la distribución de elementos en estos embalses y la efectividad de la estrategia de represas es necesario caracterizar los procesos críticos que controlan el destino de los elementos en y la interrelación de estos procesos biogeoquímicos en el sistema natural (Nordstrom, 2011; Chen *et al*.2018).

Quevedo *et al*. (2020a) indicaron que dos embalses principales regulan la salida de agua superficial de la cuenca alta del río Chicamocha: el embalse de La Playa y el Lago Sochagota. Estos embalses almacenan agua para satisfacer diversas demandas, tales como ganadería, agricultura, turismo e industria, y sus aguas reciben aportes antropogénicos de

actividades agrícolas y aguas residuales, así como aportes de aguas termales naturales, que producen aguas de alta salinidad muy eutrofizadas y sedimentos ricos en materia orgánica. Quevedo *et al*. (2020b) estudiaron los factores que controlan la contaminación por metales pesados de las aguas y sedimentos del embalse La Playa.

La presente Tesis se centra en el otro embalse significativo de la región: el Lago Sochagota. Como se describirá más detalladamente en el apartado correspondiente al área de estudio, geografía física y clima, el Lago Sochagota se encuentra ubicado en una zona de clima oceánico de altiplano subtropical situada en el área geotérmica asociada al volcán de Paipa en la Cordillera de los Andes. Los datos obtenidos indican que los sistemas geotérmicos proporcionaron importantes aportes hidrotermales de azufre y metales a las aguas del lago. El objetivo de este trabajo fue evaluar la efectividad de las represas para mejorar la calidad del agua identificando las fuentes de agua y los procesos de interacción involucrados.

Este estudio ha constituido la base del artículo. "Damming induced natural attenuation of hydrothermal waters by runoff freshwater dilution and sediment biogeochemical transformations (Sochagota Lake, Colombia)" Cifuentes, G.R.; Jiménez-Millán, J.; Quevedo, C.P.; Jiménez-Espinosa, R. que ha sido enviado a la revista Water.

1.2.2. La illitización lacustre sedimentaria promovida por el efecto de fluidos de origen hidrotermal

Existe una evidencia creciente de que las reacciones rápidas de los minerales arcillosos pueden actuar como sumideros de elementos importantes en procesos sedimentarios y diagenéticos. En este sentido,

se han propuesto diferentes transformaciones de minerales de la arcilla que secuestran a largo plazo elementos (como potasio o hierro) en entornos sedimentarios, diagenéticos e hidrotermales (Baldermann *et al*., 2017). La mayoría de las fases minerales formadas durante la diagénesis requieren largos períodos de tiempo (cientos de miles a millones de años) o altas temperaturas (o ambas) para formarse. Sin embargo, los minerales arcillosos proporcionan abundantemente superficies reactivas para la adsorción y desorción de elementos y compuestos.

La velocidad de reacción es una combinación de la estabilidad de la arcilla y el suministro de cationes que se pueden incorporar a las nuevas fases de la arcilla. Sin embargo, existe evidencia de que se pueden producir reacciones de arcilla más rápidas en sistemas donde la química de los fluidos en reacción está muy lejos del equilibrio con los minerales de la arcilla (Drief *et al*., 2002).

En ambientes sedimentarios y diagenéticos, la alta concentración de cationes en las aguas y la baja disponibilidad de oxígeno, que favorece el desarrollo de reacciones redox microbianas que involucran al hierro y al azufre, son factores que controlan determinantemente las transformaciones minerales secuenciales de las arcillas (Noël *et al*., 2017; Cuadros *et al*., 2018). La alta concentración de cationes y la actividad biológica se deben frecuentemente a la composición específica de los sedimentos, la hidrología y las condiciones climáticas, tales como las que se pueden generar en lagos salinos o suelos de manglares (Cuadros *et al*., 2018; Huggett, *et al*., 2016). En estos entornos hidrológicamente restringidos, las arcillas detríticas pueden interactuar con los fluidos salinos que conducen a la neoformación de minerales. A medida que las arcillas reaccionan en el agua salina, los cambios de catión octaédrico pueden aumentar la carga de la capa (p.ej., mediante la sustitución de magnesio por aluminio o la reducción de hierro) y la esmectita puede convertirse

en illita (Deocampo 2015). La illitización a baja temperatura puede ocurrir mediante ciclos repetidos de desecación o mediante la interacción con salmueras ricas en potasio (Deocampo, *et al*., 2009).

En lagos de regiones geotérmicas, la evolución química de las aguas puede verse influida por aportes hidrotermales. Los metales se incorporan a los sistemas geotérmicos a través de los fluidos acuosos y se transportan como iones simples o acomplejados con ligandos como Cl^-, HS^- y OH^- (p.ej., Barnes, 1997; Aiuppa., *et al*., 2005). En áreas volcánicas, la interacción progresiva agua-roca entre rocas (basálticas o riolíticas) controla la composición de los fluidos. Cuando las rocas son predominantemente riolíticas, como las del volcán Paipa (en la que se localiza este estudio), se cree que la química de los fluidos está dominada por la lixiviación de rocas (Kaasalainen *et al*., 2015), lo que produce altas concentraciones de elementos alcalinos. La descarga posterior en el lago hace que las aguas modificadas hidrotermalmente reaccionen más con los minerales detríticos, lo que puede resultar en el desarrollo de sedimentos con composiciones mineralógicas singulares. Muchas reacciones minerales a baja temperatura no están controladas por la termodinámica sino por la cinética. Las transformaciones de minerales de la arcilla como, por ejemplo, el proceso de illitización, requieren no solo suficiente tiempo de reacción o disponibilidad de cationes, sino también precursores minerales apropiados. La esmectita o los interestratificados illita-esmectita son los precursores arcillosos propuestos con más frecuencia para la formación de illita en cuencas sedimentarias (p.ej., Lanson, *et al*., 2002), paleosuelos (p.ej., Huggett *et al*., 2016) y suelos de manglares (p.ej., Andrade *et al*., 2014). Sin embargo, Dietel *et al*., (2018) observó que la transformación a illita también se puede producir a través de un interestratificado poco frecuente: illita-vermiculita dioctaédrica (I-DV).

Esta Tesis ha caracterizado los cambios mineralógicos que tienen lugar en las arcillas de los sedimentos en el Lago Sochagota (Colombia). Pueden distinguirse tres factores decisivos en el desarrollo de las transformaciones en este lago: a) la composición de los sedimentos detríticos ricos en caolinita y con presencia de I-DV en algunas zonas; b) la naturaleza de las aguas del lago como fluidos salinos de baja temperatura con aporte hidrotermal y c) el clima tropical a templado que ha permitido una gran acumulación de materia orgánica en los sedimentos. Los resultados indican que el I-DV puede actuar como un precursor mineral en la illitización rápida a baja temperatura y revelan el importante papel de los minerales arcillosos como sumidero de potasio de origen hidrotermal en lagos de regiones geotérmicas.

Los contenidos de este trabajo han sido incluidos en el artículo "Low Temperature Illitization through Illite-Dioctahedral Vermiculite Mixed-Layers in a Tropical Saline Lake rich in Hydrothermal Fluids (Sochagota Lake, Colombia)" Cifuentes, G.R.; Jiménez-Millán, J.; Quevedo, C.P.; Nieto, F.; Cuadros, J.; Jiménez-Espinosa, R." publicado en la revista Minerals. https://www.mdpi.com/2075-163X/11/5/523?-type=check_update&version=

1.2.3. Las transformaciones de minerales con azufre en sedimentos lacustres ricos en materia orgánica.

En lagos naturales o artificiales que almacenan aguas enriquecidas en azufre, los ambientes hidrológicamente restringidos pueden propiciar el desarrollo de reacciones y transformaciones minerales que impliquen a diferentes fases que incluyan este elemento. En condiciones tropicales, la alta eutrofización (Aghasian, *et al*., 2019; Zhang, *et al*., 2019) favorece la formación de depósitos ricos en materia orgánica en los que

la interacción entre los fluidos salinos y la actividad orgánica cataliza las reacciones con minerales en los sedimentos (Cuadros *et al*., 2017). Las reacciones microbiológicas redox que involucran compuestos de azufre pueden controlar algunos procesos sedimentarios autigénicos en esos ambientes (Ferreira *et al*., 2007). Rickard *et al*., 2007 revisaron exhaustivamente la química de los sulfuros de hierro. El monosulfuro de hierro resultante de la precipitación de Fe^{2+} y S^{2+} es makinawita (Kraal, *et al*., 2013). Este precipita como partículas tetragonales inestables que se transforman en cristales ordenados. La makinawita se transforma a través de diferentes pasos, en función de la concentración de O_2 y H_2S, a greigita (Fe_3S_4), pirita (FeS_2), azufre elemental (S^0) y óxidos e hidróxidos férricos. Es importante mencionar que las concentraciones de H_2S en ambientes sedimentarios de baja temperatura están asociadas a la actividad de microrganismos sulfato-reductores (Rickard, 2012). El estudio de Picard, *et al*. (2018) indicó que, aunque la mackinawita y la greigita no se suelen conservar en rocas sedimentarias, su formación puede ser controlada por microrganismos que tienen, posiblemente, una función critica en los ciclos biogeoquímicos actuales del hierro y el azufre. Entre los sulfuros, la pirita se caracteriza por su elevada estabilidad y abundancia Rickard (2012). Cosmidis *et al*. (2019) demostraron la importancia del azufre nativo (S^0) en los ciclos biogeoquímicos del azufre, el cual es producido por reacciones de oxidación (químicas o biológicas) de otras fases minerales con azufre en estado reducido.

En la presente Tesis, se ha abordado la neoformación sedimentaria de diferentes minerales con azufre en los sedimentos ricos en materia orgánica del Lago Sochagota. Los resultados obtenidos han permitido avanzar en el conocimiento de los procesos implicados en la fijación y transformación del azufre de origen hidrotermal de las aguas del lago.

Este trabajo constituye la base del artículo publicado "Transformation of S-bearing minerals in organic matter-rich sediments from a saline lake with hydrothermal inputs." Cifuentes, G.R.; Jiménez-Millán, J.; Quevedo, C.P.; Jiménez-Espinosa, R. Minerals 2020, 10, 525, https://doi.org/10.3390/min10060525"

1.2.4. El efecto de las comunidades bacterianas de los sedimentos en las transformaciones minerales y en los ciclos de los principales elementos.

Los ciclos de los principales elementos mayores y trazas sensibles a las modificaciones redox asociadas a la descomposición de la materia orgánica desempeñan un papel clave en la regulación del clima de la Tierra y en el quimismo de sedimentos, suelos, hidrósfera y atmósfera (Findlay *et al*., 2017). Algunos de los factores más comúnmente propuestos para explicar la concentración en trazas de elementos en los sedimentos de los lagos en áreas geotermales es la presencia de aportes hidrotermales que incrementan la salinidad de sus aguas (Kristmannsdóttir *et al*., 2003), la movilidad de los elementos en sedimentos ricos en materia orgánica (Andrade *et al*., 2018; Moreira *et al*., 2017) y el papel de las bacterias sulfato-reductoras (SRB) y las bacterias sulfato-oxidantes (SOB) en los ciclos bioquímicos (Niu *et al*., 2018).

Los sistemas hidrotermales activos son fuentes de fluidos que transportan metales, algunos de esos metales presentes en fluidos hidrotermales (Pb, Zn, y As) pueden tener efecto negativo sobre el ambiente por lo que es necesario determinar su comportamiento para reconocer los posibles impactos ambientales (Kristmannsdóttir *et al*., 2003).

Los fluidos hidrotermales salinos pueden ser una entrada importante de aguas ricas en trazas de elementos en lagos localizadas en áreas

geotermales activas. La abundancia de materia orgánica reactiva y las condiciones reductoras generadas en ambientes con alta producción de materia orgánica (ecosistemas tropicales) fomenta múltiples reacciones minerales asociadas frecuentemente con actividad biológica, afectando la movilidad de elementos como azufre y arsénico y la concentración de otros elementos traza (Zn, Pb, y Cu). La precipitación de sulfuros puede afectar considerablemente el comportamiento de estos elementos. Andrade *et al*., (2018) han sugerido que las reacciones reductoras mediadas por microorganismos que implican a compuestos de hierro y azufre pueden controlar la distribución de esos elementos traza en los sedimentos de esos sistemas (Noël *et al*., 2017). Los enriquecimientos en elementos traza (Cu, Ni, Co, Pb, Zn) de sedimentos de lagos que contienen framboides de azufre están frecuentemente relacionados a un alto contenido de materia orgánica (Hu *et al*., 2016; Large *et al*., 1999). La pirita es el mineral más representativo de los framboides y se encuentra principalmente en los intersticios del material orgánico (Hu *et al*., 2016), lo que sugiere que la materia orgánica favorece la precipitación de pirita a través de procesos microbianos de sulfato-reducción para convertirse en un sumidero adicional de elementos traza. Moreira *et al*., (2017) han sugerido que la materia orgánica carbonosa y la pirita tienen un efecto importante sobre la inmovilización de los metales en sedimentos depositados en regiones altamente productivas.

Las SRB se encuentran comúnmente en los sedimentos de ríos y lagos (Niu *et al*., 2018). Muyzer y Stams (2008) han indicado que esos microrganismos anaerobios procarióticos heterótrofos emplean el sulfato como aceptor de electrones para transformar materia orgánica en sedimentos bajo condiciones anaerobias. Qi *et al*. (2004) han sugerido que en este proceso se produce H_2S, el cual reacciona con los metales disponibles para estabilizarlos como sulfuros. Por lo tanto, las SRB

pueden convertir iones de metales (Cu, Pb, Cr, Zn, Hg, As) en sulfuros de metales de baja solubilidad en ambientes enriquecidos con metales pesados debido a procesos naturales como la entrada de fluidos hidrotermales (Frank *et al*., 2013), y jugar un papel importante en la eliminación de contaminantes tóxicos generados por polución antrópica (Kiran *et al*., 2017; Tarekegn *et al*., 2020; Wolfenden *et al*., 2005). Por otra parte, las SOB pueden oxidar los sulfuros a sulfatos, afectando la bioquímica del azufre (Kühl *et al*., 1992; Niu *et al*., 2018) y posibilitando la liberación de los metales asociados a los minerales con azufre. (Niu *et al*., 2018).

De acuerdo con lo anterior, las SRB y las SOB pueden definirse como los grupos de bacterias dominantes responsables de la biogeoquímica del azufre (Kühl *et al*., 1992; Niu *et al*., 2018). De hecho, la actividad de las SRB y SOB controla el balance del ciclo del azufre (Niu *et al*., 2018). Además, estos grupos de microrganismos pueden influenciar las bio-transformaciones de los metales en las aguas y los sedimentos. Las SRB pueden estar asociadas con los procesos de remoción por cristalización de los metales en agua y sedimentos (White *et al*., 1998). Estos procesos pueden ser favorecidos por la presencia de bacteria reductoras del hierro (IRB). La reducción biológica de Fe^{3+} es un mecanismo efectivo que transforma Fe^{3+} a Fe^{2+}. La actividad conjunta de SRB y IRB puede afectar la disponibilidad de los metales pesados en suelos y sedimentos (Zhang *et al*., 2019). Sin embargo, la actividad de SOB puede favorecer la oxidación del sulfuro precipitado, promoviendo de nuevo la liberación de metales tóxicos en el ambiente (Niu *et al*., 2018).

La integración de los estudios mineralógicos, geoquímicos y microbiológicos de las aguas y sedimentos del Lago Sochagota fue publicada en el trabajo "Trace element fixation in sediments rich in organic matter

from a saline lake in tropical latitude with hydrothermal inputs (Sochagota Lake, Colombia): The role of bacterial communities". Cifuentes, G.R.; Jiménez-Millán, J.; Quevedo, C.P.; Gálvez, A.; Castellanos-Rozo, J.; Jiménez-Espinosa, R. Science of the Total Environment 2021, 762, 143113. https://doi.org/10.1016/j.scitotenv.2020.143113"

1.3. Área de estudio

1.3.1. Geografía física y clima

La cuenca del Lago Sochagota está situada en la vertiente occidental de la Cordillera Oriental del Departamento de Boyacá (Colombia). En esta se ubica el Lago Sochagota que es un embalse artificial construido en 1956 sobre una zona pantanosa con un suelo mal drenado, con fertilidad baja y escasa profundidad.

El lago está ubicado en la zona turística de Paipa a 2.496 metros sobre el nivel del mar (Barco *et al*., 2010) y comprende una superficie aproximada de 8.150 hectáreas. Sus coordenas son: Latitud 5°46′05″N y Longitud 73°07′04″W

Se estima que la capacidad del lago en su nivel máximo (rebosando sobre la compuerta), es aproximadamente de 4,5 millones de m^3 (4,5 Hm^3) y que la lámina de agua, en el mismo nivel cubre una superficie de 1,6 Km^2 y una profundidad de 2,8 m. En los alrededores, la vegetación predominante está formada por pastizales y juncos en las riveras. Cabe destacar que existe una importante y desarrollada industria hotelera y de recreo alrededor de este lago.

El principal afluente del Lago Sochagota es la Quebrada Honda – Río Salitre, el cual recibe la influencia de actividades agrícolas,

pecuarias, recreativas y mineras. Dicho afluente recibe descargas provenientes de manantiales de aguas termales, mineralizadas y dulces, después de su aprovechamiento con fines recreativos (Balnearios la Playa, los Delfines, etc.). El lago también recibe aportes termales de manantiales en el área de influencia cercana, que afloran en su interior o que se articulan con el sistema regional (río Chicamocha) a través de las estructuras conocidas como "dársenas". Las dársenas, si bien no realizan aportes directos al lago, forman parte del sistema de forma integral, pues tras su uso el agua es almacenadas temporalmente en dos tanques en tierra que facilitan su regulación y vertido al río Chicamocha. El efluente del lago es regulado mediante una compuerta que a través de un canal conduce el agua hacia el río Chicamocha. Así mismo, debe existir una sincronización y regulación de apertura de las compuertas, tanto en el Lago Sochagota, como en las que existen en las dársenas y controlan el flujo hacia el río Chicamocha, pues esto puede generar un cambio en la calidad del agua y en su uso potencial (agrícola en el distrito de riego, para consumo humano, etc.). En la figura 1 se presenta el esquema general del sistema. (Díaz et al., 2015)

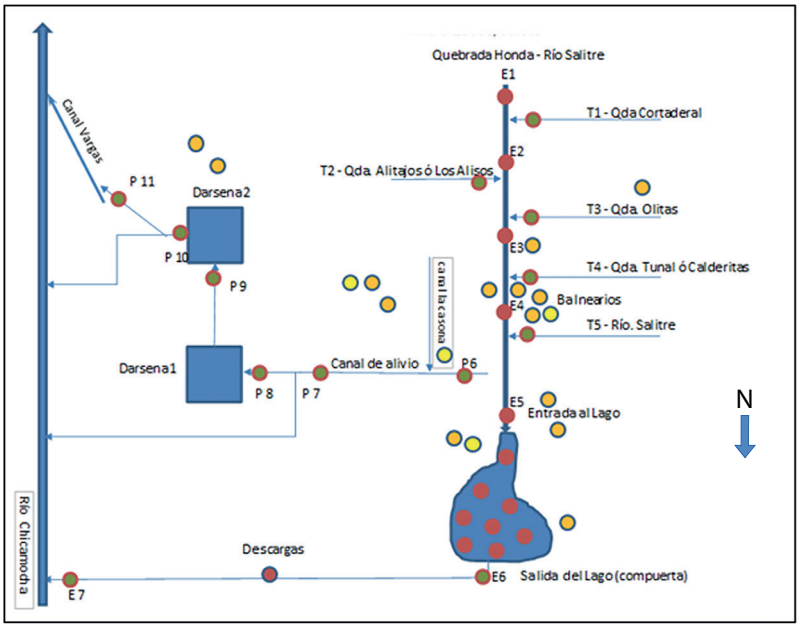

Figura 1. Esquema General del Sistema

El efluente del lago (en el canal), recibe adicionalmente aguas residuales de un sector del municipio de Paipa que presenta rezago en la conexión del sistema de alcantarillado a la Planta de Tratamiento de Agua Residual municipal (PTAR). De otra parte, en el año 1998, empezó el funcionamiento del colector perimetral (Plan de acción e inversión generación térmica 2002-2009, citado por Barco Rincón y Méndez Angarita, 2010, el cual se proyectó para la recolección de las aguas provenientes del sector hotelero, casas de recreo, cabañas, entre otras existentes en inmediaciones al Lago Sochagota. Es necesario, realizar la revisión no solo de la infraestructura existente, sino de los sectores que carecen de cobertura del sistema de alcantarillado o que disponen sus aguas en pozos sépticos u otros sistemas de tratamiento, de manera que se garantice una adecuada operación, mantenimiento y disposición final del agua residual, situación que puede comprometer no solo la calidad del agua del Lago Sochagota, del río Chicamocha, del suelo y el subsuelo.

El clima en Paipa es templado. La precipitación en Paipa es significativa, con precipitaciones incluso durante el mes más seco. El clima aquí se clasifica como Cfb (clima oceánico) por el sistema Köppen-Geiger. La temperatura media anual en Paipa se encuentra a 14,4 °C. En las horas centrales del día, la temperatura oscila entre 20 y 22°C, mientras que, durante la madrugada, la temperatura mínima está entre los 6 y los 8°C. No obstante, en la temporada seca de inicio de año, las temperaturas mínimas pueden situarse ligeramente por debajo de los 5°C. Paipa tiene un comportamiento de lluvias bimodal, es decir, dos temporadas secas y dos temporadas lluviosas. El promedio de lluvia total anual es de 881 mm. Los meses de diciembre, enero, febrero, julio y agosto son predominantes secos. Las temporadas de lluvias se extienden desde finales de marzo hasta principios de junio y desde finales de septiembre hasta noviembre. En los meses secos de inicio de año, llueve de 4 a 6 días/mes y en los meses secos de mitad del año llueve en promedio 17 días/mes. En los meses de mayores lluvias, en promedio llueve entre 18 y 20 días/mes. El sol brilla cerca de 4 horas diarias en los meses lluviosos y en los meses secos de principio de año, la insolación llega a 6 horas/día. La humedad relativa del aire es cercana al 70% en la época seca de inicio de año y en épocas de lluvias alcanza el 78%. (IDEAM, s.f.)

Para llevar a cabo este estudio se estableció una red de muestreo de 20 puntos distribuidos en el lago. Se tomaron muestras de sedimentos en cada punto de la red, obteniendo testigos de un metro que se dividieron en dos muestras en función de la profundidad (superior e inferior), empleando un tubo Shelby estándar. La zona sur del lago está caracterizada por la presencia de sedimentos pobres en materia orgánica constituidos principalmente por cuarzo y caolinita, mientras que, los sedimentos de las zonas centro y norte son negros, con granos de tamaño muy fino

y ricos en residuos de plantas. En la figura 2 se presenta el gráfico de localización del Lago Sochagota y los puntos de muestreo. (Cifuentes *et al*., 2020a)

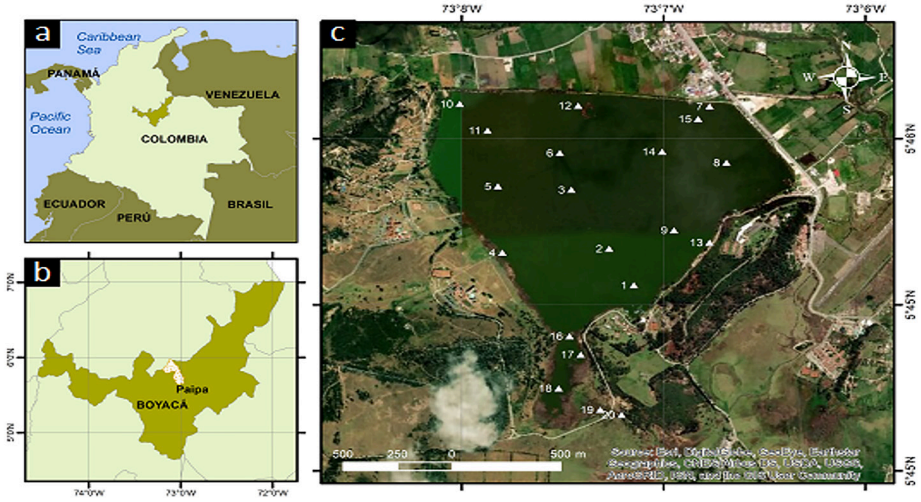

Figura 2. Localización del Lago Sochagota y los puntos de muestreo.

1.3.2. Marco geológico e hidrogeológico

Desde el punto de vista geológico, el Lago Sochagota está localizado en una importante área geotermal que desarrolla sistemas hidrotermales asociados a los volcanes de la Cordillera de Los Andes que intruye rocas sedimentarias del Cretácico (Figura 2).

Los principales afloramientos que son fuente de sedimentos al lago son rocas de las siguientes formaciones sedimentarias: a) Formación Plaeners (Cretácico), formada por radiolaritas intensamente deformadas; b) Formación Los Pinos (Cretácico), con limolitas y lechos de areniscas cuarzosas; c) Formación Labor-Tierna (Cretácico), con arcillas y areniscas que incluyen abundantes intercalaciones de areniscas cuarzosas;

d) Formación Gauduas (Maastrichtian-Paleoceno) con arcillas y limolitas que incluyen abundantes intercalaciones de areniscas cuarzosas; (e) Formación Bogotá (Paleoceno tardío- Eoceno temprano), formada por arenisca cuarzosas, limolitas y arcillas; f) Formación Tilatá (Plioceno-Pleistoceno) que se superpone discordantemente a materiales del Cretácico y Paleógeno y está formada predominantemente por niveles de arena ricos en cuarzo, lechos de limolitas y arcilla; g) Depósitos cuaternarios de arenas, limos, arcillas y conglomerados que se superponen a la Formación Tilatá y que corresponden a los materiales caracterizadas por la presencia de caolinita y cuarzo depositados por la actividad aluvial, lacustre y fluvio lacustre más reciente, también presente en la cuenca del rio Chicamocha, (Cifuentes *et al*., 2020c).

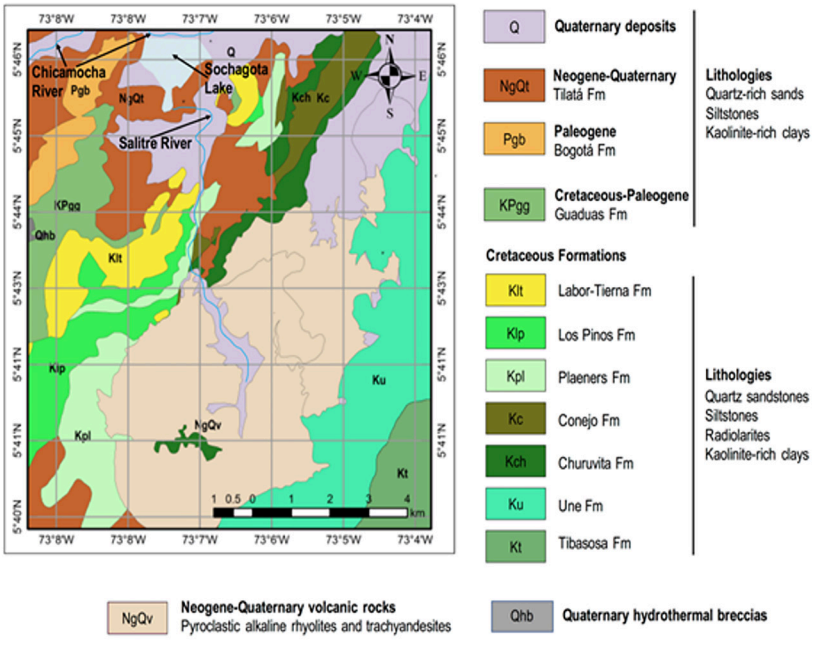

Figura 2. Mapa geológico de la cuenca del Lago Sochagota.

Además, el Lago Sochagota recibe aportes de los depósitos piroclásticos del Plioceno - Pleistoceno que constituyen el volcán Paipa (Pardo *et al*., 2005). Este edificio volcánico se caracteriza por la presencia de una caldera colapsada que incluye manantiales hidrotermales asociados a fallas profundas que descargan aguas termales ricas en SO_4-Na-K y aguas frías ricas en hierro (Cifuentes *et al*., 2020c). Esas aguas salinas hidrotermales fluyen de norte a sur a través de la Quebrada Honda - Rio Salitre (Cifuentes *et al*., 2017; Cifuentes *et al*., 2020c).

Capítulo 2.

Objetivos

Objetivo General

Determinar la influencia antrópica y natural de los procesos que controlan los parámetros fisicoquímicos de las aguas y la composición mineralógica y geoquímica de los sedimentos del Lago Sochagota (Colombia).

Objetivos Específicos

Evaluar la influencia de los aportes hidrotermales en la hidroquímica de las aguas del Lago Sochagota y la efectividad del embalse para la mejora de la calidad de las aguas.

Valorar los factores que controlan la autogénesis de arcillas, especialmente de illita, en ambientes lacustres salinos ricos en materia orgánica.

Determinar los procesos involucrados en la asimilación sedimentaria del azufre de origen hidrotermal de las aguas en fases minerales neoformadas y sus procesos de transformación.

Determinar el origen de los elementos traza en los sedimentos de un humedal de origen hidrotermal.

Evaluar el papel de las comunidades bacterianas en la formación de minerales con azufre y su influencia en la acumulación de metales mayores y en trazas en los sedimentos depositados en el Lago Sochagota.

Capítulo 3.

Composición, condiciones físico-químicas y origen de las aguas del Lago Sochagota

El contenido de este capítulo constituye el trabajo:

Damming induced natural attenuation of hydrothermal waters by runoff freshwater dilution and sediment biogeochemical transformations (Sochagota Lake, Colombia)

Cifuentes, G.R., Jiménez-Espinosa, R., Quevedo, C.P., Jiménez-Millán, J 2021.

Este manuscrito ha sido enviado a la revista Water

water

MDPI

Article

Damming induced natural attenuation of hydrothermal waters by runoff freshwater dilution and sediment biogeochemical transformations (Sochagota Lake, Colombia)

Gabriel Ricardo Cifuentes [1], Rosario Jiménez-Espinosa[2]*, Claudia Patricia Quevedo [1] and Juan Jiménez-Millán [2]

[1] Faculty of Science and Engineering, Water Resources Research Group, University of Boyacá, Campus Tunja (Colombia) (G.R.C.); grcifuentes@uniboyaca.edu.co; (C.P.Q.); patriciaquevedo@uniboyaca.edu.co
[2] Department of Geology and CEACTEMA, University of Jaén. Campus Las Lagunillas, 23071, Jaén (Spain), (J.J.-M.); jmillan@ujaen.es
* Correspondence: (R.J-E) respino@ujaen.es

Abstract: Volcanic area of Paipa system (Boyacá, Colombia) contains a magmatic heat source and deep fractures which help to flow up hot and high mineralized waters with a further combination with cold superficial inputs. This mixed water is recharging the Salitre River and downstream feeding the Sochagota Lake. This incoming water can contribute to substantial increases of hydrothermal SO_4^{2-}-Na water into the water of the Salitre river basin area, rising the salinity. An additional hydrogeochemical process is the mix with cold Fe-rich water from alluvial and surficial aquifers. This salinized Fe-rich water is feeding the Sochagota Lake, although the impact of the freshwaters from rain on the hydrochemistry of the Sochagota Lake is significant. A series of hydrogeochemical, biogeochemical and mineralogical processes occur inside the lake. The goal of this study was to examine the effect of the Sochagota Lake as a damming that acts as a natural attenuation of the contaminants. Damming in the Sochagota Lake can be considered as an effective strategy for attenuating high mineralized waters. The concentrations of dissolved elements were attenuated significantly. Dilution by rainfall runoff and precipitation of iron sulfides mediated by sulfate reducing bacteria in deposits rich in organic material were the main processes involved in the concentration attenuation of SO_4^{2-}, Fe, As Cu and Co in the lake water. Furthermore, the K-consuming illitization processes occurring in the sediments could favor the decrease of K and Al.

Keywords: Sochagota Lake; Paipa volcanic area; natural contaminant attenuation; S and Fe uptake, precipitation of pyrite.

Citation: Lastname, F.; Lastname, F.; Lastname, F. Title. *Water* **2021**, *13*, x. https://doi.org/10.3390/xxxxx

Academic Editor: Firstname Lastname

Received: date
Accepted: date
Published: date

1. Introduction

Geological ambiances with hydrothermal activity are a font of fluids that deliver and transport metals and other elements. Some of the elements found in hydrothermal liquids (eg., Fe, Pb, Zn, S and As) could induce negative effects on the environment, thus it is essential to determine their behavior to identify probable environmental impacts (e.g., [1]). These elements can be added into the hydrothermal solutions from the source water, the magmatic volatiles due to the water-rock interaction, producing salty fluids with important metal concentrations [2,3]. Saline hydrothermal solutions might be a significant contribution of iron and trace-element water to streams and lakes in geothermal areas. Damming reservoirs are frequently considered as an effective strategy for controlling dissolved pollutants transported by rivers. Dams can be utilized to monitor the water quality by regulating pollutants from anthropogenic activities (e.g., [4]) as well as from natural processes. Moreover, barriers storing water are significant instruments for local river management and offer keys for controlling and administration of water resources [5].

However, the hydrologically-limited environment produced by dams could rise eutrophication processes (e.g., [6,7]) producing organic matter-rich sediments that can interact with stored waters. Significant microorganisms communities associated with the organic matter decay (such as sulfate reducing bacteria) are present in these sediments and can work as an important factor on the immobilization and removal of S and other related elements [8, 9]. The fate of elements in these aquatic systems depends on many biogeochemical processes that control their precipitation, adsorption, desorption and transport [10, 11, 12, 13]. In order to understand the distribution of elements in these reservoirs and the effectiveness of the damming strategy it is necessary to characterize the critical processes controlling the destiny of elements in the ponds and the interrelation of these biogeochemical processes in natural system [14, 10].

[15] indicated that two principal dams control the discharge of the upper Chicamocha River basin: the La Playa dam and the Sochagota Lake dam. These barriers stock water to account for several demands, such as ranching, farming, tourism and manufacturing, and their reservoirs receive anthropogenic entries from farm actions and wastewater as well as input from geothermal waters that yield high salinity waters, important eutrophication and sediments enriched in organic matter. [16] studied the factors controlling heavy metals pollution of waters and deposits from the La Playa dam. The present study is focused on the other significant dam of the region: the Sochagota Lake. The lake is placed in a subtropical mountain region with an oceanic climate and located in the Andean geothermal Paipa volcanic area. [17,9] exposed that these geothermal structures provided remarkable hydrothermal inputs of sulfur to the waters of the Sochagota Lake. We aimed to evaluate the effectiveness of damming for improving water quality identifying the water sources and the interaction processes involved. Despite the importance of such processes, studies of types have been lacking.

2. Materials and Methods

2.1. Study area

The Sochagota Lake is an artificial pool with an entertaining utilization constructed on an earlier natural wetland. It is situated in an upland (height 2496 m) of the Department of Boyacá in the Paipa province (Colombia), extending over 1.8 km² (Figure 1). The largest depth of the lake is around 3.2 m. A tributary of the Chicamocha River, the Salitre River, feed the lake by the south.

The province of Paipa presents an average annual temperature of 14.4 °C. The rainfall is well distributed along the year with an average precipitation of 911 mm/yr. The classification of the climate is subtropical highland oceanic (Cfb by the Köppen system).

Geologically, the study zone is in the principal Andean geothermal system in Colombia, the Paipa volcanic region where hydrothermal activities associated to these volcanoes can be recognized [18]. Siliceous sedimentary rocks (Cretaceous) were intruded by different volcanic rocks (Figure 2). In this area there is an absence of any kind of evaporitic sedimentary deposits. The adjacent volcanic structure is the Paipa volcano [19] outcrops in the southern area of the Sochagota Lake appearing Pliocene-Pleistocene pyroclastic alkaline rhyolites and trachyandesites rocks. A collapsed caldera (3 km wide) with numerous hydrothermal vents, promoted by important fractures, controls the rise up of hot flow fluids and cold shallow waters with several processes of mixing producing sodium-sulfate water facies. These waters move through the Salitre River basin and are mixed with the lake and rain water in the Sochagota Lake [17,9].

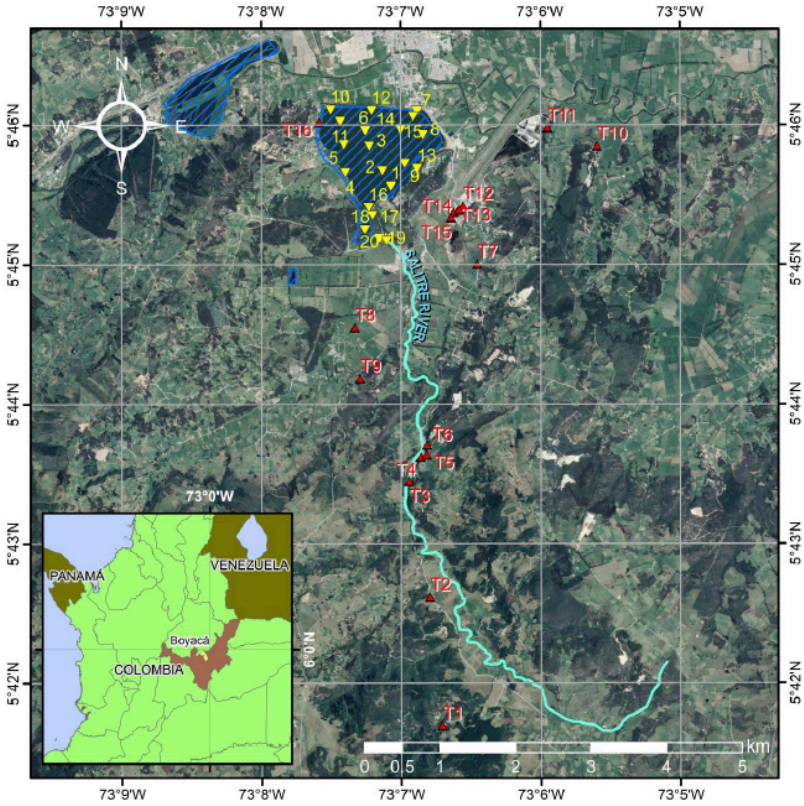

Figure 1. Geographical location of the study area and identification of samples sites. Red points represent the hydrothermal springs and the yellow points are the sites from the Sochagota Lake. Base map: Google Earth.

The conceptual model of the Paipa geothermal system [20,21] considers that the heat source is magmatic and related to the Paipa volcano. The relationship between the geothermal system and the magmatic body is derived from their proximity. The main reservoir of water is located in the old volcanic caldera formed at the end of the first eruptive epoch, in addition, a secondary reservoir would be related to the quaternary sedimentary cover. The circulation of hot spring water is carried out through faults (Figure 2). The discharge zone is structurally controlled, hot fluids rise to the surface preferentially through fault intersection zones. The main recharge zone by infiltration must occur in the southern mountains of approximately 3500m altitude, however, there is a local recharge area around the volcanic caldera.

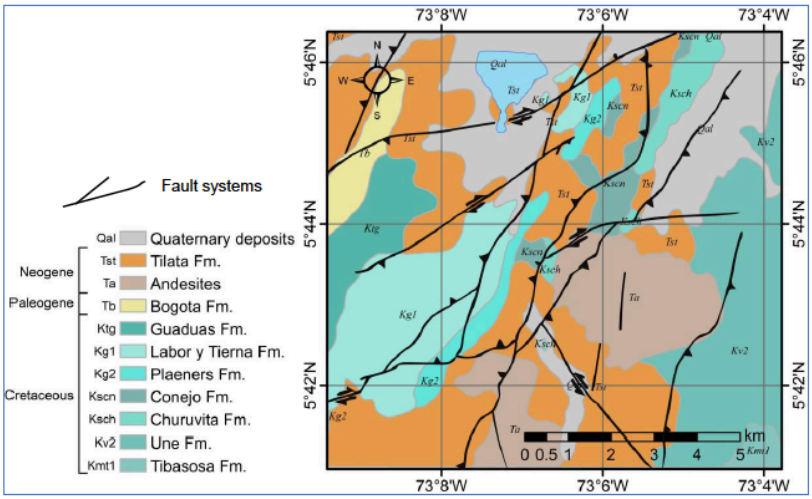

Figure 2. Map of the main geological outcropping and the principal fault system of the Pipa volcanic area related to the Sochagota Lake. Modified from [16].

[9] indicated that organic matter-poor sediments (TOC < 0.7%) with quartz and kaolinite near the south entrance of the lake (Figure 3a) were enriched in Zr (up to 603 mg/kg) and some major detrital elements (Na, Ti, Al and Si). Fine sized clay rich sediments deposited in the deep zones of the lake (central and northern segments) were characterized by high contents in organic matter (up to 11.10%) and the crystallization of S-bearing minerals, clay mineral mixed layers and illite (Figure 3b). These sediments were enriched in S, Fe, Zn, Rb, Co, K, Cr, Sb, Ni, As, Ba, Cu, Mn, Mg and Sr. The presence of Fe-sulfides nanoparticles enriched in heavy metals encrusting microbial cells and a dominant sulfate-reducing bacteria (SRB) community (*Desulfatiglans, Desulfobacterales* and Sva0485) suggested that the precipitation of the hydrothermal S and the accumulation of trace elements into the sediments was regulated by SRB activity. The crystallization of S°, barite and calcite and the good correlations between Ba, Sr and Ca indicated that previously precipitated sulfide can be oxidized by the activity of a relevant sulfur oxidizing bacterial community (*Thioalkalimicrobium, Sulfurovum, Arcobacter and Sulfurimonas*) which could favor the release of the metals.

2.2. Methods

2.2.1. Data acquisition and analytical procedures

In order to analyze the Sochagota Lake water composition, 20 samples were taken in September of 2017 at different depths: shallow, medium and deep (Figure 1). Furthermore, 16 samples from mineral and thermal waters from hydrothermal springs were collected in August of 2015 by Proagua Foundation and provided by Corpoboyaca (Regional Autonomous Corporation of Boyacá) in 2016, with the aim of establishing the influence of these waters on the water lake composition. At each site in the lake, water samples were collected in different clean high-density polyethylene bottles (HDPE), rinsed several times with the water lake to be sampled. One of the sample bottles was acidified to pH<2.0 with nitric acid (HNO_3), ACS reagent and a purity of 70%, to stabilize trace metals. The filling

of the tubes was done using sterilized syringes and filtered by 0.45 µm filter pore size then acidified. In a different bottle we kept not acidified sample, used for cations and anions analysis. These water samples were carried in iceboxes to laboratory and mantained at 4°C for forthcoming analysis. Analyses were carried out in various laboratories. Major elements were determined in an Ion Chromatograph model Metrohm 850 Professional (Scientific Instrumentation Centre, University of Jaén) with relative errors of analysis are ±1% for major anions and cations). The analysis of metals and trace elements were done by ICP-mass spectrometer Agilent Model 7500, being the errors <5% RSD (Scientific Instrumentation Centre, University of Jaén). We used the AquaChem software package (Schlumberger Water Services), and SPSS and Statgraphics Statistics software to analyze hydrochemical data. Easy_Quim [37] was used to make the graphical representation of Piper, Shöeller-Berkaloff and Salinity diagrams.

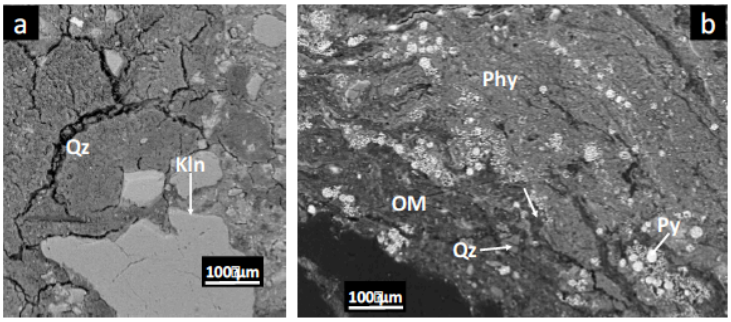

Figure 3. Images of the lake sediments by an electron microscope. (a) BSE picture of a southern area of the lake sample, where crystals of quartz in a kaolinite rich matrix can be seen. (b) BSE image of a sample taken in the north of the lake with parts rich in organic matter and framboidal pyrite in an plentiful clay-rich matrix. Phy: phyllosilicates, Kln: kaolinite, Qz: quartz, Py: pyrite, OM: Organic matter.

Different physico-chemical parameters, determined in situ, using a Hanna Instruments multiparameter device (HI 9828), such as electrical conductivity for a standard temperature of 25 °C (EC (µS/cm)), ±1 µS/cm), total dissolved solids (TDS, ppm), ±1 mg/L), pH (±0,02 pH), temperature (T) (°C, ±0,15°C). Alkalinity was obtained by volumetric determination.

Moreover, a sediment sampling survey in the same points used for water was carried out in the lake. These samples were examined under SEM using back-scattered electron (BSE) imaging and energy-dispersive X-ray (EDX) analysis in order to obtain textural and chemical data of the mineral phases using a Carl Zeiss model MERLIN. Moreover, mineral composition of these samples was examined by X-ray diffraction (XRD) using Cu-Kα radiation at 35 kV y 34 mA, with scan speed of 6º 2θ min–1, in a Siemens D-5000 diffractometer. These analyses were carried out at the Scientific Instrumentation Centre of the University of Jaén. For the chemical characterization at the nanometre scale of clay minerals, samples were prepared for transmission electron microscopy (TEM) study. Samples were prepared using Cu grid surface coated in a perforated formvar resin from a dispersion of finely ground sample particles, in alcohol or distilled water. The monomineralic character of each grain is proven by its electron diffraction pattern, checking the existence of a single network and, therefore, a single crystalline phase. The TEM data was obtained using the Philips CM20 (STEM) microscope, operated at 200 kV from the Scientific Instrumentation Centre (C.I.C.) of the University of Granada. Quantitative analyses (AEM) of particles were obtained in STEM mode with an EDAX microanalysis system in the Philips CM20. The counting time used was 100 seconds except for Na and K, which were analysed for 15 seconds to try to

minimise alkali-loss problems as short counting times improve reproducibility for K and Na [22].

We used polished sections to obtain back-scattered electrons (BSE) images and tridimensional sediment fragments to acquire secondary electron (SE) images in a field emission scanning electron microscope (FESEM, Merlin Carl Zeiss of the CICT of the University of Jaén, Spain). Polished samples used for BSE images were previously impregnated under vacuum with a polyester resin. BSE images were acquired at 15 kV with a working distance of 8 mm using an AsB detector, whereas SE images were acquired at 15 kV using conventional and In-Lens detectors. These images provided the information for a textural and microcochemical characterization.

3. Results

3.1. Physicochemical properties of the Sochagota Lake waters

As commented previously, water data acquisition was developed taking 3 different samples in the vertical line of each sampling point, deep, medium and shallow (namely B, M and S for sample labels). Nonetheless, no significant variations were found in the three different measurements, indicating that depth is not an important parameter to control geochemical behavior of the water lake, due to the shallow depth of the lake during the sampling period. This behavior led us to consider data of the middle part for the calculations, when it is possible (Table 1). Additionally, in order to better visualize the huge data set, a descriptive statistical analysis: minimum, maximum, average and standard deviation, was performed (Table 2).

Analyzing data globally, it draws attention the difference between samples from the southern area (19 and 20) and those from the rest of the lake. Samples 19 and 20 have very high contents in most of variables, such as electrical conductivity (E.C.), Cl^-, SO_4^{2-}, Na^+, K^+ and some metals. The average value for E.C. is 2925.4 µS/cm, it is high, but minimum value is 2211 µS/cm and the maximum is 8651.7 µS/cm. In order to appreciate the spatial variation of E.C. in the lake, a plot of values has been made excluding samples 19 and 20 (Figure 4). In this figure, it is possible to observe how there is a trend of dilution of saline waters through the lake in direction SW to NE and NW. Just in the center of the lake the contents of salinity show low values. This behavior is similar for most of the variables (Table 2), indicating the high influence in the main entrance of very high mineralized water to the lake which is geochemically change inside the lake. Mostly average values of lake samples have values bigger than the indications of World Health Organization and Colombian Drinking Water Legislation. In this way, total dissolved solids (TDS) show a similar trend, with high values in the south area. For example, there is a considerable difference between the two samples for the south of the lake 19 and the rest of samples. The average is 1868,39 mg/L, while maximum values are bigger than 5400 mg/L. Following indications of World Health Organization, TDS levels of TDS greater than 1000 mg/L for drinking-water becomes significantly unpalatable and the occurrence of great levels of TDS might also be unsuitable to users, due to high scaling in water pipes and household appliances [23].

In relation to pH values, there is not a problem for health, but it is very important in geochemical processes in natural waters, their values are ranging from 8.8 to 9.2, indicating an alkaline affinity of the medium. Most of the rest of ions are clearly over the recommended levels for drinking water. The average concentrations of cations followed the order as $Na^+ >> K^+ > Ca^{2+} > Mg^{2+}$, being visibly Na^+ considerable higher than the other cations in one order of magnitude. In relation to anions, $SO_4^{2-} > Cl^- > HCO_3^-$, considering that SO_4^{2-} is the most relevant anion in this water.

Table 1. Water sampling points in Sochagota Lake. M: medium vertical measurement.

SAMPLE	pH	EC	Temp	TDS	Cl	SO4	HCO3	CO3	NO3	Na	Mg	Ca	K
		µS/cm	°C	mg/L	mg/L	mg/L	mg/L	mg/L	mg/L	mg/L	mg/L	mg/L	mg/L
P1_M	9,07	2473,0	16,0	1582,9	204,80	687,34	169,88	0,70	-	432,44	8,65	24,07	54,98
P2_M	8,90	2325,0	17,0	1488,2	203,54	679,75	99,58	0,40	3,13	430,66	8,56	7,05	55,53
P3_M	9,16	2282,0	19,0	1460,3	200,94	671,69	73,77	1,30	2,94	424,24	8,35	22,89	54,17
P4_M	9,14	2329,0	18,0	1490,3	204,53	686,58	76,15	0,32	2,69	434,72	8,41	21,96	54,94
P5_M	9,17	2368,0	18,0	1515,3	204,28	687,09	102,15	0,85	2,70	433,50	8,46	21,42	54,81
P6_M	9,21	2377,0	17,0	1521,4	197,38	666,29	141,87	1,54	-	429,51	8,44	21,87	54,51
P7_M	9,16	2287,0	17,0	1463,5	194,90	652,87	107,82	0,34	2,74	416,90	8,31	26,64	52,92
P8_M	9,22	2211,0	17,0	1415,3	198,35	667,70	34,05	0,47	2,70	425,38	8,55	24,32	53,79
P9_M	9,18	2547,0	20,0	1630,3	208,36	699,74	187,27	0,64	2,68	442,88	8,71	23,87	56,12
P10_M	9,14	2485,0	19,0	1590,2	206,21	696,19	158,90	0,43	-	440,63	8,58	23,50	55,77
P11_M	9,16	2415,0	16,0	1545,9	205,51	694,10	119,17	0,68	2,67	438,32	8,55	21,39	55,46
P12_M	9,15	2371,0	19,0	1517,4	208,54	703,51	68,10	0,47	-	447,63	8,84	23,79	56,58
P13_M	9,14	2350,0	19,0	1504,0	209,71	708,17	45,40	0,60	2,72	447,04	8,90	25,00	56,45
P14_M	9,24	2355,0	19,0	1507,2	211,70	714,78	39,72	0,38	-	450,78	8,75	23,98	57,10
P15_M	9,27	2274,0	20,0	1455,1	211,09	712,57	28,37	0,73	-	419,07	9,14	21,04	53,07
P16_M	9,10	2361,0	18,0	1511,2	211,82	714,15	35,15	0,17	2,67	453,11	8,87	27,98	57,33
P17_M	9,05	2432,0	19,0	1556,5	218,03	724,41	58,58	0,15	2,76	461,27	9,06	22,23	59,97
P18_M	8,88	2489,0	18,0	1592,9	224,62	752,82	41,30	0,20	-	481,90	8,79	22,67	60,57
P19_M	8,84	7126,0	19,0	4526,3	664,50	2142,51	64,44	0,45	2,75	1470,69	8,65	28,16	178,31
P20_M	8,90	8651,8	19,0	5493,8	846,00	2598,08	80,76	0,66	3,38	1719,00	10,42	28,46	207,00

SAMPLE	NH4	F	Br	Li	Al	Mn	Fe	Ni	Cu	Zn	As	Rb	Sr	Cs
	mg/L	mg/L	mg/L	mg/L	mg/L	mg/L	mg/L	mg/L	mg/L	mg/L	mg/L	mg/L	mg/L	mg/L
P1_M	0,00	0,930	0,842	0,542	0,055	0,702	0,221	0,003	0,004	0,016	0,009	0,386	0,325	0,016
P2_M	0,00	0,577	0,834	0,586	0,063	0,709	0,219	0,003	0,001	0,054	0,008	0,386	0,329	0,016
P3_M	0,00	0,776	0,823	0,595	0,058	0,717	0,212	0,003	0,001	0,009	0,008	0,392	0,334	0,016
P4_M	0,03	0,938	0,827	0,594	0,060	0,713	0,217	0,003	0,001	0,011	0,008	0,389	0,333	0,016
P5_M	0,03	0,931	0,823	0,602	0,063	0,712	0,212	0,003	0,001	0,015	0,008	0,388	0,333	0,016
P6_M	0,04	0,902	0,813	0,603	0,055	0,694	0,205	0,002	0,001	0,006	0,008	0,385	0,329	0,016
P7_M	0,03	0,867	0,808	0,595	0,050	0,627	0,193	0,003	0,001	0,005	0,008	0,359	0,310	0,016
P8_M	0,03	0,944	0,816	0,598	0,057	0,635	0,193	0,003	0,001	0,024	0,008	0,366	0,316	0,016
P9_M	0,04	1,001	0,838	0,601	0,062	0,639	0,202	0,002	0,001	0,006	0,008	0,364	0,314	0,016
P10_M	0,08	1,004	0,819	0,599	0,048	0,645	0,199	0,002	0,001	0,005	0,008	0,370	0,317	0,016
P11_M	0,04	1,003	0,824	0,588	0,054	0,629	0,191	0,002	0,001	0,005	0,008	0,353	0,308	0,015
P12_M	0,03	1,021	0,838	0,578	0,045	0,616	0,190	0,003	0,001	0,008	0,008	0,354	0,305	0,015
P13_M	0,04	0,986	0,836	0,583	0,064	0,615	0,218	0,004	0,001	0,012	0,008	0,360	0,309	0,016
P14_M	0,06	1,037	0,838	0,572	0,054	0,632	0,194	0,003	0,001	0,023	0,008	0,365	0,315	0,016
P15_M	0,06	1,000	0,836	0,582	0,053	0,620	0,192	0,003	0,001	0,019	0,008	0,361	0,310	0,016
P16_M	0,05	1,038	0,836	0,577	0,057	0,643	0,213	0,002	0,001	0,009	0,008	0,366	0,316	0,016
P17_M	0,07	1,120	0,849	0,570	0,100	0,612	0,356	0,003	0,000	0,008	0,009	0,368	0,314	0,016
P18_M	0,05	1,078	0,850	0,610	0,024	0,006	0,033	0,002	0,000	0,000	0,007	0,379	0,317	0,017
P19_M	0,10	2,915	1,828	1,911	0,648	0,409	3,939	0,007	0,005	0,056	0,066	1,285	0,572	0,076
P20_M	0,17	3,546	2,001	2,102	0,713	0,450	4,333	0,008	0,005	0,062	0,072	1,413	0,629	0,083

Table 2. Descriptive statistics of sampled variables in Sochagota Lake (N: number of samples; Min: minimum; Max: maximum; Std.Dev. standard deviation)

Variable	N	Min.	Max.	Average	Std. Dev
pH	20	8,84	9,27	9,10	0,13
EC	20	2211,00	8651,75	2925,44	1717,38
Temp	20	16,00	20,00	18,20	1,19
TDS	20	1415,31	5493,76	1868,39	1087,10
Cl	20	194,90	846,00	261,74	171,46
SO4	20	652,87	2598,08	863,01	521,24
HCO3	20	28,37	187,27	86,62	48,09
CO3	20	0,15	1,54	0,57	0,35
NO3	13	2,67	3,38	2,81	0,21
Na	20	416,90	1719,00	554,98	358,22
Mg	20	8,31	10,42	8,75	0,45
Ca	20	7,05	28,46	23,11	4,41
K	20	52,92	207,00	69,47	42,42
NH4	20	0,00	0,17	0,04	0,037
F	20	0,57	3,55	1,18	0,72
Br	20	0,81	2,00	0,94	0,33
Li	20	0,54	2,10	0,73	0,44
Al	20	0,02	0,71	0,12	0,19
Mn	20	0,01	0,72	0,60	0,16
Fe	20	0,03	4,33	0,60	1,21
Ni	20	0,00	0,01	0,003	0,001
Cu	20	0,00	0,01	0,001	0,001
Zn	20	0,00	0,06	0,018	0,0181
As	20	0,01	0,07	0,014	0,0187
Rb	20	0,35	1,41	0,47	0,3018
Sr	20	0,31	0,63	0,35	0,0876
Cs	20	0,02	0,08	0,022	0,0195

The Shöeller-Berkalov diagram shows these high concentrations of elements like Na^+, SO_4^{2-} and Cl^-, clearly indicating the non-drinkability of this water (red crosses in Figure 5a). Moreover, this water is not even suitable for irrigation due to its extreme salinity, as SAR [24] values can indicate:

$$SAR = \frac{Na^+}{\sqrt{\frac{Ca^{2+} + Mg^{2+}}{2}}}$$

High sodium concentrations in water modifies the permeability of soil and origins infiltration complications, due to Na^+ in soils could substitute Ca^{2+} and Mg^{2+} adsorbed on the soil clays and generates dispersion of soil particles. In the Sochagota Lake, SAR values are around or bigger than 20. Samples 19 and 20 have 66 and 70, respectively, being out of the conductivity vs. SAR salinity diagram (Figure 5b).

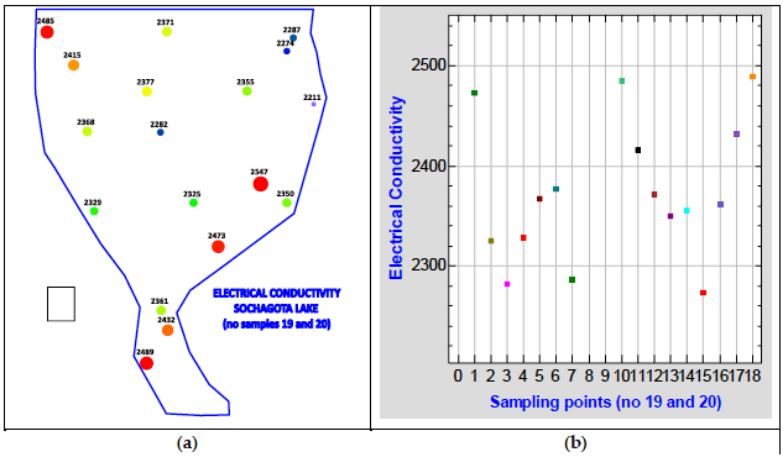

Figure 4. Values of electrical conductivity for samples 1 to 18 in the Sochagota Lake. Samples 19 and 20 have removed for better recognize the variation of the rest of samples, avoiding screen effect of these high values. (a) Map of the E.C. in the lake with scaling size and corresponding value; (b) Plot of the values of E.C. vs. samples.

Minor elements present significant values across the lake, but more remarkable in samples 19 and 20, standing out F, Mn, Fe or As. Additionally, heavy metal concentrations fluctuate relying on the water sampling position. Waters from south entrance of the lake show higher levels of heavy metals (Tables 1 and 2) following a declining order as: Fe >> Al > Mn > Zn > Cu > Ni. It is noteworthy the high contents in Fe in the lake. On the contary, lower average values of these elements in the waters from central and northern sections can be observed.

A Piper plot was carried out in order to detect hydrochemical patterns of major ion composition and water families (Figure 6). In relation to cations, there is a full concentration around the corner of Na^+K, indicating a clear sodium-potassium type water; concerning to anions, most samples are plotted in the sulfate zone with some influence of chlorides and little bicarbonates and, showing that sulfate-type water is predominant. Consequently, the principal hydrochemical family of waters is SO_4^{2-}-(Cl^-) – Na^+-(K). This is coherent with the percentage of SO_4^{2-} and Na^+ and the rest of constituents observed in the analysis.

The saline nature of the wetland and high levels of minor and metals elements could be attributed, in the first instance, to the mineralized thermomineral waters that get into the lake system through the Salitre stream entrance, as it will be shown in the next chapter of the present study [25,20; 26].

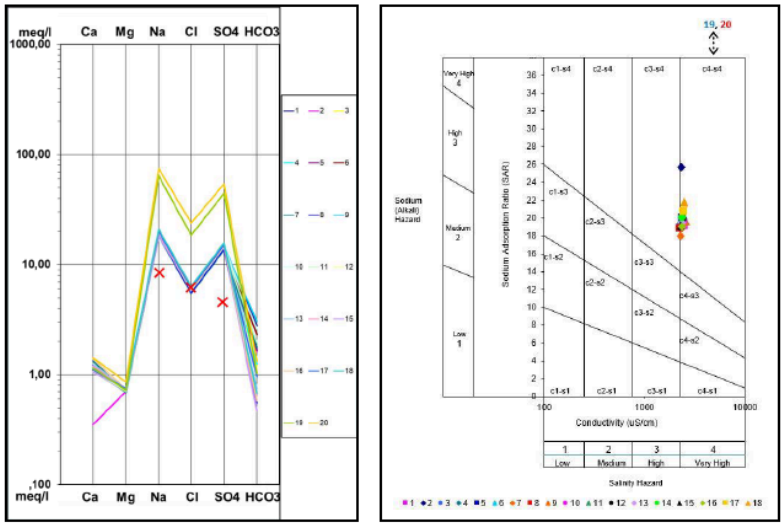

(a) (b)

Figure 5. (a) Schöeller–Berkaloff diagram highlighting the geochemical behavior of water in the Sochagota Lake. Red marks indicate health recommended values [23]. (b) Salinity Diagram for Classification of Irrigation Waters for Sochagota Lake. Samples 19 and 20 are out of the plot (19-SAR: 66; 20-SAR: 70).

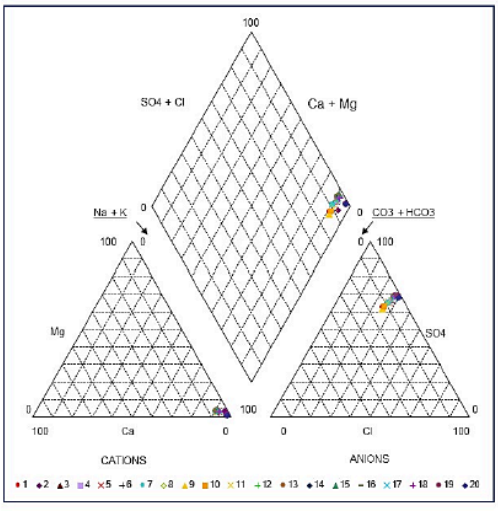

Figure 6. Piper diagram showing the hydrogeochemical facies identified for water samples of Sochagota Lake.

In the figure 7 are shown the saturation indices, SI, for anhydrite, aragonite, calcite, dolomite, fluorite, gypsum and halite in order to evaluate chemical equilibrium [27; 28]. These indices were calculated using AquaChem® 5.1 and based on the next equation:

$$SI = \log (IAP/KT)$$

IAP: ion activity product; KT: equilibrium constant at a temperature.

If SI shows positive values (SI > 0) that imply processes of mineral oversaturation and precipitation, while negative values for SI (SI < 0) indicate an unsaturated water and processes of mineral dissolution. This water is clearly oversaturated with respect to calcite, dolomite and aragonite for samples of the northern and central portion of the lake, on the contrary, in these areas the rest of minerals are unsaturated, and with a high value for halite, gypsum and anhydrite. Samples close to the Salitre River present saturation indices for all minerals < 1, indicating that waters from this part of the lake have a high potential of mineral dissolution for these minerals. These imply that, despite the high content of dissolved ions, the lake water does not favor the precipitation of these minerals, as shown the mineralogical characterization of the lake sediments [29,9,]. Furthermore, it could be considered that active biogeochemical processes have an important role in saline lakes and determine the precipitation of bacterial-induced clay mineralizations in the sediments of the Sochagota lake. Neoformed clay minerals (illite and illite-dioctahedral vermiculite mixed layers) can be found in the central and north areas of the lake, in deposits with high organic material values. [29] In these organic matter-rich sediments is frequent to find S-bearing minerals: mackinawite, pyrite, and elemental sulfur (S^o) [17].

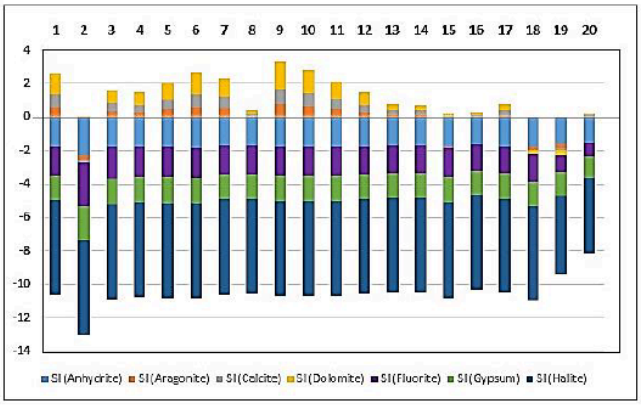

Figure 7. Saturation indices for water samples of Sochagota Lake.

3.2. Physicochemical properties of the hydrothermal waters

We aimed to characterize the impact of hydrothermal waters from the Paipa magmatic system into the Sochagota Lake. Then, a groundwater sampling campaign was carried out by Proagua in 2015. Corpoboyacá provided us a database of 16 samples, taken in different geothermal springs and they measured: i) physicochemical variables; ii) major elements, and iii) minor elements: Fe, F, B and SiO_2 (Figure 1 and Table 3). A statistical summary of these data is presented in Table 4.

Table 3. Water sampling points in Paipa geothermal area.

	Cl	SO4	HCO3	Na	Mg	Ca	K
T1. Termales Olitas	3,3	19,2	64,7	20,0	0,8	8,1	6,8
T2. El Hervidero	9,7	59,3	4,9	12,8	0,8	3,7	27,2
T3. Piscina La Playa	3050,0	9180,0	999,0	5480,0	21,0	70,0	930,0
T4. Curiosidad Caliente	100,0	60,3	360,0	130,0	4,9	59,3	13,5
T5. Curiosidad Fria	12600,0	19100,0	2598,6	14600,0	3,5	42,3	9060,0
T6. Los Delfines	6580,0	16510,0	2830,4	12460,0	8,9	83,6	1250,0
T7. Escuela Esperanza	242,0	477,0	55,6	315,0	9,9	47,3	13,7
T8. Colegio ITA	13,0	16,0	62,5	22,9	4,6	3,7	5,1
T9. Finca Entre Lomas	3,3	14,2	4,9	5,0	0,9	1,3	3,0
T10. Vereda Caños	3,3	13,3	26,8	3,1	0,6	10,7	6,9
T11. Termal Marismas	7540,0	15000,0	2976,8	12089,0	28,3	175,0	1870,0
T12. Pozo Azul	6620,0	16500,0	2635,2	11200,0	6,1	168,0	1940,0
T13. Ojo Diablo	6300,0	16400,0	2440,0	11400,0	15,9	129,0	1390,0
T14. Hotel Colsubsidio	6540,0	16600,0	2415,6	11500,0	17,6	123,0	1210,0
T15. Interior Colsubsidio	6120,0	17500,0	2403,4	11200,0	25,3	126,0	1500,0
T16. Aljive	6,0	12,5	29,5	7,2	1,6	9,2	2,2

	pH	C.E.	TDS	SiO2	Temp	Fe	F	B
T1. Termales Olitas	6,0	212,4	80,1	12,30	26,9	0,79	3,73	0,00
T2. El Hervidero	6,0	223,4	98,3	10,7	20,0	13,90	0,07	0,00
T3. Piscina La Playa	8,0	30874,8	13300,0	29,0	64,0	0,92	16,30	1,94
T4. Curiosidad Caliente	7,8	1154,6	31700,0	10,9	27,8	0,00	0,69	0,33
T5. Curiosidad Fría	7,3	90654,0	466,0	13,4	24,0	0,76	23,40	3,95
T6. Los Delfines	7,1	62099,7	28300,0	20,0	34,6	0,95	23,50	3,65
T7. Escuela Esperanza	6,4	1822,5	1010,0	3,5	21,0	2,30	0,06	0,00
T8. Colegio ITA	6,4	221,6	67,8	2,8	19,9	11,20	0,10	0,00
T9. Finca E. Lomas	6,5	84,8	44,3	2,4	19,0	19,20	0,07	0,00
T10. Vereda Caños	6,4	103,7	74,8	1,7	20,7	0,00	0,30	0,00
T11. Termal Marismas	6,4	62033,9	34500,0	13,1	22,0	9,53	6,22	4,11
T12. Pozo Azul	8,0	61073,2	26100,0	17,5	52,0	0,00	17,50	3,58
T13. Ojo Diablo	8,0	59522,0	25400,0	18,8	74,0	0,41	16,40	2,94
T14. Hotel Colsubsidio	7,0	60037,2	25800,0	17,3	52,0	0,34	16,40	3,18
T15. Interior Colsubsidio	7,3	60767,4	25500,0	16,0	44,0	0,47	16,20	2,96
T16. Aljive	6,8	108,5	53,3	1,3	17,5	0,00	0,00	0,00

Table 4. Descriptive statistics of hydrothermal water samples of Paipa.

Variable	N	Average	Std.Dev.	Min.	Max.

pH	16	7,0	0,7	6,0	8,0
EC	16	30687,1	33049,0	84,8	90654,0
Temp	16	33,7	17,9	17,5	74,0
TDS	16	13280,9	14128,8	44,3	34500,0
Cl	16	3483,2	3982,5	3,3	12600,0
SO4	16	7966,4	8384,6	12,5	19100,0
HCO3	16	1244,2	1278,1	4,9	2976,8
Na	16	5652,8	6036,1	3,1	14600,0
Mg	16	9,4	9,3	0,6	28,3
Ca	16	66,3	61,1	1,3	175,0
K	16	1201,8	2225,8	2,2	9060,0
SiO2	16	11,9	7,9	1,3	29,0
F	16	8,8	9,3	0,0	23,5
B	16	1,7	1,7	0,0	4,1
Fe	16	3,8	6,1	0,0	19,2

Two types of springs can be differentiated in Paipa region: one located in the discharge area of Pozo Azul and surroundings (samples T12-15) and sample T3 in La Playa zone, with temperatures around 40-70 ºC, more directly connected to fault systems; and a second group, mainly samples T2, 8, 9 and 11, placed in the northern sector and along the river valley, probably due to a mixing water process in relation to the alluvial aquifer and rain recharge, recognized for its low temperature and high salt content [30].

Cold waters, in general, are related with low mineralization concentrations (minor values of E.C., Cl^-, SO_4^{2-}, Na^+, K, etc.) and high values of Fe. On the other hand, samples from hot springs present very high values of electrical conductivity (Figure 8). Nevertheless, it is important to point out the high concentrations of Fe that appear in some of the samples (maximum of 19,2 mg/L in T9), indicating a process of incorporation of this element to groundwater during the evolution sequence of the thermal waters of the Paipa area.

Regarding the Piper plot (Figure 9), the hydrogeochemical facies of the geothermal waters correspond to Na^+K- SO_4^{2-}-(Cl^-) waters towards the central part of the valley of the Salitre River, while the Na^+-(Ca^{2+})- HCO_3^- waters are located towards the margins, with the exception of the Na^+-Cl^- waters for the Curiosidad Fria (T5). It is worth mentioning that El Hervidero should not be considered as a source of hot springs, but rather an emanation of steam in *steam vents*, due to the heat is related to gas release, but with little contribution of water [31]. Thus, from the genetic point of view, the classification of the waters of the Paipa geothermal system corresponds to immature waters resulting from heating with steam derived directly from magmatic sources [30]. Consequently, the main group of waters are located in the zone with a high concentration of dissolved sulfate, while a secondary group of corresponds to sulfated waters with appreciable contents of bicarbonates, which are considered as peripheral waters to the system.

Saturation indices, SI, for anhydrite, aragonite, calcite, dolomite, fluorite, goethite, gypsum, halite, hematite, pyrite and siderite (Figure 10) have been calculated in order to evaluate chemical equilibrium ([27,28]; AquaChem® 5.1). A very high pyrite dissolution capacity can be observed for these waters in most of the samples, except 2, 4, 10, 12 and 16. Siderite shows a slight negative S.I. value. On the other hand, saturation index for hematite is positive, oversaturation, but it is clear that there is not a balance between pyrite (siderite) dissolution and hematite precipitation favoring an enrichment of Fe in geothermal groundwaters, feeding the Salitre River and enabling the further entrance to the Sochagota Lake.

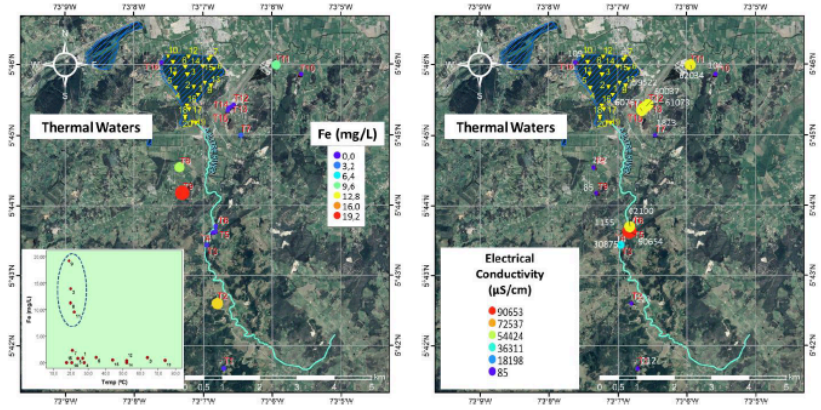

(a) (b)

Figure 8. (a) Map of Fe content in the Paipa area and the relationship of Fe concentration vs. temperature in the left corner. (b) Map of electrical conductivity in this area. In both plots, a color and size scale are used: reddish-warm colors and big dots are related to high values.

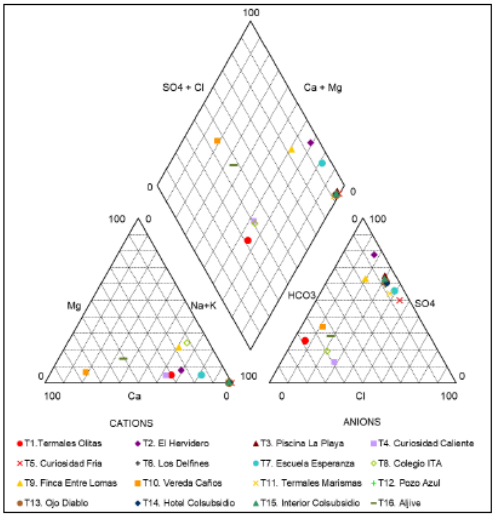

Figure 9. Piper diagram showing the hydrogeochemical facies identified for water thermal samples of Paipa.

4. Discussion

4.1. Water sources

The Sochagota Lake is recharged by the Salitre River basin waters, which are a mix of surficial and endogenous waters feeding the Salitre River (Figure 1). With the aim of the determination of the influence of different water inputs on the water of the lake, we compared available data of water composition from the geothermal groundwaters geothermal waters contribute to the chemical composition of the water of this river: (i) SO_4^{2-}-(Cl^-) Na^+-K-rich hot waters; and (ii) Fe-rich, HCO_3^- (Cl^-- SO_4^{2-}) cold waters. In Figure 11 it is possible observe the correlation between high Fe contents and the low values of temperature. [1] suggested that hydrothermal fluids associated to geothermal systems contain potential pollutant chemicals (e.g. S, Fe, As, Pb, Zn, Mn) in the liquid fraction that may occur in harmful concentrations and can cause environmental chemical pollution. Considering the water isotopic composition of the Sochagota Lake waters, 6.4‰ for $\delta^{34}S$ and 8.1 for $\delta^{18}O$, comparable to several hydrothermal liquids; see e.g. [32,33], and the lack of evaporitic rocks in the stratigraphic sequence, [17] inidcated that the high mineralzation of the water lake was produced by hydrothermal contributions of S-bearing fluids from springs feeding the Salitre River. The good correlations of SO_4^{2-} with metals in the lake waters also support an origin associated with the hydrothermal inputs that receive the Salitre River. The hydrochemistry of the cold waters can be related with water-rock interaction of an alluvial shallow aquifer made of volcanic and sedimentary particles and recharge by rain. A mixing between thermal and saline waters with cooler groundwater is produced at the the Salitre river bed causing the SO_4^{2-}- Na^+-K^+-Fe-rich waters accumulated at the south entrance of the lake. This mix of water is evidenced by samples T19 and T20, characterized by very high values of salinity, and mainly Fe.

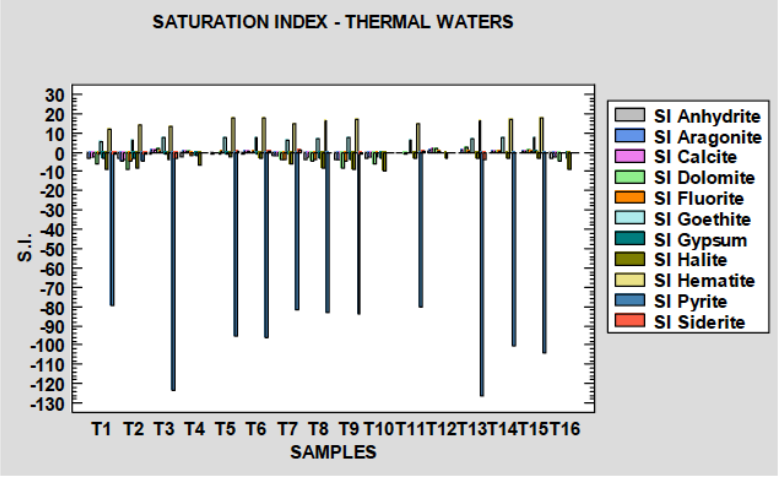

Figure 10. Saturation indices for geothermal water samples of Paipa region.

On the other hand, [34] indicated that anthropogenic inputs due to farm activities and wastewaters can pollute river basins and its impoundments in Colombia producing saline waters and organic matter-rich sediments by eutrophication. [16] proposed that these activities increased metal concentrations in the sediments of the Chicamocha River

Basin. However, the very low values for P and NO_3 and the absence of significant relationships with heavy metals caused by urban sewage and farming actions do not imply inputs associated to anthropic activity in the Sochagota Lake waters.

4.2. Chemical distribution in the lake waters: processes controlling elements concentrations

Hydrochemical analyses have exposed that two principal types of waters could be distinguished in the Sochagota Lake whose distribution could be related to several processes controlling elements concentrations: water dilution and sedimentary mineral uptake. Highly E.C. and sulfate-rich waters from the south lake entrance are characterized by higher contents in Cl^-, Li, Be, Al, K, Fe, Co, Ni, Cu, Zn, As, Rb, Cs and Pb. The concentrations of SO_4^{2-}, Cl^-, Fe and As exceed the regulatory framework for contaminants in waters (250 mg/L for SO_4^{2-} and Cl^-, 0,3 mg/L, and 0,01 mg/L, respectively) or electrical conductivity (1000 µS/cm) However, the contents of the remain heavy metals were under the limits established by Colombian regulations for human consumption and domestic use. The chemical composition of these waters suggests a strong influence of the hydrothermal and freshwater entrances into the lake through the the Salitre River. Some geothermal fluids can be considered as excessive salt content brines with that can cause direct environmental damage [1]. Ponding of these brines can be an efficient technique for fighting against water pollution. The Sochagota Lake is a pond created to preserve the water quality of the Chicamocha River), storing natural saline brines which are periodically discharged to the Chicamocha River when their salinity is reduced [15]. These waters cover organic matter-poor deposits made mostly composed of quartz and kaolinite (Figure 3a) enriched in detrital elements as Zr and Ti deriving from the adjacent sediments and low heavy metal concentrations [9], suggesting the absence of significant processes of water-sediment interaction causing mineral authigenesis or trace element incorporation from waters into the sediments.

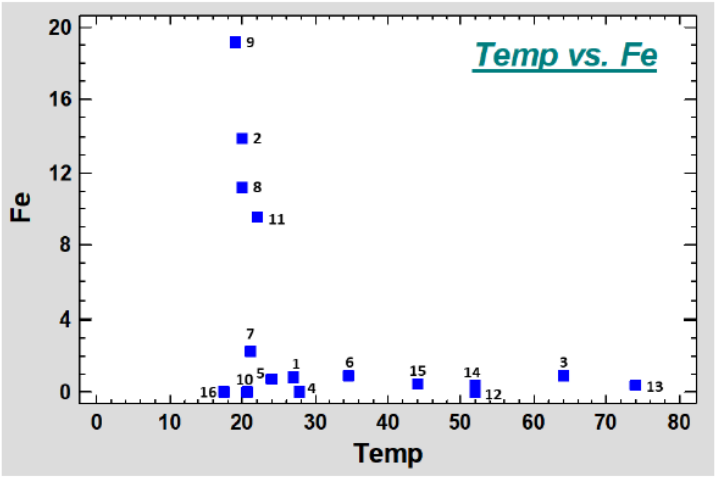

Figure 11. Relation between temperature and Fe in the geothermal water samples of Paipa region.

On the other hand, in the central and northern regions of the lake, conductivity, SO_4^{2-} and Cl^- are clearly lower than in the waters from the south entrance, although these contents slightly exceed the Colombian regulations for pollutants in waters. For the remain trace elements, a strong decrease of concentration can be observed and their contents are always below the regulatory Colombian framework. Taking into account that sediments deposited under these waters are characterized by an enrichment in organic matter. [29] indicated that these sediments are made of a fine grain sized matrix rich in illite and I-DV. The main characteristic of these deposits are the crystallization of S-bearing minerals (mackinawite, pyrite, and S°) and the enrichment in S, TOC, Fe, Zn, Mo, Rb, Co, K, Cr, Sb, Ni, As, Ba, LOI, Cu, Mn, Pb, P, Mg and Sr [17]. [9] also reported the presence of bacterial groups capable to cause reduction of sulfate (Desulfatiglans, Desulfobacterales and Sva0485) and Fe3+ (Latescibacteria), as well as the occurrence of Fe-sulfides nanoparticles coating microbial cells.

Therefore, our data propose that the water composition of the Sochagota Lake involves interactions between hydrothermal sources, freshwaters and sediments. These processes caused a sharp decrease in many element concentrations, especially for SO_4^{2-}, Fe, Cl^-, Al, As, Cu and Co (between 22 and 8-fold). Li, Rb, Na, K, Ni, Cs, Ba, Zn and Pb suffered a significant decrease (around 3-fold) while Ca, Mg and Sr were less affected (less than 1.5-fold decrease). Although fresh water from rain accumulated in the reservoir must play a key role in attenuation of the dissolved metals provided by the hydrothermal inputs, the decrease of concentration is especially important for elements involved in some the mineral processes occurring by the interaction between water, sediments and their bacterial community. Biogeochemical processes play an influence on the mobility elements. Complexation and sorption actions on sediments components such as clay minerals, organic matter, oxides, and biological fixation and transformation can be aspects that determine the water element composition. [16] indicated that in the constructed wetland of La Playa (Chicamocha River) the deposit of sediments rich in organic matter and the accumulation of saline waters generated suitable sceneries for water reduction processes, commonly related to reducing microorganism activity, that induce the production of sulfide, which can generate insoluble sulfides of divalent metals. The high contents of trace elements in the organic matter-rich sediments from the Sochagota Lake and the presence of a significant SRB community suggest that part of the decrease of SO_4^{2-}, Cl^- and trace elements in the waters of the lake was promoted by immobilization processes due to mineral reactions such as precipitation of the hydrothermal S and the accumulation of trace elements controlled by SRB in the sediments. SO_4^{2-} hydrothermal inputs of the Sochagota Lake were dropped by sedimentary processes associated with the carbonaceous matter degradation to precipitate S-bearing minerals in the sediments and caused the decrease of metals in the waters (Figure 3b). [8] showed that the process of metal sulfidation can move away the metals into low-solubility minerals. The attenuation of the concentration of K, Al and Rb could likewise be linked to mineral transformations taking place in the carbonaceous matter-rich deposits. [35] indicated that clay minerals can be rapidly transformed to illite through sequential mineral reactions in hypersaline and reducing environments. In these cases, sediments act as effective potassium sinks [36]. [15] suggested that eutrophication in a closer impoundment (La Playa dam) created an environment under reducing conditions which favored uptake of Fe into neoformed clay minerals (I-DV and Fe-smectite). [29] suggested that reducing sceneries in the carbonaceous matter-rich sediments of the Sochagota Lake favored a low-temperature illitization. At the same time, I-DV take up Fe and K via continuous dissolution-precipitation reactions. Hydrothermal K from the organic-rich pore water was fixed in the neoformed illite layers, indicating that clay minerals can be consider as sinks for K in geothermal areas.

These processes could significantly contribute to remediate the presence of some elements in the waters by natural attenuation processes. We recommend increasing the vegetation at the south entry of the lake to promote the deposit of organic matter rich sedi-

ments where these biogeochemical can take place to intensify the decrease of concentration in SO_4^{2-} and As below the Colombian regulatory framework for contaminants in waters.

5. Conclusions

The present study exposed how the effect of damming in the Sochagota Lake can be considered as an effective strategy for attenuating high salinity waters rich in SO_4^{2-}, some of them of hydrothermal origin, from the Salitre River basin. In this sense, a hydrogeochemical study of waters of the Sochagota Lake and the hydrothermal inputs conducted to the lake through the Salitre River were carried out. Concentration of major and minor elements were high in the south entrance of the lake and progressively these concentrations were attenuated significantly inside the Sochagota Lake. SO_4^{2-}, Fe, Cl^-, Al, As Cu and Co contents suffered the strongest decrease. However, SO_4^{2-} and As concentrations remained above the Colombian regulations. Li, Na, K, Ni, Cs, Ba, Zn and Pb concentration presented moderate reduction, but enough to show contents below the Colombian regulatory framework, while Ca, Mg and Sr showed a scarce variation. Dilution by rainfall runoff and precipitation of iron sulfides mediated by sulfate reducing bacteria in the organic matter rich sediments were the main processes involved in the concentration attenuation of SO_4^{2-}, Fe, As Cu and Co in the lake water. The K-consuming illitization processes occurring in the sediments could favor the decrease of K and Al.

Mineralogical, microbiological and hydrological processes might help to remediate the occurrence of different contents of harmful elements in the waters by natural attenuation procedures. In this way, a good recommendation could be to expand the vegetation at the southern entrance of the lake to stimulate the deposit of organic matter rich sediments where these biogeochemical processes can occur in order to intensify the decline the concentration in SO_4^{2-} and As, mainly, following the Colombian regulatory framework for contaminants in waters.

Author Contributions: G.R.C. and C.P.Q. managed field observations and sampling. J.J.-M., R.J.-E., G.R.C. and C.P.Q. performed water analysis procedures. G.R.C. and R.J.-E. made the hydrochemical calculations and plots All the authors deliberated the analytical results and arranged the manuscript. All authors read and approved to the published version of the manuscript.

Funding: This study has been supported by the Spanish research project PGC2018-094573-B-I00 from the MCIU-AEI-FEDER. and research group RNM-325 of the Junta de Andalucía (Spain). Our gratefulness to the Asociación Universitaria Iberoamericana de Posgrado (AUIP) and the Universidad de Boyacá. Added appreciations to Colombian Research groups Gestión Ambiental COL0005468 and Gestión de Recursos Hídricos COL0005477.

Acknowledgments: We would like to acknowledge to anonymous reviewers for their suggestions and comments that helped to improve the manuscript.

Conflicts of Interest: The authors declare no conflict of interest.

References

1. Kristmannsdóttir, H.; Ármannsson, H. Environmental aspects of geothermal energy utilization. Geothermics, **2003**, *32(4-6)*, 451-461.
2. Aiuppa, A.; Dongarra, G.; Capasso, G.; Allard, P.. Trace elements in the thermal groundwaters of Vulcano Island Sicily. J. Volcanol Geotherm. Res., **2000**, *98*, 189–207.
3. Aiuppa, A.; Federico, C.; Giudice, G.; Gurrieri, S. Chemical mapping of a fumarolic field: la Fossa crater, Vulcano Island (Aeolian Islands, Italy). Geophysical Research Letters, **2005**, *32(13)*.
4. Khadse, G.K.; Meshram, D.B.; Deshmukh, P.; Labhasetwar, P.K. Water quality of Tehri dam reservoir and contributing rivers in the Himalayan region. India. **2019**, Sustain. Water Resour. Manag. *5*, 1951–1961.
5. Aghasian, K.; Moridi, A.; Mirbagheri, A.; Abbaspour, M. Selective withdrawal optimization in a multipurpose water use reservoir. **2019**, Int. J. Environ. Sci. Technol. *10*, 5559–5568.

6. Willis, C.M.; Griggs, G.B. Reductions in fluvial sediment discharge by coastal dams in California and implications for beach sustainability. **2003**, J. Geol. *111*, 167–182.
7. Zhang, Y., Liao, J., Pei, Z., Lu, X., Xu, S., Wang, X., 2019. Effect of dam construction on nutrient deposition from a small agricultural karst catchment. Ecol. Indic. 107.
8. Niu Z.S.; Pan H.; Guo X.P; Lu D.P; Feng, J.N.; Chen, Y.R.; Tou, F.Y; Liu, M.; Yang, Y. Sulphate-reducing bacteria (SRB) in the Yangtze estuary sediments: abundance, distribution and implications for the bioavailibility of metals. **2018**, Sci. Total Environ. *634*, 296–304.
9. Cifuentes, G.R.; Jiménez-Millán, J.; Quevedo, C.P.; Gálvez; A.; Castellanos-Rozo, J.; Jiménez-Espinosa, R. Trace element fixation in sediments rich in organic matter from a saline lake in tropical latitude with hydrothermal inputs (Sochagota Lake, Colombia): The role of bacterial communities Sci. Total Environ. **2021**, *762*, 143113.
10. Chen, M.; Lu, G.; Wu, J.; Yang, C.; Niu, X.; Tao, X.; Zhenqing, S.; Xiaoyun, Y.; Dang, Z. Migration and fate of metallic elements in a waste mud impoundment and affected river downstream: a case study in Dabaoshan Mine, South China. Ecotoxicology and Environmental Safety, **2018**, *164*, 474-483.
11. Wang, W.H.; Wang, W.X. Trace metal behavior in sediments of Jiulong River Estuary and implication for benthic exchange fluxes. Environ. Pollut., **2017**, *225*, 598-609.
12. Acero, P.; Ayora, C.; Torrentó, C.; Nieto, J.M. The behavior of trace elements during schwertmannite precipitation and subsequent transformation into goethite and jarosite. Geochim. Cosmochim. Acta, **2006**, *70*, 4130-4139.
13. Schaider, L.A.; Senn, D.B.; Estes, E.R.; Brabander, D.J; Shin, J.P. Sources and fates of heavy metals in a mining-impacted stream:Temporal variability and the role of iron oxides. Sci. Total Environ. **2014**, *490*, 456-466.
14. Nordstrom, D.K. Hydrogeochemical processes governing the origin, transport and fate of major and trace elements from mine wastes and mineralized rock to surface waters. 2011, App. Geochem. 26(11), 1777-1791. https://doi.org/10.1016/j.apgeochem.2011.06.002.
15. Quevedo, C.P.; Jiménez-Millán, J.; Cifuentes, G.R.; Jiménez-Espinosa, R. Clay mineral transformations in anthropic organic matter-rich sediments. under saline water environment. Effect on the detrital mineral assemblages in the Upper Chicamocha River Basin, Colombia. Applied Clay Sci., 2020, 196, 105776.
16. Quevedo, C.P.; Jiménez-Millán, J.; Cifuentes, G.R.; Jiménez-Espinosa, R.Electron Microscopy Evidence of Zn Bioauthigenic Sulfides Formation in Polluted Organic Matter-Rich Sediments from the Chicamocha River (Boyacá-Colombia). Minerals, **2020**, *10(8)*, 673.
17. Cifuentes, G.R.; Jiménez-Millán, J.; Quevedo, C.P.; Jiménez-Espinosa, R. Transformation of S-Bearing Minerals in Organic Matter-Rich Sediments from a Saline Lake with Hydrothermal Inputs. Minerals, *2020, 10(6)*, 525.
18. Alfaro, C.; Velandia, F.; Cepeda, H. Colombian geothermal resources. Proceedings. World Geothermal Congress, Antalya, Turkey, April 24–29, 2005, pp. 1–11.
19. Pardo, N.; Cepeda, H.; Jaramillo, J.M. The Paipa volcano, eastern cordillera of Colombia, South America: volcanic stratigraphy. Earth Sci. Res. J. 2005, 9, 3–18.
20. Alfaro, C.; Velandia, F.; Cepeda, H.; Pardo, N. Preliminary Conceptual Model of the Paipa Geothermal System, Colombia Proceedings World Geothermal Congress 2010 Bali, Indonesia, 25-29 April 2010.
21. Alfaro, C. Improvement of Perception of the Geothermal Energy as a Potential Source of Electrical Energy in Colombia, Country Update Proceedings World Geothermal Congress 2015, Melbourne, Australia, 19-25 April 2015.
22. Nieto, F.; Ortega-Huertas, M.; Peacor, D.R.; Arostegui, J. Evolution of illite/smectite from early diagenesis through incipient metamorphism in sediments of the Basque-Cantabrian Basin. Clay Clay Miner. **1996**, *44*, 304–323.
23. WHO (World Health Organization). *Guidelines for drinking-water quality: fourth edition incorporating the first Addendum*. WHO Library Cataloguing-in-Publication Data, 2017. ISBN 978-92-4-154995-0
24. USSL (US Salinity Laboratory). *Diagnosis and improvement of saline and alkaline soils*. Agriculture Handbook No. 60 USDA, 1954, p 160.
25. Velandia, F. *Cartografía geológica y estructural Sector Sur del Municipio de Paipa. Informe Técnico*. 2003. INGEOMINAS. 31 p. (In Spanish).
26. Usaquén, O.L. Desarrollo de una metodología para la gestión ambiental de humedales costeros y continentales sometidos a presiones agrícolas. PhD. University of Cantabria (Spain). 2007. (In Spanish).
27. Parkhurst, D.L.; Appelo, C.A.J. User's guide to PHREEQC (Version 2): A computer program for speciation, batch-reaction, one-dimensional transport, and inverse geochemical calculations. Water-resources investigations report. **1999**, *99(4259)*, 312.
28. Drever, J.I. *The Geochemistry of Natural Waters*, 3rd edition, Prentice Hall, Upper Saddle River, New Jersey, 1997, 436 pp.
29. Cifuentes, G.R.; Jiménez-Millán, J.; Quevedo, C.P.; Nieto, F.; Cuadros, J.; Jiménez-Espinosa, R. Low Temperature Illitization through Illite-Dioctahedral Vermiculite Mixed Layers in a Tropical Saline Lake Rich in Hydrothermal Fluids (Sochagota Lake, Colombia). Minerals, 2021, 11(5), 523.
30. Alfaro, C. *Geoquímica del sistema geotérmico de Paipa*. Ingeominas, informe inédito. Bogotá, 2002, 88. (In Spanish)
31. Corpoboyacá - Corporación Autónoma Regional de Boyacá. Lineamientos para la Gestión Integral de Aguas Termales y Termominerales en el Municipio de Paipa, Departamento de Boyacá. 2006. Fundación Profesional para el Manejo Integral del Agua, 2016. (In Spanish).
32. Rye, R.O.; Bethke, P.M.; Wasserman, M.D. The stable isotope geochemistry of acid sulfate alteration. Econ. Geol. **1992**, *87*, 225–262.

33. John, D.A.; Lee, R.G.; Breit, G.N.; Dilles, J.H.; Calvert, A.T.; Muer, L.J.P.; Clynne, M.A. Pleistocene hydrothermal activity on Brokeo volcano and in the Maidu volcanic center, Lassen Peak area, northeast California: Evolution of magmatic-hydrothermal systems on stratovolcanoes. Geosphere, **2019**, *15*, 946–982.
34. Marrugo-Negrete, J.; Pinedo, J.; Díez, S. Assessment of heavy metal pollution, spatial distribution and origin in agricultural soils along the Sinú River Basin, Colombia. Environ. Res. **2017**, *154*, 380–388.
35. Andrade, G.R.P.; Cuadros, J.; Partiti, C.M.S.; Cohen, R.; Vidal-Torrado, P. Sequentialmineral transformation from kaolinite to Fe-illite in two Brazilian mangrove soils. Geoderma, **2018**, *309*, 84–99.
36. Cuadros, J.; Andrade, G.; Ferreira, T.O.; Partiti, C.S.M.; Cohen, R.; Vidal-Torrado, P. The mangrove reactor: fast clay transformation and potassium sink. Appl. Clay Sci. **2017**, *140*, 50–58.
37. Vazquez-Suñe, E. & Serrano-Juan, A. (2012) Easy Quim v5.0. Grupo de Hidrología Subterránea. https://h2ogeo.upc.edu/

Capítulo 4.

Mineralogía de arcillas de los sedimentos del lago: illitización sedimentaria promovida por fluidos hidrotermales

El contenido de este capítulo constituye el trabajo:

Low Temperature Illitization through Illite-Dioctahedral Vermiculite Mixed-Layers in a Tropical Saline Lake rich in Hydrothermal Fluids (Sochagota Lake, Colombia)

Cifuentes, G.R., Jiménez-Millán, J.,
Quevedo, C.P., Nieto F., Cuadros J.,
Jiménez-Espinosa, R.,

Este artículo ha sido publicado en Minerals. 2021
DOI:10.3390/min11050523
Recibido:15 abril 2021; Aceptado: 12 mayo 2021;
Publicado: 15 mayo 2021

minerals

MDPI

Article

Low Temperature Illitization through Illite-Dioctahedral Vermiculite Mixed Layers in a Tropical Saline Lake Rich in Hydrothermal Fluids (Sochagota Lake, Colombia)

Gabriel Ricardo Cifuentes [1], Juan Jiménez-Millán [2,*], Claudia Patricia Quevedo [1], Fernando Nieto [3], Javier Cuadros [4] and Rosario Jiménez-Espinosa [2]

[1] Faculty of Science and Engineering, Campus Tunja, University of Boyacá, Tunja 15003, Colombia; grcifuentes@uniboyaca.edu.co (G.R.C.); patriciaquevedo@uniboyaca.edu.co (C.P.Q.)
[2] Department of Geology and CEACTEMA, Campus Las Lagunillas, University of Jaén, 23071 Jaén, Spain; respino@ujaen.es
[3] Department of Mineralogy and Petrology and IACT (CSIC-UGR), Faculty of Sciences, Campus Fuentenueva, University of Granada, s/n, 18002 Granada, Spain; nieto@ugr.es
[4] Department of Earth Sciences, Natural History Museum, London SW7 5BD, UK; j.cuadros@nhm.ac.uk
* Correspondence: jmillan@ujaen.es

check for updates

Citation: Cifuentes, G.R.; Jiménez-Millán, J.; Quevedo, C.P.; Nieto, F.; Cuadros, J.; Jiménez-Espinosa, R. Low Temperature Illitization through Illite-Dioctahedral Vermiculite Mixed Layers in a Tropical Saline Lake Rich in Hydrothermal Fluids (Sochagota Lake, Colombia). *Minerals* **2021**, *11*, 523. https://doi.org/10.3390/min11050523

Academic Editors: Manuel Pozo Rodríguez and André Sampaio Mexias

Received: 15 April 2021
Accepted: 12 May 2021
Published: 15 May 2021

Publisher's Note: MDPI stays neutral with regard to jurisdictional claims in published maps and institutional affiliations.

Abstract: In this investigation, we showed that high salinity promoted by hydrothermal inputs, reducing conditions of sediments with high content in organic matter, and the occurrence of an appropriate clay mineral precursor provide a suitable framework for low-temperature illitization processes. We studied the sedimentary illitization process that occurs in carbonaceous sediments from a lake with saline waters (Sochagota Lake, Colombia) located at a tropical latitude. Water isotopic composition suggests that high salinity was produced by hydrothermal contribution. Materials accumulated in the Sochagota Lake's southern entrance are organic matter-poor sediments that contain detrital kaolinite and quartz. On the other hand, materials formed at the central segment and near the lake exit (north portion) are enriched in organic matter and characterized by the crystallization of Fe-sulfides. X-ray diffraction (XRD), field emission scanning electron microscopy (FESEM), high resolution transmission electron microscopy (HRTEM), and energy dispersive X-ray spectrometry (EDX) data allowed for the identification of illite and illite-dioctahedral vermiculite mixed layers (I-DV), which are absent in the southern sediments. High humidity and temperate climate caused the formation of small-sized metastable intermediates of I-DV particles by the weathering of the source rocks in the Sochagota Lake Basin. These particles were deposited in the low-energy lake environments (middle and north part). The interaction of these sediments enriched in organic matter with the saline waters of the lake enriched in hydrothermal K caused a reducing environment that favored Fe mobilization processes and its incorporation to I-DV mixed layers that acted as mineral precursor for fast low temperature illitization, revealing that in geothermal areas clays in lakes favor a hydrothermal K uptake.

Keywords: Sochagota Lake; hydrothermal inputs; illite–dioctahedral vermiculite mixed layers; illitization

1. Introduction

There is increasing evidence that fast clay mineral reactions can act as important element sinks in sedimentary and diagenetic processes. Thus, different clay mineral transformations have been proposed to lead to long-term sequestration of elements (such as K or Fe) in sedimentary, diagenetic, and hydrothermal settings [1,2]. Time and temperature are the most important variables that control the mineral phases formed by burial diagenesis. Extended time lapses combined with temperature increases are commonly required for the crystallization of diagenetic minerals. However, reactive clay surfaces can influence adsorption–desorption processes. The presence of high concentrations of elements able to

be included in the clay structure affects the reaction rates, promoting an increase of clay transformation speed [3]. In sedimentary and diagenetic systems, clay reactions can be influenced by elevated water salinity and oxygen-depleted conditions that favor reducing transformations (e.g., of Fe) mediated by microorganisms [4–6]. High concentration of cations and biological activity are frequently due to specific sediment composition, hydrology, and climatic conditions, such as those that can be generated in saline lakes or mangrove soils [6–9]. In these environments with hydrologically restricted conditions, clays of detrital origin interact with high salinity waters, producing phase authigenesis. Singer and Stoffers [10] revealed that K-enriched paleo-lake waters produced the diagenetic transformation of smectite into illite in two East African lakes. Deconinck et al. [11,12] also evidenced syndepositional smectite illitization in Purbeckian sediments under hypersaline conditions. Eberl et al. [13] suggested that cycles of wetting and drying cycles can be involved in the formation mechanism of illite.

The effect of high salinity waters on clays favors the modification of the octahedral layer charge (through Fe reduction and Fe-Mg for Al substitution), producing the transformation of smectite to illite [14]. Deocampo [7] suggested that the interaction of clays with K-rich waters can yield sedimentary illitization. In this paper, we study the illite formation process in the Sochagota Lake (Paipa Colombia), a saline lake located in a geothermal area [15].

In lakes from geothermal regions, the chemical evolution of the waters can be influenced by hydrothermal inputs. Metals can be included in the geothermal systems from a magmatic source and/or through dissolution of rocks processes (e.g., [16–19]). In volcanic areas, fluid–rock (basaltic or rhyolitic) reactions play an important control on the composition of the hydrothermal waters. When the rocks are predominantly rhyolitic, such as those of the Paipa volcano [20], the fluid chemical composition is mainly controlled by water–rock interaction [21], producing high concentrations of alkaline elements. A later discharge into rivers and lakes causes hydrothermally-modified waters that further react with detrital minerals, which may result in singular sediment mineralogies.

Many mineral reactions at low temperature are not controlled by thermodynamics but kinetics. Clay transformations such as the illitization process require not only sufficient reaction time or cation availability but also an appropriate mineral precursor. Smectite or illite–smectite mixed layers are the most frequently proposed clay precursors for illite formation in sedimentary basins (e.g., [22]), paleosoils (e.g., [9]), and mangrove soils (e.g., [8]). However, Dietel et al. [23] observed that the transformation to illite can also be produced through illite–dioctahedral vermiculite (I-DV) interstratification.

This investigation characterizes the mineralogical changes taking place in the clays from the Sochagota Lake sediments (Colombia). The detrital sediments are kaolinite-rich. The waters are low-temperature and saline fluids with a hydrothermal input. The climate is tropical to temperate, which allows for large organic matter accumulation in the sediments. The aim of this study is to clarify whether I-DV could act as a mineral precursor in a fast low-temperature illitization and to provide evidence of the relevant effect of clays on the hydrothermal K uptake in lakes from geothermal areas.

2. Geological Context

We studied sediments from the Sochagota Lake, which is situated in the province of Paipa at the Boyacá region (Colombia) (Figure 1). This lake has an extension of 1.7 km^2. A deepest point of 3.15 m can be observed. This lake is fed by the Salitre River from the south entrance and forms a small artificial basin by the effect of a dam constructed at the north border of the lake. The Sochagota Lake accumulates saline waters of hydrothermal origin [24]. These waters are periodically discharged through the north exit of the dam into the Chicamocha River (flowing from east to west), in which basin the Sochagota Lake is included (Figure 2) [25,26]. The climate of the area can be classified as Cfb by the Köppen system, corresponding to a climate of subtropical highland (height, 2496 m) under oceanic

conditions. The average temperature of the Sochagota Lake region is around 15 °C, and the rainfall is around 900 mm/y.

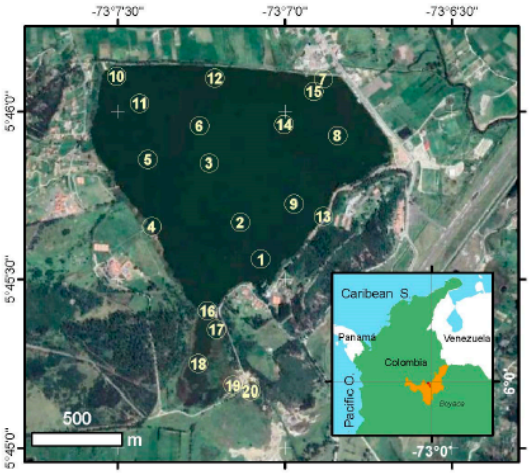

Figure 1. Location of the study region and sample positions (numbers 1 to 20) in the Sochagota Lake. The small map represents the regional context of the global area, i.e., situation of the Paipa province (Boyaca region) in Colombia. Modified from [25].

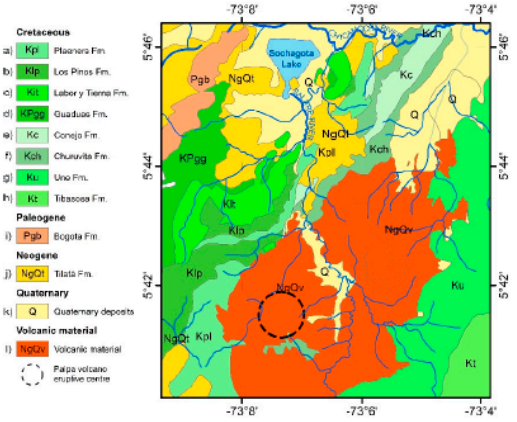

Figure 2. The Sochagota Lake Basin. Modified from [15].

From the geological perspective, the Sochagota Lake belongs to an important geothermal area that develops hydrothermal systems associated to volcanoes of the Andean Cordillera intruding cretaceous sediments rich in silicates (Figure 2). The most important outcrops as a source of sediments to the lake are rocks from the following formations:

(a) Plaeners Formation (Cretaceous), made of intensely deformed radiolarites; (b) Los Pinos Formation (Cretaceous), formed by siltstones and quartz sandstone beds; (c) Labor-Tierna Formation (Cretaceous), made of coarse to fine-grained quartz sandstones; (d) Guaduas Formation (Maastrichtian–Paleocene), with clays and siltstones that include abundant intercalations of quartz sandstones; other siliceous cretaceous formations such as (e) Conejo Formation, (f) Churuvita Formation, (g) Une Formation, and (h) Tibasosa Formation; (i) Bogotá Formation (Late Paleocene–Early Eocene), consisting of quartz sandstones, siltstones and clays; (j) Tilatá Formation (Pliocene-Pleistocene) that discordantly overlies the Cretaceous and Paleogene materials and is predominantly made of quartz-rich sandy levels with beds of siltstones and clays; (k) Quaternary deposits of sands, silts, clays, and conglomerates overlying the Tilatá Formation corresponding to the most recent alluvial, lacustrine, and fluvio-lacustrine activity also deposited in the Chicamocha River Basin, mainly made of kaolinite and quartz [25,26]. The southern part of the Sochagota Lake basin is occupied by the Pliocene–Pleistocene acid pyroclastic deposits of the Paipa volcano (1 in Figure 2) [20]. This volcanic building is characterized by the presence of a collapsed caldera that includes hydrothermal vents associated to deep faults discharging SO_4-Na-K-rich thermal waters and Fe-rich cold waters [27]. These hydrothermal saline waters mixed with rain waters flow from N to S through the Salitre River to feed the Sochagota Lake [24,27,28].

The Waters and Sediments of the Lake

Natural hydrothermal saline waters feed the Sochagota Lake at the south entrance from El Salitre River [27]. These hydrothermal waters are mixed at the lake with rain surface waters, causing waters to be rich in SO_4^{2-} (around 2150 mg/L), Na^+ (around 1500 mg/L), and K^+ (around 280 mg/L) [27,28]. The waters of the lake are alkaline (pH around 9.3) and show very high electric conductivity (around 2500 µS/cm). Cifuentes et al. [27,28] suggested that the mean values of $\delta^{34}S$ (6.4‰) and $\delta^{18}O$ (8.1‰) reveal an isotopic composition of the water analogous to other hydrothermal waters (see e.g., [29,30]). Considering these data and that evaporitic rocks are absent in the geological framework, Cifuentes et al. [27] argued that hydrothermal inputs are responsible of the S-enrichment of the waters and its high salinity.

Cifuentes et al. [28] documented an important variation in the geochemical distribution of sediments in the Sochagota Lake. Sediments near the south entrance have high contents of some elements commonly considered as detrital (Zr, Si, Al, Ti, and Na) and show low organic-matter contents (Total Organic Carbon, TOC < 0.7 wt.%). Cifuentes et al. [27,28] indicated that the deposit of this type of materials is related to the prevalence of transport conditions over the deposit of particles due to the higher hydraulic energy of the waters at this segment of the lake. The deposit of clay-rich sediments with high contents of organic matter (values of TOC around 11 wt.%) is characteristic of the deepest sections of the lake (located at the center and north parts). These sediments have Eh (redox potential) near −150 mV and high contents in S and metal transition elements. Cifuentes et al. [27,28] also showed that these materials contain Fe sulfide nanoparticles enriched in heavy metals caused by sulfate reducing bacteria (SRB) activity.

The 20 points of sediment sampling in the lake are shown Figure 1. Cores up to 0.5 m deep were collected using a standard stainless Shelby tube. Sediments from the entrance of the lake (south segment) have light colors and a sandy aspect. Samples near the lake exit (at the deepest parts located at the center and north) are dark, rich in very fine grain fractions, and have a great amount of plant remains.

3. Methods

The drying of sediments was carried out at 45 °C for 72 h. Samples were ground, and then the silt and clay fractions were separated and washed (eliminating salts) by wet sieving. After successive washing with deionized water, the <0.2 µm fraction was separated from the existing <2 µm fraction by consecutive cycles of centrifugation (10 to 15 times, at 4200 rpm for 20 min).

We obtained X-ray diffraction (XRD) diagrams from random powders and oriented the aggregates from the whole sample and from the <2 μm and <0.2 μm fractions. A dispersion on a glass slide was used to make the oriented aggregates, which were treated in several ways to identify expandable minerals. They were analyzed as air-dried, intercalated with ethylene glycol (obtained in saturated environment at 60 °C for 24 h), intercalated with glycerol (obtained in a saturated environment at 40 °C for 24 h), and heated at 300 °C during 1 h. The diffraction patterns were obtained with a PANalytical X'Pert Pro diffractometer (CuKα radiation, 45 kV, 40 mA) equipped with an automatic slit and an X'Celerator solid-state linear detector (University of Jaén, Spain). This detector continuously scans and integrates the diffracted intensity in an arc of 2.1 °2θ. The conditions used were equivalent to a 0.008 °2θ step increment and a 10 s/step counting time. Random powders as well as air-dried oriented mounts were scanned from 3 to 65 °2θ, while all other samples were scanned from 2 to 30 °2θ to identify expandable minerals.

A field emission scanning electron microscope (FESEM, Merlin Carl Zeiss, University of Jaén) was used for textural and chemical observations. Polished sections of sediments previously consolidated with a polyester resin were studied with backscattered electrons (BSE). Secondary electron (SE) mode of unconsolidated sediment fragments were also used for obtaining topographical images. Chemical analyses of minerals were obtained with an Oxford Inca energy dispersive X-ray spectrometry (EDX) system.

A high resolution transmission electron microscopy (HRTEM) study of the nanometric textural and compositional features was carried out on finely powdered samples. Selected samples (according to the XRD and FESEM results) were finely ground and dispersed in distilled water. After settling dispersion for some minutes to allow the coarser particles to settle, a drop was deposited on Au or Cu grids coated with formvar resin. We used two microscopes from the University of Granada: the HAADF FEI Titan G2 microscope, operated at 300 kV, and the Philips CM20 microscope, operated at 200 kV. Quantitative analyses of particles were acquired in scanning transmission mode (STEM) with an EDX microanalysis system. A 100-s counting time was used, excluding Na and K, for which 15 s of analysis were used to minimize alkali-loss and improve K and Na determinations [31].

4. Results

4.1. XRD Data

XRD patterns of random powders and oriented aggregates from the <2 μm and 0.2 size fractions are shown in Figure 3 (samples from the southern part of the lake) and Figure 4 (samples from the deepest parts at the center and northern part of the lake).

Quartz and kaolinite are the dominant phases in the southern sediments. The presence of kaolinite was documented by intense and sharp 7.18 Å and 3.57 Å reflections of the <2 μm and <0.2 μm fractions patterns (Figure 3b,c). These peaks do not vary after ethylene glycol treatment, indicating kaolinite–smectite mixed-layer minerals (K-S) were absent.

Random powders patterns from the central and northern sediments show a more intense peak of phyllosilicates at 4.47 Å and a broad peak of low intensity around 10.20 Å (Figure 4a). Oriented air-dried aggregates from the <2 μm fraction are characterized by a broad and asymmetric peak with an abrupt side at 10 Å (Figure 4b). Ethylene glycol treatment produces a more symmetric peak at 10 Å, and the presence of a zone of slightly higher intensities around 16.50 Å d-spacings (Figure 4b). The abrupt right edge of the 10 Å peak and the 3.33 Å peak (which interferes with the 3.34 Å reflection of quartz) in the air-dried pattern and the 10 Å symmetric peak in the ethylene glycol pattern (Figure 4b) were interpreted as due to the presence of illite in the <2 μm fraction.

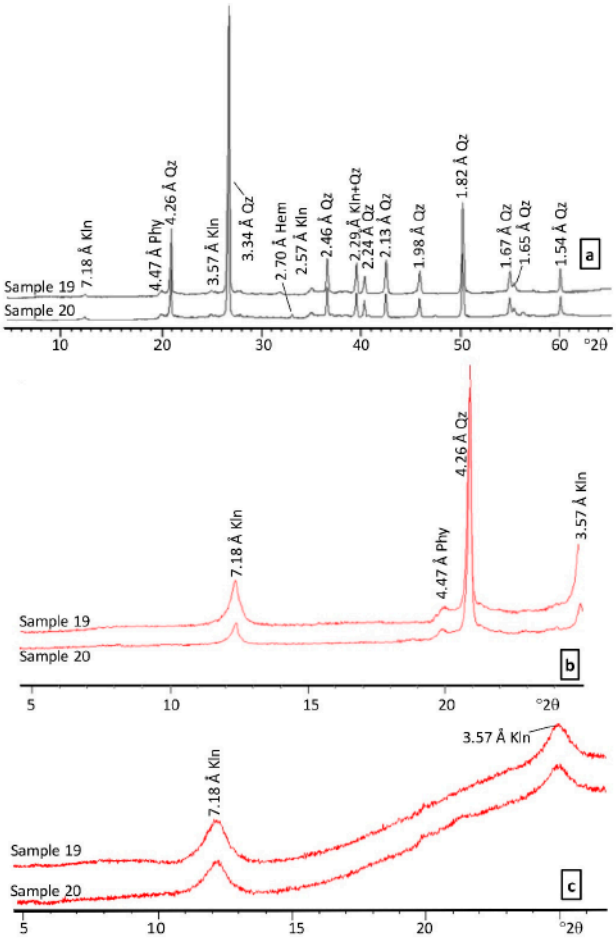

Figure 3. Representative XRD diagrams of samples from the southern entrance of the Sochagota Lake. (**a**) Whole random powders. (**b**) Air-dried oriented aggregates of the <2 µm size fraction; XRD diagrams of the ethylene glycol treated samples completely overlap the air-dried diagrams. (**c**) Air-dried oriented aggregates of the <0.2 µm size fraction; XRD diagrams of the ethylene glycol treated samples completely overlap the air-dried diagrams. Phy: phyllosilicates, Kln: kaolinite, Qz: quartz.

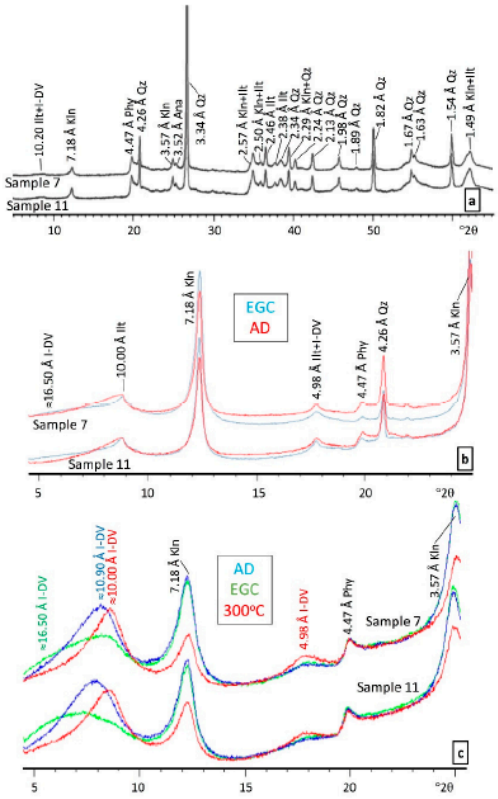

Figure 4. Representative XRD diagrams of samples from the central and northern parts of the Sochagota Lake. **(a)** Whole random powders. **(b)** Oriented aggregates of the <2 µm size fraction. **(c)** Oriented aggregates of the <0.2 µm size fraction. AD: air-dried samples. EGC: samples treated with ethylene-glycol. 300 °C: samples heated to 300 °C. Kln: kaolinite, I-DV: illite–dioctahedral vermiculite mixed layers, Ilt: illite, Qz: quartz.

To characterize the nature of the phases that form the broad peak around 16.50 Å in the ethylene glycol pattern of the <2 µm fraction, a detailed study of the <0.2 Å size fraction was carried out (Figure 4c). In this size fraction, the intensity of the kaolinite peaks decreases, and the 10 Å peak of illite was not observed in the air-dried patterns. However, a broad peak around 10.9 Å was identified, suggesting the presence of mixed layers. After ethylene glycol treatment, this peak decreases its intensity, and although part of the peak slightly changes its position toward higher d-spacings, the characteristic peak of the smectitic phases around 17 Å was not observed. The peak collapses to 10 Å after heating to 300 °C. On the other hand, the peak does not change after glycerol treatment, which ruled out a smectitic nature of the expansible component of the mixed layer. Therefore, the partial swelling character with ethylene glycol and the collapse after 300 °C of the mixed layer need to be explained by a vermiculitic component [32]. The chemical data obtained

in TEM (see below) show that this vermiculitic component is dioctahedral, and hence I-DV are present in the sediments from central and northern lake segments.

This I-DV mineral is rich in illite layers (85–90% illite layers) as indicated by the intensity and minor modifications of the peak at ≈10 Å in the ethylene glycol samples and also by the lack of a peak at ≈17 Å in the same samples. According to the relative peak intensities, the I-DV mineral phase can be up to 50% of the <0.2 um fraction.

In summary, several facts can be highlighted from the above results. Sediments highly rich in kaolinite are located in the southern part of the lake where illite is absent. In the sediments from the north part of the lake, I-DV and illite are abundant in the <2 and <0.2 µm fractions.

4.2. SEM-EDX Data

The light colored and compact sediments deposited at the south lake entrance are characterized in the scanning electron microscope images by the presence of large crystals of quartz (from 100 to 800 µm, Figure 5a) included in a phyllosilicate matrix rich in small flakes of subhexagonal kaolinite (Figure 5b). Small amounts of K and Fe in the EDX spectra of kaolinite can be associated to the adsorption of these elements from the interstitial waters of the sediments of hydrothermal origin. Sediment micropores are cemented by microcrystal aggregates of calcite (Figure 5c).

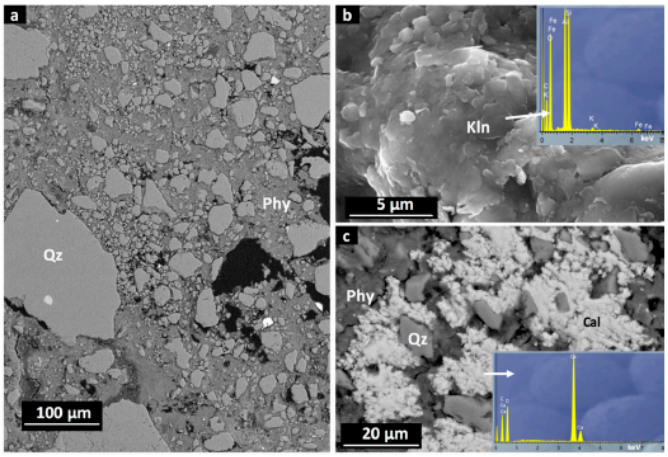

Figure 5. FESEM images of samples from the southern entrance of the lake. (**a**) BSE image of grains of quartz in a phyllosilicate matrix; (**b**) SE image of kaolinite aggregate crystals. (**c**) BSE image of calcite filling sediment micropores. Phy: phyllosilicates, Kln: kaolinite, Qz: quartz, Cal: calcite.

The clay-rich matrix is predominant in the very fine grain sized sediments from the central and northern areas (Figure 6a). The sediment matrix commonly contains long plant fragments of up to 60 µm of diameter (Figure 6a). The SEM images show that clay aggregates of massive aspect are frequent with EDX analyses, indicating the presence of K, Fe, and a higher Si/Al ratio than in kaolinite (Figure 6b). Pyrite framboids are frequently found in these areas (Figure 6a,c).

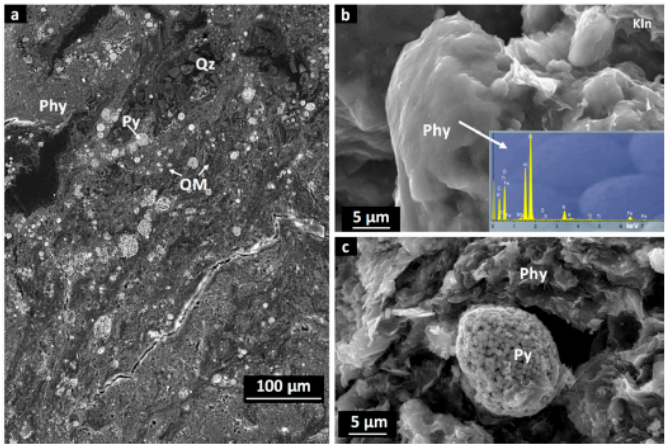

Figure 6. FESEM images of lake samples from the central and northern parts. (**a**) Elongated areas rich in organic matter (plant remains) and sulfide framboids included in a matrix rich in clay-minerals (BSE image); (**b**) SE picture showing massive clay aggregates in which EDX analyses indicate the presence of K, Fe, and a higher Si/Al ratio than in kaolinite. (**c**) SE image of a framboid of pyrite. Phy: phyllosilicates, Qz: quartz, OM: organic matter, Py: pyrite.

4.3. HRTEM-EDX Data

According to the grain morphology, the composition, and lattice fringe images, three groups of clays can be identified through the HRTEM-EDX study of the Sochagota Lake sediments. Selected compositions of these minerals are shown in Table 1.

Table 1. HRTEM-EDX chemical analyses. I-DV and illite standardized to $O_{10}(OH)_2$. Kaolinite standardized to $O_{10}(OH)_8$. $^{IV}Al = (4 - Si)$.

Sample-Analysis	Si	Al^{IV}	Al^{VI}	Fe	Mg	$\sum^{VI}$	Ca	K	Na	$\sum^{XII}$
Illite-dioctahedral vermiculite mixed layers (I-DV)										
7-1	3.50	0.50	1.75	0.12	0.10	1.97	0.04	0.60	0.01	0.65
7-2	3.35	0.65	1.80	0.15	0.05	2.00	0.04	0.62	0.00	0.66
7-3	3.40	0.60	1.72	0.16	0.12	2.00	0.03	0.64	0.02	0.69
7-4	3.43	0.57	1.79	0.13	0.05	1.97	0.05	0.60	0.01	0.66
7-5	3.38	0.62	1.73	0.16	0.13	2.02	0.04	0.58	0.03	0.65
8-1	3.48	0.52	1.78	0.11	0.10	1.99	0.03	0.58	0.01	0.62
8-2	3.36	0.64	1.72	0.16	0.14	2.02	0.05	0.61	0.01	0.67
8-3	3.47	0.53	1.75	0.15	0.08	1.98	0.05	0.56	0.01	0.62
8-4	3.37	0.63	1.70	0.18	0.14	2.02	0.05	0.60	0.01	0.66
8-5	3.42	0.58	1.74	0.12	0.15	2.01	0.04	0.60	0.02	0.66
8-6	3.39	0.61	1.73	0.15	0.12	2.00	0.03	0.63	0.03	0.69
11-1	3.36	0.64	1.71	0.15	0.14	2.00	0.05	0.61	0.01	0.67
11-2	3.36	0.64	1.89	0.12	0.05	2.06	0.03	0.62	0.02	0.67
11-3	3.46	0.54	1.77	0.15	0.09	2.01	0.05	0.56	0.01	0.62
11-4	3.44	0.56	1.81	0.12	0.05	1.98	0.04	0.61	0.02	0.67
13-1	3.37	0.63	1.71	0.17	0.13	2.01	0.04	0.58	0.03	0.65
13-2	3.49	0.51	1.79	0.12	0.10	2.01	0.02	0.59	0.02	0.63
13-3	3.41	0.49	1.73	0.12	0.13	1.98	0.04	0.61	0.01	0.66
13-4	3.38	0.62	1.71	0.18	0.12	2.01	0.05	0.60	0.01	0.66
13-5	3.49	0.51	1.76	0.12	0.11	1.99	0.04	0.60	0.01	0.65

Table 1. *Cont.*

Sample-Analysis	Si	Al ^{IV}	Al ^{VI}	Fe	Mg	$\sum^{VI}$	Ca	K	Na	$\sum^{XII}$
					Illite					
7-1	3.36	0.64	1.59	0.31	0.1	2.00	0.00	0.68	0.06	0.74
7-2	3.30	0.7	1.57	0.29	0.16	2.02	0.03	0.7	0.04	0.77
7-3	3.33	0.67	1.55	0.32	0.14	2.01	0.02	0.7	0.04	0.76
8-1	3.39	0.61	1.62	0.24	0.12	1.98	0.01	0.71	0.03	0.75
8-2	3.37	0.63	1.58	0.3	0.12	2.00	0.01	0.71	0.03	0.75
11-1	3.32	0.68	1.56	0.3	0.15	2.01	0.03	0.69	0.03	0.75
11-2	3.34	0.66	1.56	0.31	0.14	2.01	0.02	0.69	0.05	0.76
13-1	3.38	0.62	1.62	0.25	0.11	1.98	0.01	0.7	0.02	0.73
					Kaolinite					
11-1	4.03	0.00	3.87	0.09	0.00	3.96	-	-	-	-
11-2	4.00	0.00	3.94	0.05	0.00	3.99	-	-	-	-
19-1	4.01	0.00	3.91	0.07	0.00	3.98	-	-	-	-
20-1	4.02	0.00	3.92	0.08	0.00	4.00	-	-	-	-
20-2	4.01	0.00	3.93	0.07	0.00	4.00	-	-	-	-

Note: Al ^{IV}: tetrahedral Al; Al ^{VI}: octahedral Al; $\sum^{VI}$: total octahedral cations; $\sum^{XII}$: total interlayer cations.

Kaolinite pseudohexagonal crystals are predominant in the sediments from the south entrance of the lake, although irregular crystals can also be observed with quartz grains in the sediment matrix (Figure 7). However, the chemical compositions are very similar in both types of grains (Table 1). Interlayer cations (K, Ca, and Na) are almost absent. Kaolinite composition displays low values of iron in all analyzed grains (<0.1 atoms p.f.u.), and magnesium was not detected.

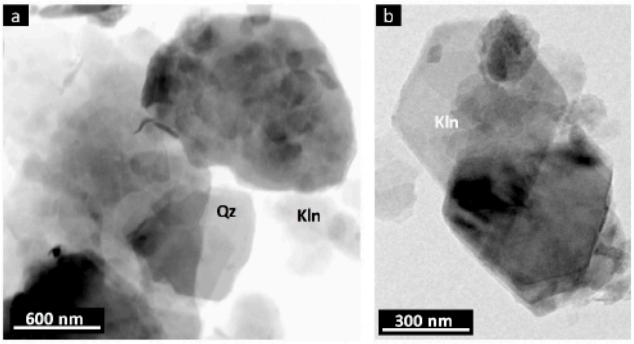

Figure 7. HRTEM pictures of sediments from the lake's southern entrance. (**a**) Low-magnification image displaying an aggregate of quartz and kaolinite. (**b**) Detail of pseudohexagonal crystals of kaolinite. Kln: kaolinite, Qz: quartz.

Lake sediments from the center and the northern part also contain kaolinite, but they are characterized by the presence of two additional groups of clays: (a) very fine grain sized clay particles with irregular shapes forming massive aggregates (Figures 8 and 9) and (b) coarser (up to 1 μm) subidiomorphic tabular to prismatic crystals (Figures 8 and 10).

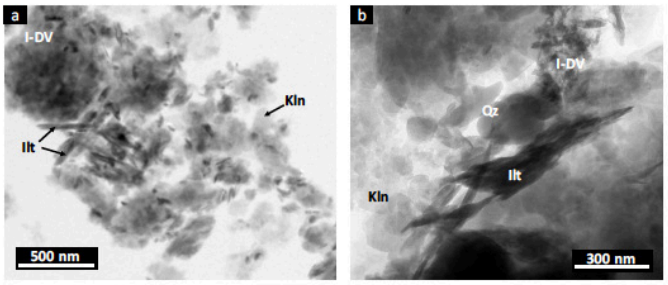

Figure 8. HRTEM pictures of sediments of the central and northern parts of the lake. (**a**) Textural image of a sediment from the central area; (**b**) Textural image of a sediment from the north area. Kln: kaolinite, Qz: quartz, I-DV: illite-dioctahedral vermiculite mixed layers, Ilt: illite.

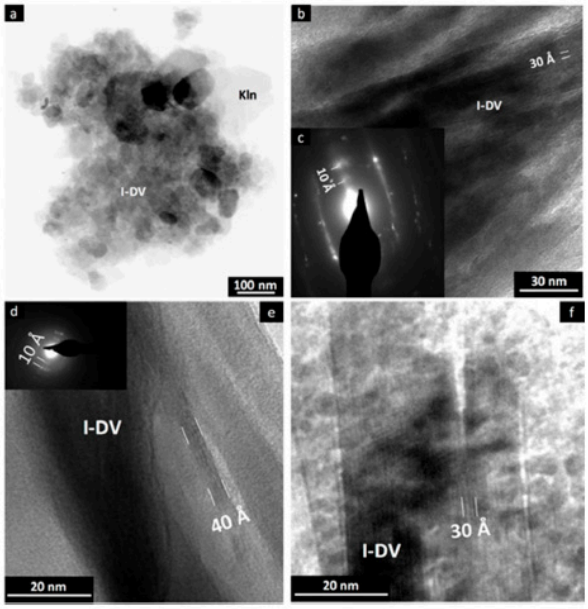

Figure 9. HRTEM pictures showing I-DV details. (**a**) Textural image of I-DV aggregates. (**b**,**e**), and (**f**) Lattice fringe images of I-DV flakes with some layers of 10 Å. (**c**,**d**) SAED patterns of I-DV flakes showing 10 Å d-spacing diffraction peaks. Kln: kaolinite, Qz: quartz, I-DV: illite–dioctahedral vermiculite mixed layers.

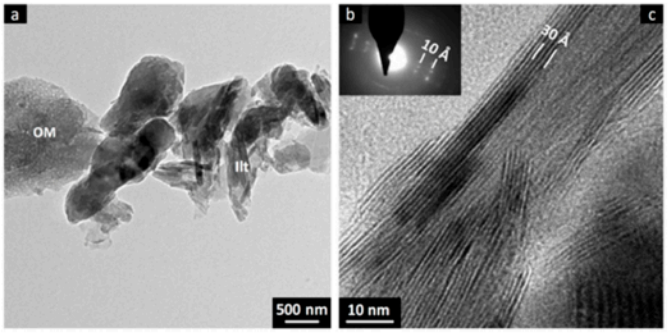

Figure 10. HRTEM images showing details of illite in samples from the central and northern parts of the lake. (**a**) Textural image of illite in clay aggregates. (**b**) SAED pattern of illite. (**c**) HRTEM image of illite showing wide areas of well-defined 10 Å lattice fringes. OM: organic matter, Ilt: illite.

The HRTEM and the selected area electron diffraction (SAED) images of the fine particles show clay flakes where narrow areas with some and discontinuous layers of 10 Å alternate with zones where lattice fringes cannot be observed (Figure 9b–d). The EDX chemical analyses of these particles revealed important contents of tetrahedral Al (>0.50 a.p.f.u.) and small amounts of octahedral Fe (less than 0.18 a.p.f.u.) and Mg (less than 0.1 a.p.f.u). The layer charge p.f.u. of these minerals oscillates between 0.69 and 0.72. K was found to be the dominant interlayer cation (0.58–0.64) in the clay composition, indicating a high proportion of illitic layers. According to the high layer charge and high K content, we relate these minerals with the illite-rich I-DV identified by XRD (Figure 4c). In spite of the presence of the vermiculitic component, this mixed layer shows an octahedral sum very near to 2 a.f.u, which suggests its dioctahedral character.

On the other hand, the SAED and HRTEM images of the tabular subidiomorphic particles (Figure 10a) show wide areas with well-defined 10 Å lattice fringes (Figure 10b,c), suggesting a higher crystallinity than that observed for the I-DV interstratifications. The EDX composition of these crystals has higher Fe (0.24–0.31 a.p.f.u.) and K (0.68–0.71 a.p.f.u.) than that of the I-DV minerals (Table 1). According to these features, we relate these particles with the illite phase identified by XRD in the oriented aggregates of the <2 μm size fraction (Figure 4b).

5. Discussion

5.1. Source Materials: Weathering and Transport

Sedimentary rocks of Cretaceous and Paleogene ages and the outcrops of acidic vulcanites are the main geological materials in the surrounding areas of the Sochagota Lake (Figure 2) [15], which develop highly weathered soils that are rich in kaolinite and quartz, as expected for soils weathered under a subtropical highland oceanic climate. Quevedo et al. [21] showed that very fine particles of I-DV minerals were formed in the materials draining the Chicamocha River Basin (which also includes the Sochagota Lake Basin) as a consequence of weathering transformations under the high humidity and moderate climate in the Tunja region of Colombia. These materials also feed the Sochagota Lake [15,28].

Yin et al. [33] indicated that the presence of weathering materials that include I-V has been described in different areas, such as in the Appalachians [34], Greenland [35], New Zealand [36], the Adirondacks [37], Virginia [38], Scotland [39], the Southern Taiga [40], and South China [41].

High humidity with chemical percolating environments favors the crystallization of clays that include vermiculite layers [42]. Under these temperate climatic conditions, the weathering of micaceous minerals can form vermiculitic mixed layers [36,38,39,43,44]. Vanderaveroet et al. [45,46] suggested that the I-V are the result of soil transformations of primary minerals in a temperate climate.

Therefore, climatic conditions in the Sochagota Lake area could produce a partial transformation of primary minerals to kaolinite and vermiculitic minerals as the main clay minerals in the source materials draining the basin, and they favored the formation of small-sized metastable intermediates of I-DV minerals, which were transported to the deposit areas of the basin.

5.2. Detrital Deposit

Kaolinite is the prevalent clay from the floodplains of the global Chicamocha River Basin and the Sochagota Lake Basin [25]. In fact, the Sochagota Lake drains to the Chicamocha River [15,25]. FESEM and HRTEM images as well as the sharp XRD peaks of the Sochagota Lake sediments clearly indicate that kaolinite is the main detrital mineral of the clay assemblage, especially in the zones of higher hydraulic energy, such as the southern part of the lake characterized by the presence of sediments enriched in coarse grain size fraction due to the prevalence of transport for the fine size fraction enriched in I-DV. We did not find mineral evidence of the reaction of the detrital kaolinite to form K-S mixed layers in the Sochagota Lake sediments. Andrade et al. [6] described this reaction in the soils of Brazilian mangrove forests and indicated the importance of the high salinity of the pore waters and the reducing conditions for this reaction to take place.

Quevedo et al. [25] documented the presence of small amounts of I-DV mixed layers in the floodplain sediments and dam deposits of the Chicamocha River Basin (where waters flow from east to west), suggesting that the small sized particles of I-DV were only deposited in the very low hydraulic energy environments of the basin, whereas sediments deposited under higher hydraulic energy conditions were characterized by the absence of I-DV and high concentrations of bigger-sized kaolinite. A similar process can explain the detrital mineral assemblage distribution in the Sochagota Lake, i.e., higher hydraulic conditions at the south entrance of the lake (Figure 2) avoiding the deposit of the fine grain sized I-DV and producing sediments enriched in kaolinite grains of larger size. When the water flow loses energy in the deepest parts of the Sochagota Lake (center and northern part), the deposit of the fine size particle fractions produces sediments enriched in I-DV.

5.3. Neoformation of Clay Minerals

An important clay assemblage change of the Chicamocha River sediments can be observed after receiving the inputs from the Sochagota Lake: illite is absent in the sediments from the eastern upper part of this Chicamocha River Basin located upstream the Sochagota Lake, while traces of illite can be found in the western downstream sediments of the Chicamocha River Basin [25] after including waters from the Sochagota Lake.

This evidence and our results on the distribution of illite and I-DV in the sediments of the Sochagota Lake indicate that the interaction of the hydrothermal waters of the lake, enriched in K an Fe (see [15,27,28]), and the organic matter-rich sediments promoted changes in the chemistry of clays from the sediments studied. In the central and northern parts of the lake, a significant enrichment of I-DV mixed-layer minerals and an Fe-bearing illite can be observed, which is absent in the southern sediments feeding the Sochagota Lake (and in the eastern floodplains of the Chicamocha River Basin before the Sochagota Lake). Illite is present in all samples of the northern and central areas of the Sochagota Lake, but it was not detected in significant amount in the sediments of the south entrance of the lake (neither in the sediments of the upper part of the Chicamocha River Basin, above the lake). Moreover, Fe content is clearly higher in illite (0.24–0.31 a.p.f.u.) than in I-DV (0.11–0.18 a.p.f.u.). The crystallization of illite is a common feature of the Sochagota Lake sediments enriched in organic matter with pyrite, mackinawite and S° [11,24]. Cifuentes et al. [11,24] have showed

that the neoformation of the S-bearing phases was produced by sedimentary processes that occurred under the saline and reduced conditions of the sediments (−150 eV), which allowed for the fixation of elements of hydrothermal origin (such as S and other trace metals, see Cifuentes et al. [24]) enriched in the lake water. These waters are also enriched in hydrothermal potassium. Cuadros et al. [2] indicated that organic matter-rich sediments (such as those of mangroves in tropical environments) can promote quick transformations of clays that favor K uptake under rapid sedimentation conditions, the percolation of saline waters, the existence of Fe easily mobilized by oxidation–reduction reactions, high activity of organisms, and the existence of precursors able to be transformed into illite. Andrade et al. [6,8] suggested that Fe–illite was formed by the reaction of detrital kaolinite through the formation of mixed-layer minerals in Brazilian mangrove sediments. High concentrations of cations in saline waters and reducing conditions in soils triggered this transformation [2,6,47]. However, in the Sochagota Lake sediments we did not find any evidence of the dissolution of kaolinite or its transformation to mixed layers, which excludes kaolinite as the clay mineral precursor to form illite.

However, the mineralogical composition of the sediments as well as the environmental conditions provided by the hydrothermal input to the waters of the lake are consistent with illitization reactions from I-DV mixed layers. I-DV can be an intermediate mineral more reactive under extremely saline conditions than the vermiculitic and smectitic end members [33]. The vermiculite to illite transformation could implicate the exchange of hydrated cations for K^+ [48–50]. Dietel et al. [23] described I-DV in very low grade metamorphic rocks from Hungary. The characterization of this reported composition suggested that such an interstratified phase could possibly act as an intermediate stage of a steady illite conversion series. Skiba et al. [51] indicated that low hydration energy cations, such as K^+ or NH_4^+, can be selectively adsorbed or fixed by vermiculite. Clays saturated with NH_4^+ produced the transformation of dioctahedral vermiculitic layers to form an illite-like phase, which is frequently found in organic matter-rich sediments and soils.

The waters of the lake are enriched in K (more than 280 mg/L) of hydrothermal origin [23,24]. Foersters et al. [52] suggested that the increase of potassium concentrations controlled by the hydrochemistry of the paleolake from the Chew Bahir basin was an important factor controlling the authigenic illitization of smectites, which was enhanced by Al-by-Mg substitution in the octahedral sheet. In the Sochagota Lake samples, the presence of a K (0.68–0.71 a.p.f.u.) and Fe (0.24–0.31 a.p.f.u.) rich phase suggests that Fe-bearing illite appears to be the end product of the illitization process. Thus, high K concentration in the waters of the lake and Fe uptake in the octahedral sheet can promote the illitization of the precursor clays (I-DV). The incorporation of Fe during illitization should be produced by the coupled substitutions of Al for Si in the tetrahedral sheet and of Mg and Fe for Al in the octahedral sheet, promoting the incorporation of K to the interlayer. An I-DV mixed-layer mineral that is progressively richer in K would be formed as an intermediate in the reaction process. Interstratified clay minerals from the Sochagota lake sediments are dominated by illite-rich phases. Andrade et al. [6] indicated that mixed-layer phases with an intermediate composition of illite layers have a fast reaction rate towards more illitic phases, which can also explain that the relatively high proportion of the illite-rich interstratification of the studied sediments.

6. Conclusions

1. Illitization takes place in the Sochagota Lake (Tunja, Colombia). The mineral precursor is detrital mixed-layer I-DV incorporated into the lake by the El Salitre River, which discharges to the south of the lake. The illitization process within the lake is supported by (a) the absence of illite in the sediments of both the El Salitre River, which feeds the lake, and of the Chicamocha River, which receives water from the lake, above the lake mouth, and (b) by the presence of illite both in the lake and in the Chichamocha River below the lake mouth.

2. TEM-EDS data revealed that neoformed illite has more Fe than I-DV, revealing that the uptaking of Fe played an important role during the illitization process.
3. The chemistry of the lake water, which is enriched in K and Fe by hydrothermal input, and the reducing conditions generated by the decay of abundant organic matter caused Fe mobilization and the incorporation of K and Fe into detrital mixed-layer I-DV. This low-temperature illitization process highlights the importance of clays in the uptake of K from hydrothermal waters in geothermal areas.

Author Contributions: C.P.Q. and G.R.C. conducted field observations and sampling. J.J.-M., R.J.-E., C.P.Q., G.R.C., F.N., and J.C. performed microscopic observations SEM and TEM (mineralogical, textural, chemical analyses) and interpreted the X-ray diffractograms and TOC. All the authors discussed the analytical results and prepared the manuscript. All authors have read and agreed to the published version of the manuscript.

Funding: This work has been financed by the Spanish research project PGC2018-094573-B-I00 from the MCIU-AEI-FEDER. and research group RNM-325 of the Junta de Andalucía (Spain). Our gratitude is also extended to Asociación Universitaria Iberoamericana de Posgrado (AUIP) and the Universidad de Boyacá. Additional thanks to Colombian Research groups Gestión Ambiental COL0005468 and Gestión de Recursos Hídricos COL0005477.

Data Availability Statement: Not applicable.

Acknowledgments: We would like to thank three anonymous reviewers for their suggestions and comments that helped to improve the manuscript.

Conflicts of Interest: The authors declare no conflict of interest. The funders had no role in the design of the study; in the collection, analyses, or interpretation of data; in the writing of the manuscript, or in the decision to publish the results.

References

1. Baldermann, A.; Warr, L.; Letofsky-Papst, I.; Mavromatis, V. Substantial iron sequestration during green-clay authigenesis in modern deep-sea sediments. *Nat. Geosci.* **2015**, *8*, 885–890. [CrossRef]
2. Cuadros, J.; Andrade, G.; Ferreira, T.O.; Partiti, C.S.M.; Cohen, R.; Vidal-Torrado, P. The mangrove reactor: Fast clay transformation and potassium sink. *Appl. Clay Sci.* **2017**, *140*, 50–58. [CrossRef]
3. Drief, A.; Martinez-Ruiz, F.; Nieto, F.; Sanchez, N. Transmission electron microscopy evidence for experimental illitization of smectite in K-enriched seawater solution at 50 degrees C and basic pH. *Clays Clay Miner.* **2002**, *50*, 746–756. [CrossRef]
4. Noël, V.; Boye, K.; Kukkadapu, R.K.; Bone, S.; Pacheco, J.S.L.; Cardarelli, E.; Janot, N.; Fendorf, S.; Williams, K.H.; Bargar, J.R. Understanding controls on redox processes in floodplain sediments of the Upper Colorado River Basin. *Sci. Total Environ.* **2017**, *603–604*, 663–675. [CrossRef]
5. Kasina, M.; Bock, S.; Wurdemann, H.; Pudlo, D.; Picard, A.; Lichtschlag, A.; Marz, C.; Wagenknecht, L.; Wehrmann, L.M.; Vogt, C.; et al. Mineralogical and geochemical analysis of Fe-phases in drill-cores from the Triassic Stuttgart Formation at Ketzin CO_2 storage site before CO_2 arrival. *Environ. Earth Sci.* **2017**, *76*, 161. [CrossRef]
6. Andrade, G.R.P.; Cuadros, J.; Partiti, C.M.S.; Cohen, R.; Vidal-Torrado, P. Sequential mineral transformation from kaolinite to Fe-illite in two Brazilian mangrove soils. *Geoderma* **2018**, *309*, 84–99. [CrossRef]
7. Deocampo, D.M.; Cuadros, J.; Wing-Dudek, T.; Olives, J.; Amouric, M. Saline lake diagenesis as revealed by coupled mineralogy and geochemistry multiple ultrafine clay phases: Pliocene Olduvai Gorge, Tanzania. *Am. J. Sci.* **2009**, *309*, 834–868. [CrossRef]
8. Andrade, G.R.P.; Azevedo, A.C.; Cuadros, J.; Furquim, S.A.C.; Souza, V.S., Jr.; Kiyohara, P.K.; Vidal-Torrado, P. Transformation of kaolinite into smectite and Fe-illite in Brazilian mangrove soils. *Soil Sci. Soc. Am. J.* **2014**, *78*, 655–672. [CrossRef]
9. Huggett, J.; Cuadros, J.; Gale, A.S.; Wray, D.; Adetunji, J. Low temperature, authigenic illite and carbonates in a mixed dolomite-clastic lagoonal and pedogenic setting, Spanish Central System, Spain. *Appl. Clay Sci.* **2016**, *132–133*, 296–312. [CrossRef]
10. Singer, A.; Stoffers, P. Clay mineral diagenesis in two East African lake sediments. *Clay Miner.* **1980**, *15*, 291–307. [CrossRef]
11. Deconinck, J.F.; Strasser, A.; Debrabant, P. Formation of illitic minerals at surface temperatures in Purbeckian sediments (Lower Berriasian, Swiss and French Jura). *Clay Miner.* **1988**, *23*, 91–103. [CrossRef]
12. Deconinck, J.F.; Gillot, P.Y.; Steinberg, M.; Strasser, A. Syn-depositional, low temperature illite formation at the Jurassic-Cretaceous boundary (Purbeckian) in the Jura Mountains (Switzerland and France): K/Ar and $\partial^{18}O$ evidence. *Bull. Soc. Geol. France* **2001**, *172*, 209–213. [CrossRef]
13. Eberl, D.D.; Srodon, J.; Northrop, H.R. Potassium fixation in smectite by wetting and drying. In *Geochemical Processes at Mineral Surfaces*; Davis, J.A., Hayes, K.F., Eds.; American Chemical Society: Washington, DC, USA, 1986; pp. 296–326.
14. Deocampo, D.M. Authigenic clays in lacustrine mudstones. In *Paying Attention to Mudstones: Priceless*; Egenhoff, S., Ed.; Geological Society of America Special Paper; Geological Society of America: Boulder, CO, USA, 2015; pp. 49–64. [CrossRef]

15. Cifuentes, G.R.; Jiménez-Millán, J.; Quevedo, C.P.; Jiménez-Espinosa, R. Transformation of S-bearing minerals in organic matter-rich sediments from a saline lake with hydrothermal inputs. *Minerals* **2020**, *10*, 525. [CrossRef]
16. Barnes, H.L. Solubilities of ore metals. In *Geochemistry of Hydrothermal Ore Deposits*, 2nd ed.; John Wiley and Sons: New York, NY, USA, 1997; pp. 404–460.
17. Seward, T.M.; Barnes, H.L. Metal transport by hydrothermal ore fluids. In *Geochemistry of Hydrothermal Ore Deposits*, 3rd ed.; John Wiley and Sons: New York, NY, USA, 1997; pp. 435–486.
18. Aiuppa, A.; Dongarra, G.; Capasso, G.; Allard, P. Trace elements in the thermal groundwaters of Vulcano Island Sicily. *J. Volcanol. Geotherm. Res.* **2000**, *98*, 189–207. [CrossRef]
19. Aiuppa, A.; Federico, C.; Allard, P.; Gurrieri, S.; Valenza, M. Trace metal modeling of groundwater-gas-rock interactions in a volcanic aquifer: Mount Vesuvius, Southern Italy. *Chem. Geol.* **2005**, *216*, 289–311. [CrossRef]
20. Pardo, N.; Cepeda, H.; Jaramillo, J.M. The Paipa volcano, Eastern Cordillera of Colombia, South America: Volcanic stratigraphy. *Earth Sci. Res. J.* **2005**, *9*, 3–18. Available online: http://www.scielo.org.co/scielo.php?script=sci_arttext&pid=S1794-61902005000100001&lng=en&nrm=iso (accessed on 14 May 2021).
21. Kaasalainen, H.; Stefánsson, A.; Giroud, N.; Arnórsson, S. The geochemistry of trace elements in geothermal fluids. Iceland. *App. Geochem.* **2015**, *62*, 207–223. [CrossRef]
22. Lanson, B.; Beaufort, D.; Berger, G.; Bauer, A.; Cassagnabere, A.; Meunier, A. Authigenic kaolin and illitic minerals during burial diagenesis of sandstones: A review. *Clay Miner.* **2002**, *37*, 1–22. [CrossRef]
23. Dietel, J.; Ufer, K.; Kaufhold, S.; Dohrmann, R. Unusual illite–dioctahedral vermiculite interstratification with Reichweite 2 in clays from northern Hungary. *Eur. J. Mineral.* **2018**, *30*, 747–757. [CrossRef]
24. Cifuentes, G.R.; Jiménez-Espinosa, R.; Quevedo, C.P.; Jiménez-Millán, J. El ciclo del azufre en sedimentos de lagos con aportes hidrotermales y antrópicos: El Lago Sochagota (Boyacá-Colombia). *Macla* **2017**, *22*, 27–28.
25. Quevedo, C.P.; Jiménez-Millán, J.; Cifuentes, G.R.; Jiménez-Espinosa, R. Clay mineral transformations in anthropic organic matter-rich sediments under saline water environment. Effect on the detrital mineral assemblages in the upper Chicamocha river basin, Colombia. *Appl. Clay Sci.* **2020**, *196*, 105576. [CrossRef]
26. Quevedo, C.P.; Jiménez-Millán, J.; Cifuentes, G.R.; Jiménez-Espinosa, R. Electron microscopy evidence of Zn bioauthigenic sulfides formation in polluted organic matter-rich sediments from the Chicamocha River (Boyacá-Colombia). *Minerals* **2020**, *10*, 673. [CrossRef]
27. Cifuentes, G.R.; Jiménez-Espinosa, R.; Quevedo, C.P.; Jiménez-Millán, J. Damming induced natural attenuation of hydrothermal waters by runoff freshwater dilution and sediment biogeochemical transformations (Sochagota Lake, Colombia). *Water* **2021**, in press.
28. Cifuentes, G.R.; Jiménez-Millán, J.; Quevedo, C.P.; Gálvez, A.; Castellanos-Rozo, A.; Jiménez-Espinosa, R. Trace element fixation in sediments rich in organic matter from a saline lake in tropical latitude with hydrothermal inputs (Sochagota Lake, Colombia): The role of bacterial communities. *Sci. Total Environ.* **2021**, *762*, 143113. [CrossRef]
29. Rye, R.O.; Bethke, P.M.; Wasserman, M.D. The stable isotope geochemistry of acid sulfate alteration. *Econ. Geol.* **1992**, *87*, 225–262. [CrossRef]
30. John, D.A.; Lee, R.G.; Breit, G.N.; Dilles, J.H.; Calvert, A.T.; Muffler, L.J.P.; Clynne, M.A. Pleistocene hydrothermal activity on Brokeoff volcano and in the Maidu volcanic center, Lassen Peak area, northeast California: Evolution of magmatic—hydrothermal systems on stratovolcanoes. *Geosphere* **2019**, *15*, 946–982. [CrossRef]
31. Nieto, F.; Ortega-Huertas, M.; Peacor, D.R.; Aróstegui, J. Evolution of illite/smectite from early diagenesis through incipient metamorphism in sediments of the Basque-Cantabrian Basin. *Clays Clay Miner.* **1996**, *44*, 304–323. [CrossRef]
32. Moore, D.M.; Reynolds, R.C.J. *X-ray Diffraction and the Identification and Analysis of Clay Minerals*; Oxford University Press: New York, NY, USA, 1997; p. 378.
33. Yin, K.; Honga, H.; Churchman, G.J.; Li, Z.; Fang, Q. Mixed-layer illite-vermiculite as a paleoclimatic indicator in the Pleistocene red soil sediments in Jiujiang, southern China. *Palaeogeogr. Palaeoclimatol. Palaeoecol.* **2018**, *510*, 140–151. [CrossRef]
34. Fagel, N.; Robert, C.; Hillaire-Marcel, C. Clay mineral signature of the NW Atlantic boundary undercurrent. *Mar. Geol.* **1996**, *130*, 19–28. [CrossRef]
35. Petersen, L.; Rasmussen, K. Mineralogical composition of the clay fraction of two fluvio-glacial sediments from East Greenland. *Clay Miner.* **1980**, *15*, 135–145. [CrossRef]
36. Churchman, G.J. Clay minerals formed from micas and chlorites in some New Zealand soils. *Clay Miner.* **1980**, *15*, 59–76. [CrossRef]
37. April, R.H.; Hluchy, M.M.; Newton, R.M. The nature of vermiculite in Adirondack soils and till. *Clays Clay Miner.* **1986**, *34*, 549–556. [CrossRef]
38. McCartan, L. *Geology and Paleontology of the Haynesville Cores Northeastern Virginia Coastal Plain*; U.S. Geological Survey: Denver, CO, USA, 1989; p. 1489.
39. Bain, D.C.; Mellor, A.; Wilson, M.J. Nature and origin of an aluminous vermiculitic weathering product in acid soils from upland catchments in Scotland. *Clay Miner.* **1990**, *25*, 467–475. [CrossRef]
40. Bonifacio, E.; Falsone, G.; Simonov, G.; Sokolova, T.; Tolpeshta, I. Pedogenic processes and clay transformations in bisequal soils of the Southern Taiga zone. *Geoderma* **2009**, *149*, 66–75. [CrossRef]

41. Yin, K.; Hong, H.; Churchman, G.J.; Li, R.; Li, Z.; Wang, C.; Han, W. Hydroxyinterlayered vermiculite genesis in Jiujiang late-Pleistocene red earth sediments and significance to climate. *Appl. Clay Sci.* **2013**, *74*, 20–27. [CrossRef]
42. Hong, H.; Churchman, G.J.; Yin, K.; Li, R.; Li, Z. Randomly interstratified illite–vermiculite from weathering of illite in red earth sediments in Xuancheng, southeastern China. *Geoderma* **2014**, *214*, 42–49. [CrossRef]
43. Berry, R.W.; Johns, W. Mineralogy of the claysize fractions of some North Atlantic Arctic Ocean bottom current. *Geol. Soc. Am. Bull.* **1966**, *77*, 183–196. [CrossRef]
44. Srodon, J. Nature of mixed-layer clays and mechanisms of their formation and alteration. *Annu. Rev. Earth Planet. Sci.* **1999**, *27*, 19–53. [CrossRef]
45. Vanderaveroet, P.; Averbuch, O.; Deconinck, J.F.; Chamley, H. A record of glacial/interglacial alternations in Pleistocene sediments off New Jersey expressed by clay mineral, grain-size and magnetic susceptibility data. *Mar. Geol.* **1999**, *159*, 79–92. [CrossRef]
46. Vanderaveroet, P.; Bout-Roumazeilles, V.; Fagel, N.; Chamley, H.; Deconinck, J.F. Significance of random illite/vermiculite mixed-layers in Pleistocene sediments of the northwestern Atlantic Ocean. *Clay Miner.* **2000**, *35*, 679–691. [CrossRef]
47. Vilhena, M.P.S.P.; Costa, M.L.; Berrêdo, J.F. Continental and marine contributions to formation of mangrove sediments in an eastern Amazonian mudplain: The case of Marapanin estuary. *J. S. Am. Earth Sci.* **2010**, *79*, 427–438. [CrossRef]
48. Barnishel, R.I.; Bertsch, P.M. Chlorites and hydroxy-interlayered vermiculite and smectite. In *Minerals in Soil Environments*, 2nd ed.; Dixon, J.B., Weed, S.B., Eds.; Soil Science Society of America: Madison, WN, USA, 1989.
49. Meunier, A. Soil hydroxy-interlayered minerals: A re-interpretation of their crystallochemical properties. *Clays Clay Miner.* **2007**, *55*, 380–388. [CrossRef]
50. Velde, B.; Meunier, A. *The Origin of Clay Minerals in Soils and Weathered Rocks*; Springer: Berlin/Heidelberg, Germany, 2008.
51. Skiba, M.; Skiba, S.; Derkowski, A.; Maj-Szeliga, K.; Dziubińsk, B. Formation of NH_4-Illite-like phase at the expense of dioctahedral vermiculite in soil and diagenetic environments—An experimental approach. *Clays Clay Miner.* **2018**, *66*, 74–85. [CrossRef]
52. Foerster, V.; Deocampo, D.; Asrat, A.; Günter, C.; Junginger, A.; Kraemer, K.H.; Stroncik, N.; Trauth, M. Towards an understanding of climate proxy formation in the Chew Bahir basin, southern Ethiopian Rift. *Palaeogeogr. Palaeoclimatol. Palaeoecol.* **2018**, *501*. [CrossRef]

Capítulo 5.

Asociación de minerales con azufre de los sedimentos: fijación y transformación del azufre de origen hidrotermal

El contenido de este capítulo constituye el trabajo:

Transformation of S-Bearing Minerals in Organic Matter-Rich Sediments from a Saline Lake with Hydrothermal Inputs

Cifuentes, G.R., Jiménez-Millán, J.,
Quevedo, C.P., Nieto F., Cuadros J.,
Jiménez-Espinosa, R.,

Este artículo ha sido publicado en Minerals. 2020
DOI: 10.3390/min10060525
Recibido:17 mayo 2020; Aceptado: 5 junio 2020;
Publicado: 9 junio 2020

minerals

MDPI

Article

Transformation of S-Bearing Minerals in Organic Matter-Rich Sediments from a Saline Lake with Hydrothermal Inputs

Gabriel Ricardo Cifuentes [1], Juan Jiménez-Millán [2,*], Claudia Patricia Quevedo [1] and Rosario Jiménez-Espinosa [2]

[1] Faculty of Science and Engineering, Water Resources Research Group, University of Boyacá, Campus Tunja 15003, Colombia; grcifuentes@uniboyaca.edu.co (G.R.C.); patriciaquevedo@uniboyaca.edu.co (C.P.Q.)

[2] Department of Geology and CEACTEMA, University of Jaén, Campus Las Lagunillas, 23071 Jaén, Spain; respino@ujaen.es

* Correspondence: jmillan@ujaen.es

Received: 17 May 2020; Accepted: 5 June 2020; Published: 9 June 2020

check for updates

Abstract: Geothermal systems can provide significant amounts of hydrothermal sulfur to surface waters, increasing salinity and avoiding some of the common anthropic uses. The objective of this study was to investigate the sedimentary neoformation of S-bearing phases in organic matter-rich sediments from a saline lake with hydrothermal inputs (Sochagota Lake, Colombia). Detrital kaolinite and quartz are the main minerals of the materials deposited in the Sochagota Lake. Neoformed clay minerals (illite and illite-dioctahedral vermiculite mixed layers) are concentrated in the central and northern part of the lake in sediments with high organic matter content. The most organic matter-rich materials are characterized by S-bearing minerals: mackinawite, pyrite, and elemental sulfur (S°). FESEM, high-resolution transmission electron microscopy (HRTEM), EDS, and Raman microspectrometry have revealed the presence of cell-shape aggregates of mackinawite nanoparticles filling the inner part of plant fragments, indicating that microorganisms were involved in the hydrothermal sulfur uptake. The alteration of mackinawite in free sulfide excess environment produced the formation of framboidal pyrite. The evolution to conditions with the presence of oxygen favored the formation of complex S° morphologies.

Keywords: Sochagota Lake; hydrothermal sulfur; sedimentary sulfur uptake; mackinawite; pyrite; elemental sulfur

1. Introduction

The presence of sulfur as an important component is widely extended in many hydrothermal systems controlling the geochemistry and distribution of most of the trace elements in geothermal systems [1,2]. In geothermal systems, the presence of alkaline hot springs is very frequently found as surface waters, representing the composition of the geothermal reservoir [3]. The boiling of the reservoir can produce fluids enriched in volatile gases such as CO_2 and H_2S, which proportion can change depending on the degree of boiling (H_2S content increases with increasing of boiling). H_2S hydrothermal fluids mix with non-thermal surface waters producing SO_4^{2-}-rich waters due to the oxidation of the hydrothermal H_2S [1,4]. Spring discharges of SO_4^{2-}-rich fluids may alter the surface waters, producing important environmental effects in downstream waters, e.g., increasing salinity and avoiding some of the anthropic uses of the waters. The presence of natural or constructed lakes that accumulate this type of waters generates hydrologically restricted environments. Under tropical conditions, strong eutrophication [5,6] favors the deposit of organic matter-rich materials where the

interaction with saline fluids and organic activity catalyze mineral reactions in the sediments [7]. Microbial redox reactions involving S compounds can control some mineral authigenic sedimentary processes in these environments [8–10]. These reactions are commonly influenced by the formation of sulfide minerals. Rickard and Luther [11] exhaustively reviewed the chemistry of iron sulfides. The Fe monosulfide resulting from the precipitation of Fe^{2+} and S^{2-} is mackinawite (see, e.g., [12]). It precipitates as unstable tetragonal particles that transform to ordered crystals. Mackinawite is transformed through different pathways, according to O_2 and H_2S concentrations, to greigite (Fe_3S_4), pyrite (FeS_2), elemental sulfur (S°), and ferric oxides and hydroxides. H_2S concentrations in sedimentary environments under low-temperature conditions are associated with the activity of the sulfate-reducing microorganisms [13]. Some studies (e.g., [14]) indicated that mackinawite and greigite are infrequently conserved in the sedimentary rocks, but its formation can be controlled by microorganisms and they possibly have a critical reactive function in the current biogeochemical cycles of Fe and S. Among sulfide minerals, pyrite is characterized by its high stability and abundance [13]. Recent research [15] has indicated the importance of the sulfur biogeochemical cycle of native sulfur (S°), which is produced by oxidation reactions (chemical or biological) of other S-bearing phases with lower oxidation state.

This study aims to investigate the sedimentary neoformation of S-bearing phases in organic matter-rich sediments from a saline lake with hydrothermal inputs. High-resolution microscopy techniques, such as field emission scanning electron microscopy (FESEM), high-resolution transmission electron microscopy (HRTEM)), coupled to high spectral resolution techniques, such as energy dispersive X-ray spectrometry (EDX) and Raman spectroscopy, were used in a fine-scale characterization to reveal the processes involved in the sedimentary uptake and transformation of the hydrothermal S.

2. Materials and Methods

2.1. Study Site

The Sochagota Lake is located in the Paipa province (Boyacá department, Colombia) (Figure 1a,b). This lake has, mainly, a recreational use. The surface area of the lake is 1.8 km^2 and the deepest point is 3.20 m. It is an artificial lake on a previous natural wetland forming a small endorheic basin in the lower course of the Salitre River (Paipa), a tributary of the Chicamocha River.

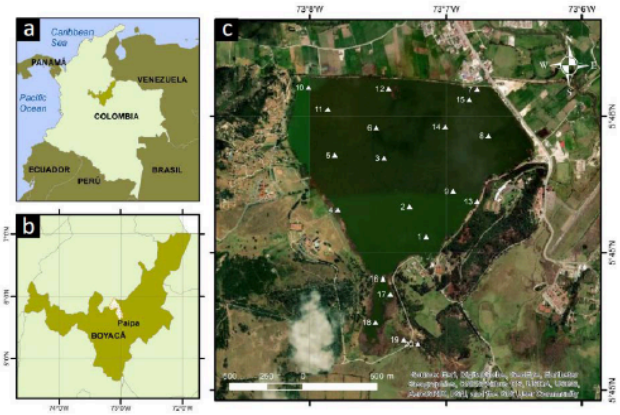

Figure 1. Geographical setting of the study area and sampling location. **(a)** Global context of the area; **(b)** Local situation in Colombia; **(c)** Location of the sampling points 1 to 20 at the Sochagota Lake.

The average annual temperature in Paipa is 14.4 °C. The average rainfall is 911 mm/year, with this precipitation well distributed throughout the year. The climate is subtropical highland (altitude, 2496 m) oceanic (classified as Cfb by the Köppen system).

From the geological perspective, the Sochagota Lake is situated in the main geothermal area of the Andean Cordillera in the Colombian territory, with hydrothermal systems located mainly around the volcanoes of the Andean Cordillera in the Colombian territory. These volcanoes predominantly intrude cretaceous siliceous sedimentary rocks (conglomerates, sandstones, shales, and claystones) (Figure 2). The presence of evaporitic rocks or other types of salt-bearing rocks has not been described in the stratigraphic column of the area. To the south of the small endorheic basin of the Sochagota Lake outcrop the materials of one of these volcanoes, the Paipa volcano [16], which is an eroded explosive volcanic building formed by acid pyroclastic deposits (alkaline rhyolites and trachyandesites) of Pliocene-Pleistocene age. This structure includes a collapsed caldera of 3 km diameter that has several hydrothermal vents. The presence of these materials may be related to the heat source of the intense geothermal system in the area as well as to the presence of S-bearing materials. A high-temperature geothermal system related to a magmatic heat source has been proposed for the area [17]. The heat upflow is controlled by deep faults and a shallow mixing process producing a highly mineralized sodium-sulfate water that hides the chemical composition of the deep reservoir fluid.

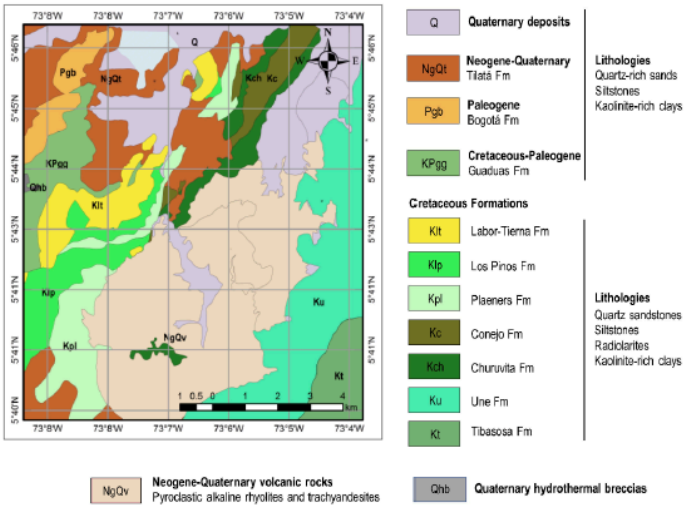

Figure 2. Geological map of the Sochagota Lake Basin. The lake does not receive sediments from the north area. Modified from Reference [16].

The Sochagota Lake stores natural hydrothermal saline waters [18] mixed with rain surface waters. Table 1 shows that lake waters have high electrical conductivity (2440 µS/cm) and pH (9.27). These waters are enriched in SO_4^{2-} (2165 mg/L), Na^+ (1493 mg/L), and K^+ (280 mg/L). The isotopic composition of the water samples is characterized by mean values of 6.4‰ for $\delta^{34}S$ and 8.1 for $\delta^{18}O$ [19]. The isotope contents (see, e.g., [20,21]) and the absence of evaporitic deposits in the geological context strongly suggest the hydrothermal origin of the S responsible for the high salinity of the lake.

Table 1. Average physical-chemical parameters of the Sochagota Lake waters from Reference [19].

Physical-Chemical Parameters and Units	Average Values
Cl^- (mg/L)	672.3
SO^{2-}_4 (mg/L)	2165.0
HCO^-_3 (mg/L)	204.2
CO^{2-}_3 (mg/L)	1.5
NO^-_3 (mg/L)	314.9
Na^+ (mg/L)	1493.1
Mg^{2+} (mg/L)	9.1
Ca^{2+} (mg/L)	55.5
K^+ (mg/L)	280.7
pH	9.27
E.C. (µS/cm)	2440.0
Temperature (°C)	22.0

E.C. Electrical conductivity.

The sediments were sampled from 20 points in a grid covering the entire area of the lake (Figure 1c). A standard stainless Shelby tube was used for sampling, and cores up to 50 cm deep were obtained. Coring polypropylene tubes with samples were capped at top and bottom with silicone rubber preserved in frozen tubes with dry ice at −80 °C, included in closed polyethylene bags that were transported to the laboratory until further processing. The extracted cores were divided into two sections: (a) 0–25 cm depth segment (samples ending with –s in Table 2) and (b) 25–50 cm segment (samples ending with –p in Table 2).

Table 2. Content in inorganic carbon (IC), total organic carbon (TOC), and total carbon from the materials deposited in the Sochagota Lake. *: 0–25 cm core segment; **: 25–50 cm core segment; ***: 0–50 cm core segment. Standard deviation is indicated in parenthesis.

Sample	IC (%)	TOC (%)	Total C (%)
1p **	0.149 (0.01)	9.15 (0.04)	9.30
1s *	0.142 (0.01)	4.11 (0.02)	4.25
2p **	0.269 (0.03)	1.01 (0.01)	1.28
2s *	0.176 (0.01)	1.17 (0.01)	1.34
3p **	0.290 (0.02)	1.88 (0.02)	2.17
3s *	0.188 (0.01)	1.74 (0.01)	1.93
4p **	0.161 (0.01)	0.996 (0.01)	1.16
4s *	0.090 (0.01)	2.01 (0.01)	2.10
5p **	0.131 (0.01)	3.04 (0.03)	3.18
5s *	0.121 (0.01)	2.51 (0.03)	2.63
6p **	0.123 (0.02)	11.1 (0.01)	11.20
6s *	0.142 (0.01)	3.59 (0.04)	3.73
M7 ***	<0.100	1.16 (0.01)	1.24
7p **	0.253 (0.01)	1.41 (0.01)	1.66
7s *	0.229 (0.01)	1.21 (0.01)	1.43
M8 ***	<0.10 (0.01)	1.25 (0.03)	1.33
8p **	0.181 (0.01)	2.12 (0.01)	2.30
8s *	0.264 (0.01)	2.26 (0.01)	2.52
M9 ***	<0.100	2.10 (0.01)	2.11
9p **	1.26 (0.03)	0.66 (0.01)	1.93
9s *	0.683 (0.02)	0.62 (0.01)	1.31
10p **	0.199 (0.01)	3.64 (0.04)	3.84
10s *	0.194 (0.01)	3.18 (0.02)	3.38
11p **	0.195 (0.01)	1.52 (0.01)	1.72
11s *	0.200 (0.01)	1.57 (0.01)	1.77
12p **	0.206 (0.01)	1.24 (0.01)	1.45
12s *	0.141 (0.01)	1.80 (0.01)	1.94

Table 2. *Cont.*

Sample	IC (%)	TOC (%)	Total C (%)
13p **	0.216 (0.01)	1.27 (0.01)	1.48
13s *	0.957 (0.01)	0.37 (0.01)	1.33
M14 ***	<0.10	0.96 (0.01)	0.96
14p **	0.218 (0.01)	3.45 (0.04)	3.67
14s *	0.149 (0.01)	2.24 (0.01)	2.38
15p **	0.218 (0.01)	1.73 (0.01)	1.94
15s *	0.188 (0.01)	1.59 (0.01)	1.78
16p **	0.408 (0.01)	0.48 (0.01)	0.89
17p **	0.156 (0.01)	0.64 (0.01)	0.80
17s *	0.309 (0.01)	0.31 (0.01)	0.62
18p **	0.212 (0.01)	4.35 (0.05)	4.56
18s *	1.180 (0.02)	0.29 (0.01)	1.48
19p **	0.257 (0.01)	1.64 (0.02)	1.89
19s *	0.137 (0.01)	1.78 (0.01)	1.89
M20 ***	<0.100	0.69 (0.01)	0.70
20p **	0.158 (0.01)	1.79 (0.02)	1.95
20s *	0.189 (0.01)	2.59 (0.03)	2.78

2.2. Methods

We prepared oriented aggregates (whole sample and <2 μm fraction) to obtain X-ray diffraction (XRD) data. Samples were previously washed with ultrapure water to remove salts [22]. Oriented aggregates were obtained by sedimentation in a glass. Centrifugation was used to separate the <2 μm fraction. Ethylene glycol and heating treatments at 400 °C and 550 °C were carried out to identify expandable clay minerals.

The diffractograms were obtained in a PANalytical X'Pert Pro diffractometer (CuKα radiation, 45 kV, 40 mA), equipped with an X'Celerator solid-state linear detector, which was used to obtain the diffraction patterns (0.008° 2θ step increment and 10 s/step of counting time) (CICT, University of Jaén, Jaén, Spain). A scan between 3° and 62° 2θ was carried on the air-dried samples, while for the treated samples, the scan was done between 2° and 30° 2θ to help with the identification of clay minerals [22].

We used polished sections to obtain back-scattered electrons (BSE) images and tridimensional sediment fragments to acquire secondary electron (SE) images in a field emission scanning electron microscope (FESEM, Merlin Carl Zeiss of the CICT of the University of Jaén, Jaén, Spain). Polished samples used for BSE images were previously impregnated under vacuum with a polyester resin [23]. BSE images were acquired at 15 kV with a working distance of 8 mm using an AsB detector, whereas SE images were acquired at 15 kV using conventional and in-lens detectors, according to Reference [24]. These images provided the information for a textural and microchemical characterization.

The nanometric characterization was carried out by high-resolution transmission electron microscopy (HRTEM) following the experimental procedure indicated by Nieto and collaborators [25] in two electron microscopes at the CIC of the University of Granada (FEI TITAN and the Philips CM20) (Granada, Spain). Au and Cu grids were used to prepare samples from alcohol or distilled water of sample particles dispersion.

A FESEM with a Raman spectrometer (CIC, University of Granada, Granada, Spain) was used for the Raman spectrometry following the experimental procedure indicated by Guerra and Cardell [26] (Zeiss Supra 40Vp FESEM with a Renishaw spectrometer In Via fitted with a Nd:YAG 532 nm laser and a near-infrared diode 785 nm laser, maximum powers of 500 mW and 100 mW, respectively, coupled to a Peltier-cooled CCD detector and single-grating monochromators, 1200 and 1800 lines mm^{-1}).

Total organic carbon (TOC) was measured after preparing five replicate samples for every core segment using high-temperature (720 °C) catalytic oxidation (Pt-alumina) on a Shimadzu TOC-V CSH Total Organic Carbon Analyzer [27] from the IRNAS at CSIC-Sevilla (Sevilla, Spain). Sediment samples were precisely weighed (2–3 mg ± 0.01 mg) on silver capsules. Analytical replication of reference

material (PACS-2) was run every 10 samples. The limit of quantification was calculated as 0.03%. Standard deviation for every core segment is indicated in Table 1.

3. Results

The materials accumulated in the Sochagota Lake are microlaminated sediments. There are important differences between the materials sampled in the south part of the lake and those from the central and north areas.

Samples from the south part are light-colored and compact. XRD analyses reveal the presence of high amounts of kaolinite, quartz, and feldspars (Figure 3a). Scanning electron microscope images show that quartz and feldspar appear as large sub-idiomorphic crystals sized from 100 to 800 µm (Figure 4a). Feldspar crystals are characterized by the presence of very altered surfaces (Figure 4b). Acid volcanic glass particles very rich in microvesicles, whose size varies between 2 and 10 µm, can also be observed.

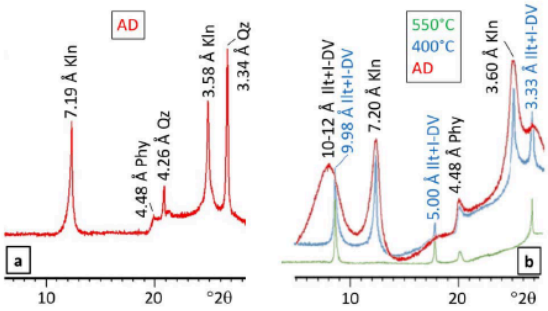

Figure 3. XRD diagrams of air-dried oriented aggregates from samples of the Sochagota Lake. (**a**) Representative sample from the south part of the lake (segment 0–25 cm depth). (**b**) Representative sample from the central and north areas (segment 25–50 cm depth). Kln: kaolinite, I-DV: illite-dioctahedral vermiculite mixed layers, Ilt: illite, Qz: quartz. Red: air-dried (AD) pattern; blue: 400 °C heated pattern; green: 550 °C heated pattern.

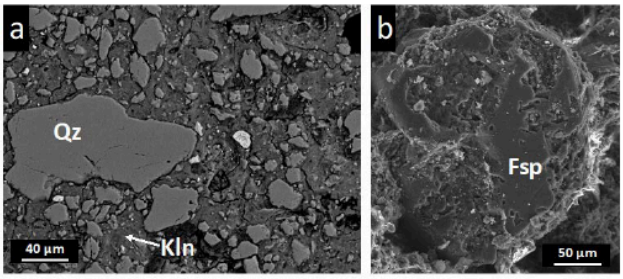

Figure 4. FESEM images of samples from the south part of the lake. (**a**) back-scattered electrons (BSE) image of crystals of quartz in a kaolinite-rich matrix (sample from segment 25–50 cm depth); (**b**) SE image of feldspar crystal with altered surface (sample from segment 0–25 cm depth). Kln: kaolinite, Qz: quartz, Fsp: feldspar.

On the other hand, sediments from the central and north areas are very fine grain sized. X-ray diffraction analysis shows that these materials are frequently enriched in clay minerals (Figure 3b), of which mineral assemblage is made of illite, illite-dioctahedral vermiculite mixed layers, and kaolinite (Figure 5a) [28]. FESEM images show that the clay-rich matrix of the sediments is often crossed by elongated plant rests, diameter of which can reach up to 50 μm (Figure 5b).

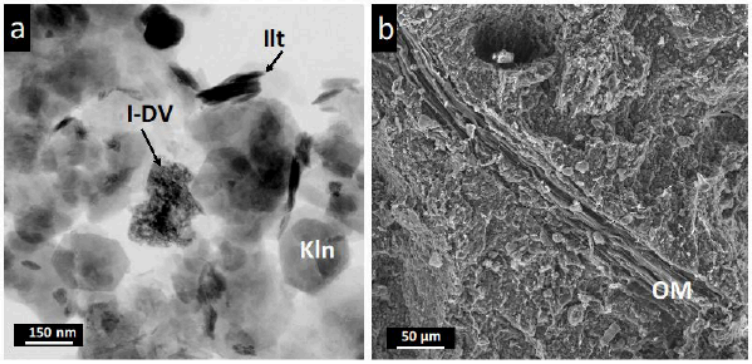

Figure 5. FESEM images of samples from the north part of the lake. (**a**) HRTEM image showing the mineral assemblage made of illite, illite-dioctahedral vermiculite mixed layers, and kaolinite (sample from segment 0–25 cm depth); (**b**) FESEM-SE image showing the clay-rich matrix of the sediments crossed by elongated plant rests (sample from segment 25–50 cm depth). Kln: kaolinite, Ilt: illite, I-DV: illite-dioctahedral vermiculite mixed layers, OM: organic matter.

Sulfur-bearing minerals are especially concentrated in materials rich in organic matter from the central and north areas. Figures 6 and 7 show FESEM and HRTEM micrographs, as well as EDX and micro-Raman spectra of sulfur-containing minerals from the Sochagota Lake sediments.

Pyrite is the most abundant S-bearing mineral in the organic matter-rich materials. Microcrystals and pyrite spherules of around 500 nm appear between the micropores of the sediment (Figure 6a). EDX microanalyses of these grains show a Fe:S ratio close to 2. The aggregation of pyrite crystals produces less than 10 μm sized framboids (Figure 6b–d). Accumulations of framboidal pyrite is especially important in areas rich in organic matter remains (Figure 6e). Near these pyrite-rich zones appear individual grains of elemental S of around 10 μm in size (Figure 6f) and S-aggregates formed by microfilaments and micro-spherules that generate a vesicular texture (Figure 6g). Raman spectra of these regions (Figure 6h) allow the identification of pyrite, with peaks at 344 and 379 cm^{-1} [29] and elemental S with peaks at 152 and 220 cm^{-1} [30]. Weak mackinawite peaks (208, 260, and 298 cm^{-1}) were also observed [31].

In contrast, other Fe^{2+} sulfides were detected in the inner part of some cores enriched in organic matter (Figure 7). EDX analyses indicates that its Fe-S atomic ratio is close to 1 for some of these minerals filling plant fragments, which corresponds to the mackinawite composition FeS (Figure 7a,b).

Detailed high magnification images of the inner part of the plant fragments revealed the presence of clusters of fine FeS nanoparticles (around 80 nm) forming aggregates, which shape and size (1–2 μm) is similar to the bacterial cell morphology (Figure 7c–e). HRTEM images also show scattered extracellular nanoparticles (Figure 7f). EDX microanalyses of nanoparticles from the HRTEM study also shows the same Fe:S ratio. Raman spectra of the FeS minerals filling plant rests confirmed the presence of mackinawite with an important peak at 298 cm^{-1}, a secondary one at 208 cm^{-1}, and a very weak peak at 260 cm^{-1} (Figure 7g) [31]. Greigite was not identified in any samples.

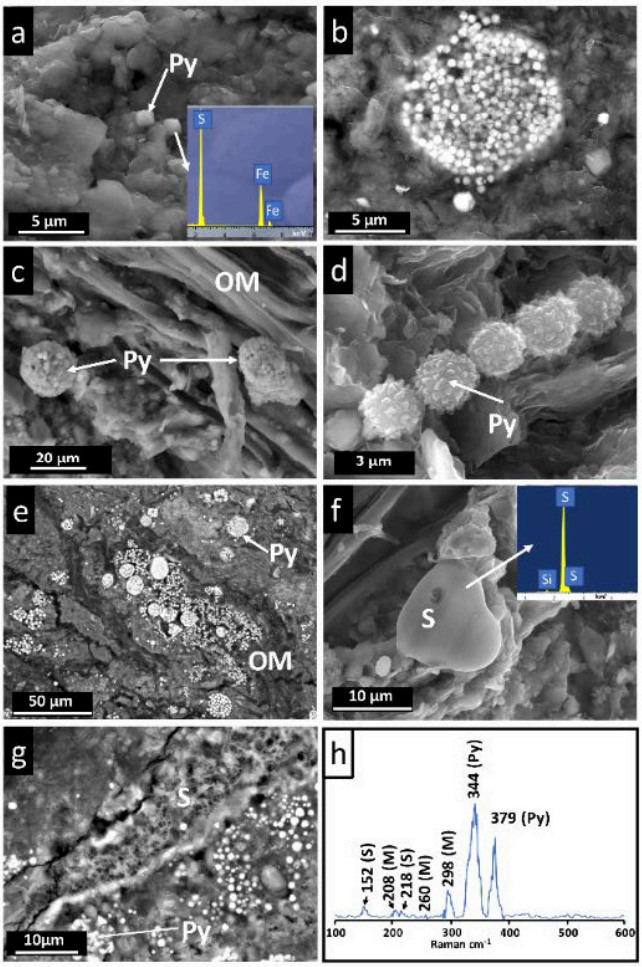

Figure 6. Electron microscope image and spectroscopy data (EDS and Raman) of pyrite and S° in the organic matter-rich materials of the lake (samples from segments 0-(samples from segments 25–50 cm depth, except for a) 25 cm depth, except for a). **(a)** SE image of microcrystals of pyrite between the micropores of the sediment; **(b)**, **(c)** and **(d)** SE images of pyrite framboids; **(e)** BSE image of an accumulation of framboidal pyrite near organic matter rests; **(f)** SE image of an individual grain of native sulfur near pyrite-rich zones; **(g)** BSE image of a S-aggregate formed by microfilaments that generate a vesicular texture; **(h)** Raman spectrum of pyrite-rich region. Py: pyrite, OM: organic matter, S: elemental sulfur, M: mackinawite.

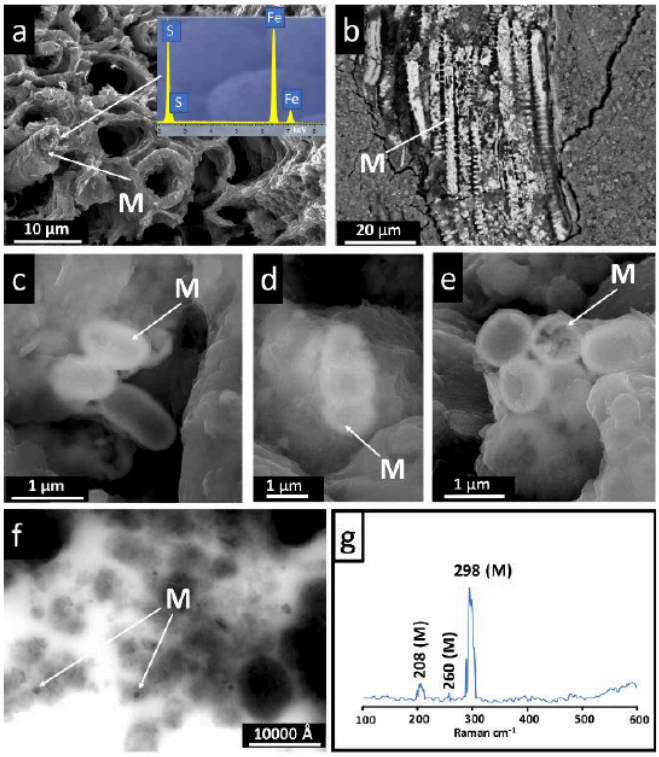

Figure 7. Electron microscope image and spectroscopy data (EDS and Raman) of mackinawite in the organic matter-rich materials of the lake (samples from segments 25–50 cm depth, except for a). (**a**) and (**b**) FeS filling plant fragments in a SE image (**a**) and in a BSE image (**b**); EDX analysis indicates that its Fe-S atomic ratio is close to 1; (**c**), (**d**) and (**e**) Detailed high magnification SE images of the inner part of the plant fragments revealing FeS nanoparticles aggregates with bacterial cell morphology; (**f**) HRTEM image showing scattered FeS nanoparticles; (**g**) Raman spectrum of the FeS minerals filling plant rests confirming the presence of mackinawite. M: mackinawite.

Regarding the organic matter content, TOC in the sediments oscillated from 0.28% to 11.1% (Table 2). The lowest concentrations were located in materials rich in kaolinite, quartz, and feldspars formed in the south part of the lake, near the El Salitre hydrothermal input, and where plant vegetation is scarce. The highest concentrations of total organic carbon were found in the materials rich in 2:1 phyllosilicates (illite-dioctahedral vermiculite mixed layers (I-DV) and illite) at the central and northern part of the lake, frequently close vegetation rich zones. These fine sized sediments have the highest contents of sulfide minerals.

4. Discussion

The relationship between detrital materials, hydrothermal input, high organic matter content, and S-containing mineral precipitation occurring in the Sochagota lake was evaluated in this study.

4.1. Detrital Minerals and Neoformed Clay Minerals

The results of this study revealed that the materials formed at the Sochagota Lake exhibited significant differences in the grain size, mineral assemblage, and organic matter content according to the distance from the entrance of the hydrothermal inputs (El Salitre). From the entrance to the inner portion and the northern border of the lake, the amount of fine particles of clay minerals (illite and mixed-layer clay mineral) increases. The formation of illite and I-DV was occurred during the strong interaction of the sediments with the saline water-pore under the reduced conditions provided by the high content in organic matter [32]. Similar illitization processes in other saline and organic matter-rich environments, such as those occurring in mangroves, have been described [7]. On the other hand, the higher hydrodynamic conditions of the lake entrance and the low organic matter content of these materials avoided the formation and accumulation of the fine clay mineral particles in the southern area of the Sochagota Lake [32].

4.2. Hydrothermal Inputs and Reduced Microenvironments Favored by Organic Matter

Isotopic composition of the waters from the Sochagota Lake (mean values of 6.4‰ for $\delta^{34}S$ and 8.1 for $\delta^{18}O$) is inside the reference fields indicated in several studies [20,21] for active hydrothermal systems. These data and the absence of evaporitic deposit or any other type of sulfate-bearing rocks in the geological context [16] clearly indicate that sulfur dissolved in the water and precipitated in the materials of the lake is of hydrothermal origin.

S-bearing minerals are concentrated at the organic matter-rich materials from the deeper central and northern part of the lake. Organic matter-rich layers are able to maintain oxygen depleted conditions due to the capability of decaying organic matter to provide electrons for reactions of reduction. In saline environments, such as that of the Sochagota Lake, following the availability of easily degradable organic matter, microorganisms most likely can create microenvironments with reduced Fe and aqueous sulfides in which some processes lead to the precipitation of insoluble sulfides (see, e.g., [33]).

4.3. The S Cycle in the Materials of the Sochagota Lake

Figures 4–7 suggest that the presence of S-bearing minerals is not associated to the sediment depth. The main factor controlling the formation of these minerals was the amount of organic matter, which is heterogeneously distributed among both depths (Table 2). Pyrite is the more extended S-bearing mineral from these organic matter-rich materials. This indicates that the uptake of Fe is associated with the existence of S-bearing phases in the materials with finest particles and close to vegetation-rich areas, suggesting the association of a pyritization process to the organic matter abundance. Crystallization of individual pyrite crystals and framboidal aggregates associated with organic matter have been extensively described in anoxic sediments (e.g., [34,35]). For example, nanobacterial cells are frequently found coating pyrite microcrystals associated with decaying organic matter [35]. Pyrite framboids can be formed within templates provided by organic carbon matrix [36]. Experimental studies and field observations suggest that pyrite framboids formation is promoted by the nucleation and growth of iron monosulfides, which are later converted to pyrite (e.g., [37–39]). According to Hu and collaborators, most of the organic matter-rich materials are thought to undergo three processes that contribute to the crystallization of pyrite in framboids [40]: (a) formation and development of precursors (FeS); (b) transformation of FeS to FeS_2; and (c) pyrite growth.

In the materials investigated in this study, high spatial and spectral resolution spectromicroscopy techniques allow to identify textural traces of microorganisms' activity associated with the first stage

of the framboidal sulfides formation. High-resolution electron microscopy studies are one of the best tools to determine the presence of sulfide nanoparticles, its volume, morphology, composition, and disposition in organic matter-rich environment, allowing to elucidate the importance of the factors controlling its formation, such as the microbial-mineral interactions or the changes in aqueous and sediment chemistry (see, e.g., [14,41,42]). Figure 7c–e shows the remarkable morphological and dimensional features of spherical and oval-shaped FeS nanoparticle aggregates in the organic matter-rich sediments of the Sochagota Lake materials, suggesting bacterially induced precipitation of FeS. Raman microspectrometry confirmed the accumulation of these mackinawite particles at the inner part of plant fragments.

Therefore, the FESEM, HRTEM, and Raman microspectrometry data from this study reveal that sulfate-reducing bacteria cells facilitated decisively the uptake of Fe particles from the Sochagota Lake materials through the formation of mackinawite FeS nanoparticles. The experimental study of Picard and collaborators [14] has confirmed the ability of microbial cells to uptake metals (Fe) that concentrate in crusts on the surface of microorganisms as sulfide minerals, suggesting that the cell membrane of sulfate-reducing microorganisms and their extracellular materials can act as templates for the formation and growth of sulfide minerals. Kraal and collaborators [12] suggested that rapid burial under anoxic conditions prevent dissolution of FeS in organic-rich reducing sediments.

Pyrite and S° were likely produced by the alteration of mackinawite produced by a free sulfide excess that generate iron monosulfide dissolution and a later pyrite recrystallization [11,43]. The conversion of monosulfides to pyrite can also be influenced by sulfate-reducing bacteria activity, supplying H_2S, or organic sulfur able to accept electrons, which facilitate the formation of FeS_2 [44–46].

The transformation of sulfide to S° by inorganic oxidation reaction is very slowly produced, which suggest that oxidation by microorganisms is the prevalent process for S° crystallization in low-temperature environments [47]. However, Cosmidis and Templeton [48] discovered that H_2S can interact with organic matter under an oxygenated environment to form inorganic S°, producing filamentous and complex morphologies similar to those observed in the Lago Sochagota materials.

5. Conclusions

We have investigated the sedimentary neoformation of S-bearing phases in organic matter-rich sediments from the Sochagota Lake (Colombia), a saline lake in tropical latitude with hydrothermal inputs. The sedimentary processes occurring under saline and reduced conditions carried out the fixation of the hydrothermal sulfur enriched in the water lake.

Most of the materials deposited in the Sochagota Lake are made of detrital quartz and kaolinite. Sediments from the central and northern part of the lake are enriched in neoformed clay minerals (illite and I-DV) by saline transformations due to the interaction with the waters of the lake and high content in organic matter. The isotopic composition of these waters suggest that the sulfur dissolved in these waters is of hydrothermal origin. The hydrothermal input was responsible for the salinity of the waters.

The cycle of sulfur in the lake is related to a pyritization process associated with the abundance of organic matter. The first step of the process was evidenced by FESEM, HRTEM, EDS, and Raman microspectrometry, which revealed the presence of mackinawite particles (sometimes forming cell-shape aggregates) at the inner part of plant fragments of some organic matter-rich cores. The crystallization of mackinawite strongly support that hydrothermal SO_4^{2-} dissolved in the waters of the Sochagota Lake underwent sulfate reduction processes associated with the decay of the organic matter to form S-bearing minerals in the sediments. Microorganisms favored the formation and growth of mackinawite and its transformation to pyrite and S°. Pyrite was formed by mackinawite alteration in an environment with excess of free sulfide. Filamentous and complex morphologies of S° were formed inorganically by H_2S and organic matter reaction in an oxygen-richer environment.

Author Contributions: C.P.Q. and G.R.C. conducted field observations and sampling. J.J.-M., R.J.-E., C.P.Q., and G.R.C. performed microscopic observations SEM and TEM (mineralogical, textural, chemical analyses, and Raman spectrometry) and interpreted the X-ray diffractograms and TOC. All authors discussed the analytical results and prepared the manuscript. All authors have read and agreed to the published version of the manuscript.

Funding: This work has been financed by the Spanish research project PGC2018-094573-B-I00 from the MCIU-AEI-FEDER and research group RNM-325 of the Junta de Andalucía (Spain). Our gratitude is also extended to Asociación Universitaria Iberoamericana de Posgrado (AUIP) and the Universidad de Boyacá. We would also like to thank Colombian Research groups Gestión Ambiental COL0005468 and Gestión de Recursos Hídricos COL0005477.

Acknowledgments: We would like to acknowledge to two anonymous reviewers for their suggestions and comments that helped to improve the manuscript.

Conflicts of Interest: The authors declare no conflict of interest. The funders had no role in the design of the study; in the collection, analyses, or interpretation of data; in the writing of the manuscript; or in the decision to publish the results.

References

1. Kaasalainen, H.; Stefánsson, A. Sulfur speciation in natural hydrothermal waters, Iceland. *Geochim. Cosmochim. Acta* **2011**, *75*, 2777–2791. [CrossRef]
2. Kaasalainen, H.; Stefánsson, A.; Giroud, N.; Arnórsson, S. The geochemistry of trace elements in geothermal fluids, Iceland. *App. Geochem.* **2015**, *62*, 207–223. [CrossRef]
3. Björke, J.K.; Stefánsson, A.; Arnórsson, S. Surface water chemistry at Torfajökull, Iceland—Quantification of boiling, mixing, oxidation and water-rock interaction and reconstruction of reservoir fluid composition. *Geothermics* **2015**, *58*, 75–86. [CrossRef]
4. Nordstrom, D.K.; McCleskey, R.B.; Ball, J.W. Sulfur geochemistry of hydrothermal waters in Yellowstone National Park: IV Acid-sulfate waters. *App. Geochem.* **2009**, *24*, 191–207. [CrossRef]
5. Aghasian, K.; Moridi, A.; Mirbagheri, A.; Abbaspour, M. Selective withdrawal optimization in a multipurpose water use reservoir. *Int. J. Environ. Sci. Technol.* **2019**, *16*, 5559–5568. [CrossRef]
6. Zhang, Y.; Liao, J.; Pei, Z.; Lu, X.; Xu, S.; Wang, X. Effect of dam construction on nutrient deposition from a small agricultural karst catchment. *Ecol. Indic.* **2019**, *107*. [CrossRef]
7. Cuadros, J.; Andrade, G.; Ferreira, T.O.; Partiti, C.S.M.; Cohen, R.; Vidal-Torrado, P. The mangrove reactor: Fast clay transformation and potassium sink. *Appl. Clay Sci.* **2017**, *140*, 50–58. [CrossRef]
8. Ferreira, T.O.; Vidal-Torrado, P.; Otero, X.L.; Macías, F. Are mangrove forest substrates sediments or soils? A case study in southeastern Brazil. *Catena* **2007**, *70*, 79–91. [CrossRef]
9. Noël, V.; Boye, K.; Kukkadapu, R.K.; Bone, S.; Pacheco, J.S.L.; Cardarelli, E.; Janot, N.; Fendorf, S.; Williams, K.H.; Bargar, J.R. Understanding controls on redox processes in floodplain sediments of the Upper Colorado River Basin. *Sci. Total Environ.* **2017**, *603–604*, 663–675. [CrossRef]
10. Andrade, G.R.P.; Cuadros, J.; Partiti, C.M.S.; Cohen, R.; Vidal-Torrado, P. Sequential mineral transformation from kaolinite to Fe-illite in two Brazilian mangrove soils. *Geoderma* **2018**, *309*, 84–99. [CrossRef]
11. Rickard, D.; Luther, G.W. Chemistry of Iron Sulfides. *Chem. Rev.* **2007**, *107*, 514–562. [CrossRef]
12. Kraal, P.; Burton, E.D.; Bush, R.T. Iron monosulfide accumulation and pyrite formation in eutrophic estuarine sediments. *Geochim. Cosmochim. Acta* **2013**, *122*, 75–88. [CrossRef]
13. Rickard, D.T. Microbial sulfate reduction in sediments. In *Developments in Sedimentology: Sulfidic Sediments and Sedimentary Rocks*; van Loon, A.J., Ed.; Elsevier: Oxford, UK, 2012; pp. 319–351. [CrossRef]
14. Picard, A.; Gartman, A.; Clarke, D.R.; Girguis, P.R. Sulfate-reducing bacteria influence the nucleation and growth of mackinawite and greigite. *Geochim. Cosmochim. Acta* **2018**, *220*, 367–384. [CrossRef]
15. Cosmidis, J.; Nims, C.; Diercks, D.; Templeton, A.S. Formation and stabilization of elemental sulfur through organomineralization. *Geochim. Cosmochim. Acta* **2019**, *247*, 59–82. [CrossRef]
16. Pardo, N.; Cepeda, H.; Jaramillo, J.M. The Paipa volcano, Eastern Cordillera of Colombia, South America: Volcanic stratigraphy. *Earth Sci. Res. J.* **2005**, *9*, 3–18.
17. Alfaro, C.; Velandia, F.; Cepeda, H. Colombian Geothermal Resources. In Proceedings of the World Geothermal Congress, Antalya, Turkey, 24–29 April 2005; pp. 1–11.
18. Cifuentes, G.R.; Jiménez-Espinosa, R.; Quevedo, C.P.; Jiménez-Millán, J. El ciclo del azufre en sedimentos de lagos con aportes hidrotermales y antrópicos: El Lago Sochagota (Boyacá-Colombia). *Macla* **2017**, *22*, 27–28. (In Spanish)

19. Cifuentes, G.R.; Jiménez-Millán, J.; Quevedo, C.P.; Jiménez-Espinosa, R. Isotopic evidence of the hydrothermal origin of the waters of the Sochagota Lake (Colombia). In Proceedings of the AGU Fall Meeting, San Francisco, CA, USA, 7–11 December 2020.
20. Rye, R.O.; Bethke, P.M.; Wasserman, M.D. The stable isotope geochemistry of acid sulfate alteration. *Econ. Geol.* **1992**, *87*, 225–262. [CrossRef]
21. John, D.A.; Lee, R.G.; Breit, G.N.; Dilles, J.H.; Calvert, A.T.; Muffler, L.J.P.; Clynne, M.A. Pleistocene hydrothermal activity on Brokeoff volcano and in the Maidu volcanic center, Lassen Peak area, northeast California: Evolution of magmatic-hydrothermal systems on stratovolcanoes. *Geosphere* **2019**, *15*, 946–982. [CrossRef]
22. Sánchez-Roa, C.; Jiménez-Millán, J.; Abad, I.; Faulkner, D.R.; Nieto, F.; García-Tortosa, F.J. Fibrous clay mineral authigenesis induced by fluid-rock interaction in the Galera fault zone (Betic Cordillera, SE Spain) and its influence on fault gouge frictional properties. *Appl. Clay Sci.* **2016**, *134*, 275–288. [CrossRef]
23. Sánchez-Roa, C.; Faulkner, D.R.; Boulton, C.; Jimenez-Millan, J.; Nieto, F. How phyllosilicate mineral structure affects fault strength in Mg-rich fault systems. *Geophys. Res. Lett.* **2017**, *44*, 5457–5467. [CrossRef]
24. Jiménez-Millán, J.; Abad, I.; García-Tortosa, F.J.; Nieto, F.; Jiménez-Espinosa, R. Clay saline diagenesis in lake Plio-Pleistocene sediments rich in organic matter from the Guadix-Baza Basin (Betic Cordillera, SE Spain). *Appl. Clay Sci.* **2020**, in press.
25. Nieto, F.; Ortega-Huertas, M.; Peacor, D.R.; Arostegui, J. Evolution of illite/smectite from early diagenesis through incipient metamorphism in sediments of the Basque-Cantabrian Basin. *Clay Clay Miner.* **1996**, *44*, 304–323. [CrossRef]
26. Guerra, I.; Cardell, C. Optimizing use of the structural chemical analyser (variable pressure FESEM-EDX Raman spectroscopy) on micro-size complex historical paintings characterization. *J. Microsc.* **2015**, *260*, 47–61. [CrossRef]
27. Benner, R.; Strom, M. A critical evaluation of the analytical blank associated with DOC measurements by high-temperature catalytic oxidation. *Mar. Chem.* **1993**, *41*, 153–160. [CrossRef]
28. Cifuentes, G.R.; Jiménez-Millán, J.; Quevedo, C.P.; Jiménez-Espinosa, R.; Nieto, F. Fijación de K hidrotermal a través de transformaciones secuenciales de formación de illita en ambiente lacustre hipersalino reductor (Lago Sochagota, Colombia). In *Sociedad Española de Arcillas 2018*; Sociedad Española de Arcillas: Granada, Spain, 2018. (In Spanish)
29. Kleppe, A.K.; Jephcoat, A.P. High-pressure Raman spectroscopic studies of FeS_2 pyrite. *Mineral. Mag.* **2004**, *68*, 433–441. [CrossRef]
30. Meyer, B. Elemental Sulfur. *Chem. Rev.* **1976**, *76*, 367–388. [CrossRef]
31. Bourdoiseau, J.A.; Jeannin, M.; Sabot, R.; Rémazeilles, C.; Refait, P. Characterisation of mackinawite by Raman spectroscopy: Effects of crystallisation, drying and oxidation. *Corrosion Sci.* **2008**, *50*, 3247–3255. [CrossRef]
32. Cifuentes, G.R.; Jiménez-Millán, J.; Quevedo, C.P.; Jiménez-Espinosa, R. Low temperature illitization through illite-dioctahedral vermiculite mixed layers in a tropical latitude hypersaline lake rich in hydrothermal fluids (Lago Sochagota, Colombia). In Proceedings of the AGU Fall Meeting, San Francisco, CA, USA, 7–11 December 2020.
33. Smieja-Król, B.; Janeczek, J.; Bauerek, A.; Thorseth, I.H. The role of authigenic sulfides in immobilization of potentially toxic metals in the Bagno Bory wetland, southern Poland. *Environ. Sci. Pollut. Res.* **2015**, *22*, 15495–15505. [CrossRef]
34. Love, L.G.; Al-Kaisy, A.T.H.; Brockley, H. Mineral and organic material in matrices and coatings of framboidal pyrite from Pennsylvanian sediments, England. *J. Sediment. Res.* **1984**, 54. [CrossRef]
35. Folk, R.L. Nannobacteria and the formation of framboidal pyrite: Textural evidence. *J. Earth Syst. Sci.* **2005**, *114*, 369–374. [CrossRef]
36. MacLean, L.C.W.; Tyliszczak, T.; Gilbert, P.U.P.A.; Zhou, D.; Pray, T.J.; Onstott, T.C.; Southam, G. A high-resolution chemical and structural study of framboidal pyrite formed within a low temperature bacterial biofilm. *Geobiology* **2008**, *6*, 471–480. [CrossRef] [PubMed]
37. Wilkin, R.; Barnes, H. Formation processes of framboidal pyrite. *Geochim. Cosmochim. Acta* **1997**, *61*, 323–339. [CrossRef]
38. Schoonen, M.A.A. Mechanisms of sedimentary pyrite formation. *Geol. Soc. Am. Spec. Pap.* **2004**, *379*, 117–134.

39. Ohfuji, H.; Rickard, D. High resolution transmission electron microscopic study of synthetic nanocrystalline mackinawite. *Earth Planet. Sci. Lett.* **2006**, *241*, 227–233. [CrossRef]
40. Hu, S.Y.; Evans, K.; Fisher, L.; Rempel, K.; Craw, D.; Evans, N.J.; Cumberland, S.; Robert, A.; Grice, K. Associations between sulfides, carbonaceous material, gold and other trace elements in polyframboids: Implications for the source of orogenic gold deposits, Otago Schist, New Zealand. *Geochim. Cosmochim. Acta* **2016**, *180*, 197–213. [CrossRef]
41. Cosmidis, J.; Benzerara, K.; Menguy, N.; Arning, E. Microscopy evidence of bacterial microfossils in phosphorite crusts of the Peruvian shelf: Implications for phosphogenesis mechanisms. *Chem. Geol.* **2013**, *359*, 10–22. [CrossRef]
42. Xu, J.; Murayama, M.; Roco, C.M.; Veeramani, H.; Michel, F.M.; Rimstidt, J.D.; Winkler, C.; Hochella, M.F.J. Highly-defective nanocrystals of ZnS formed via dissimilatory bacterial sulfate reduction: A comparative study with their abiogenic analogues. *Geochim. Cosmochim. Acta* **2016**, *180*, 1–14. [CrossRef]
43. Rickard, D.; Grimes, S.T.; Butler, I.; Oldroyd, A.; Davies, K.L. Botanical constraints on pyrite formation. *Chem. Geol.* **2007**, *236*, 228–246. [CrossRef]
44. Nabbefeld, B.; Grice, K.; Schimmelmann, A.; Sauer, P.E.; Böttcher, M.E.; Twitchett, R. Significance of $\delta D_{kerogen}$, $\delta^{13}C$, $\delta\ ^{13}C_{kerogen}$ and $\delta^{34}S_{pyrite}$ from several Permian/Triassic (P/Tr) sections. *Earth Planet. Sci. Lett.* **2010**, *295*, 21–29. [CrossRef]
45. Jaraula, C.M.; Grice, K.; Twitchett, R.J.; Böttcher, M.E.; LeMetayer, P.; Dastidar, A.G.; Opazo, L.F. Elevated pCO_2 leading to Late Triassic extinction, persistent photic zone euxinia, and rising sea levels. *Geology* **2013**, *41*, 955–958. [CrossRef]
46. Melendez, I.; Grice, K.; Schwark, L. Exceptional preservation of Palaeozoic steroids in a diagenetic continuum. *Sci. Rep.* **2013**, *3*. [CrossRef] [PubMed]
47. Luther, G.W.; Findlay, A.; MacDonald, D.J.; Owings, S.M.; Hanson, T.E.; Beinart, R.A.; Girguis, P.R. Thermodynamics and kinetics of sulfide oxidation by oxygen: A look at inorganically controlled reactions and biologically mediated processes in the environment. *Front. Microbiol.* **2011**, *2*, 62. [CrossRef] [PubMed]
48. Cosmidis, J.; Templeton, A.S. Self-assembly of biomorphic carbon/sulfur microstructures in sulfidic environments. *Nat. Commun.* **2016**, *7*, 12812. [CrossRef] [PubMed]

Capítulo 6.

Caracterización geoquímica y microbiológica de los sedimentos: papel de la comunidad bacteriana en el ciclo de los elementos

El contenido de este capítulo constituye el trabajo:

Trace element fixation in sediments rich in organic matter from a saline lake in tropical latitude with hydrothermal inputs (Sochagota Lake, Colombia): The role of bacterial communities.

Cifuentes, G.R., Jiménez-Millán, J., Quevedo, C.P., Gálvez A., Castellanos-Rozo J., Jiménez-Espinosa, R.,

Este artículo ha sido publicado en Science of The Total Environment. 2020
DOI: 10.1016/j.scitotenv.2020.143113.
Recibido:21 agosto 2020; Aceptado: 13 octubre 2020;
Publicado: marzo 2021

Science of the Total Environment 762 (2021) 143113

Contents lists available at ScienceDirect

Science of the Total Environment

journal homepage: www.elsevier.com/locate/scitotenv

Trace element fixation in sediments rich in organic matter from a saline lake in tropical latitude with hydrothermal inputs (Sochagota Lake, Colombia): The role of bacterial communities

Gabriel Ricardo Cifuentes [a], Juan Jiménez-Millán [b,*], Claudia Patricia Quevedo [a], Antonio Gálvez [c], José Castellanos-Rozo [d], Rosario Jiménez-Espinosa [b]

[a] Faculty of Sciences and Engineering, Water Resources Research Group, University of Boyacá, 150003 Tunja, Colombia
[b] Department of Geology and CEACTEMA, University of Jaén, Campus Las Lagunillas, 23071 Jaén, Spain
[c] Microbiology Division, Department of Health Sciences, Campus Las Lagunillas, 23071 Jaén, Spain
[d] Department of Biology and Microbiology, Faculty of Sciences and Engineering, Environmental Management Group, University of Boyacá, 150003 Tunja, Colombia

HIGHLIGHTS

- Hydrothermal and anthropic inputs influenced Sochagota Lake sediment composition.
- Most metal were enriched in the organic matter-rich sediments.
- Bacterial biodiversity controls organic matter decay and mineral authigenesis
- SRB promoted metal sulphide precipitation and trace metal uptake.
- SOB could promote metal sulphide oxidation and metal release.

GRAPHICAL ABSTRACT

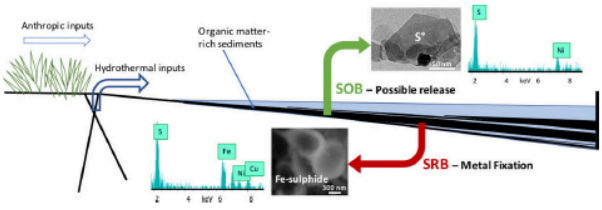

ARTICLE INFO

Article history:
Received 21 August 2020
Received in revised form 13 October 2020
Accepted 13 October 2020
Available online 20 October 2020

Editor: Filip M.G. Filip M.G.Tack

Keywords:
Trace elements
S-bearing minerals
Hydrothermal fluid
Lake sediment
Bacterial community
Sochagota Lake

ABSTRACT

We studied the relationships between the trace element concentration in sediments from a saline lake at a tropical latitude (Sochagota Lake, Colombia) containing hydrothermal and anthropic inputs with the organic matter content, the mineral assemblage composition and the activity of the bacterial communities of the sediments. Organic matter-poor sediments (TOC < 0.7%) with quartz and kaolinite near the southern entrance of the lake were enriched in Zr (up to 603 mg/kg) and some major detrital elements (Na, Ti, Al and Si). Fine-sized clay-rich sediments deposited in the deep zones of the lake (central and northern segments) were characterized by substantial organic matter (up to 11.10%) and the crystallization of S-bearing minerals, clay mineral mixed layers and illite. These sediments were enriched in S, Fe, Zn, Mo, Rb, Co, K, Cr, Sb, Ni, As, Ba, Cu, Mn, Pb, P, Mg, and Sr. The presence of Fe sulfide nanoparticles enriched in heavy metals encrusting microbial cells and a dominant sulfate-reducing bacteria (SRB) community (*Desulfatiglans*, *Desulfobacterales* and Sva0485) suggested that the precipitation of the hydrothermal S and the accumulation of trace elements in the sediments was regulated by SRB activity. The crystallization of S°, barite and calcite and the good correlations between Ba, Sr and Ca indicated that previously precipitated sulfide can be oxidized by the activity of a relevant sulfur-oxidizing bacterial community (*Thioalkalimicrobium*, *Sulfurovum*, *Arcobacter* and *Sulfurimonas*), possibly facilitating the release of the metals.

1. Introduction

Some of the frequently proposed factors to explain trace element concentration in lake sediments from geothermal areas are the presence

* Corresponding author.
E-mail address: jmillan@ujaen.es (J. Jiménez-Millán).

https://doi.org/10.1016/j.scitotenv.2020.143113
0048-9697/

of hydrothermal inputs that increase lake salinity (Kristmannsdóttir and Ármannsson, 2003), the mobility behavior of elements in organic matter-rich sediments (e.g. Andrade et al., 2018; Moreira et al., 2017) and the role of sulfate-reducing bacteria and sulfur oxidizing bacteria on biochemical cycles (e.g. Niu et al., 2018).

Active hydrothermal systems are a source of fluids that provide and transport metals. Some of these metals present in hydrothermal fluids (eg, Pb, Zn, and As) can have negative effects on the environment, so it is necessary to determine their behavior to recognize possible environmental impacts (e.g., Kristmannsdóttir and Ármannsson, 2003). Metals can be included in the hydrothermal fluids from the source water, the igneous volatiles and as a consequence of the water-rock interaction, causing saline fluids with high metal concentrations (Aiuppa et al., 2000, 2005). Saline hydrothermal fluids can constitute an important input of trace element-enriched water to lakes in active geothermal areas.

The abundance of reactive organic matter and the reducing conditions generated in environments with high organic matter production (e.g., ecosystems at tropical latitudes) foster multiple mineral reactions frequently associated with biological activity, affecting the mobility of elements such as S and As as well as the concentrations of several trace elements (e.g., Zn, Pb, and Cu). Sulfide mineral precipitation can largely affect all these reactions. Andrade et al. (2018) have suggested that reducing reactions mediated by microbes involving Fe and S compounds can control the distribution of trace elements in the sediments of these systems (see also Noël et al., 2017). Trace element (e.g., Cu, Ni, Co, Pb, Zn) enrichment in lake sediments containing sulfide framboids is frequently related to high contents of organic matter (Hu et al., 2016; Large et al., 1999). Pyrite, as the main representative mineral of the framboids, is frequently found in the interstices of organic matter (Hu et al., 2016), suggesting that organic matter favors pyrite precipitation through microbial sulfate reduction, which may constitute an additional trace element sink. Moreira et al. (2017) have suggested that carbonaceous matter and pyrite have an important effect on metal immobilization in sediments deposited in highly productive regions.

Sulfate-reducing bacteria (SRB) are common in lake and river sediments (Niu et al., 2018). Muyzer and Stams (2008) have indicated that these anaerobic prokaryotic microorganisms use sulfate as an electron acceptor to degrade organic matter in sediments under anaerobic conditions. Qi et al. (2004) have suggested that this process produces H_2S, which reacts with available metals to stabilize those in sulfide minerals. Therefore, SRB are able to convert metal ions (e.g., Cu, Pb, Cr, Zn, Hg, As) into low-solubility metal sulfides in heavy metal-enriched environments due to natural processes such as hydrothermal inputs (Frank et al., 2013), or play an important role in removing the toxic pollutants of anthropic pollution (Kiran et al., 2017; Tarekegn et al., 2020; Wolfenden et al., 2005). On the other hand, sulfur oxidizing bacteria can oxidize reduced sulfide to sulfate, affecting the sulfur biogeochemistry (Kühl and Jørgensen, 1992; Niu et al., 2018) and enabling the release of the metals included in sulfide minerals (Niu et al., 2018). Therefore, SRB and SOB are the dominant bacterial groups responsible for sulfur biogeochemistry (Kühl and Jørgensen, 1992; Niu et al., 2018). Indeed, SRB and SOB activities control the balance of the sulfur cycle (Niu et al., 2018). Moreover, SRB and SOB can influence metal biotransformations in water and sediments. SRB can be involved in removal processes by metal crystallization in water and sediments (White and Shaman, 1998). This process can be reinforced by the presence of iron-reducing bacteria (IRB). Bacteria-mediated Fe^{3+} reduction is an effective mechanism that transforms Fe^{3+} to Fe^{2+}. The joint activity of SRB and IRB can affect heavy metals' availability in sediments and soils (Zhang et al., 2019). However, SOB activity can favor the oxidation of precipitated reduced sulfide, again promoting the release of toxic metals into the environment (Niu et al., 2018).

The Sochagota Lake (Colombia) is situated in a subtropical highland oceanic climate zone, in a geothermal area associated with Paipa volcano in the Andean Cordillera. Cifuentes et al. (2020a, 2020b) have revealed that the geothermal systems here provide significant hydrothermal inputs of sulfur to the lake waters. The climatic conditions here favor the deposition of organic matter-rich sediments. The present study evaluated the role of bacterial communities in the formation of S-bearing minerals and their influence on major and trace element accumulation in sediments deposited in Sochagota Lake. We quantified the composition of sediments (some of them containing sulfide framboids), focusing on the concentration and distribution of metals, and the association of metals with carbonaceous material. We tried to improve knowledge of metal behavior in this saline lake environment, identifying the main microbial communities related to the biogeochemical processes occurring in the sediments of the lake. We aimed to combine comprehensive geochemical and mineralogical analysis with microbiological analysis to reveal the origin of trace element in the sediments of wetlands with inputs of hydrothermal origin.

2. Materials and methods

2.1. Study area

Sochagota Lake is an artificial lake intended for recreational use, constructed from a previous natural wetland. It is located in a highland (altitude 2496 m) of the department of Boyacá in Paipa province (Colombia), and occupies a total surface area of 1.8 km2 (Fig. 1A and B). The deepest point of the lake is 3.20 m. The lake is fed by a tributary of the Chicamocha River, the El Salitre River.

Paipa province has an average annual temperature of 14.4 °C. Rainfall is well distributed throughout the year, with precipitation averaging 911 mm/yr. The climate is classified as subtropical highland oceanic (Cfb by the Köppen system).

From a geological point of view, the study area is located in the main Andean geothermal system in Colombia. Hydrothermal systems associated with the area's volcanoes can be identified (Alfaro et al., 2005). Siliceous sedimentary rocks of Cretaceous age are intruded by these volcanoes (Fig. 2). The area is characterized by a lack of any type of evaporitic sedimentary deposits. The nearest volcanic building is Paipa (Pardo et al., 2005), outcropping to the south of Sochagota Lake with Pliocene-Pleistocene pyroclastic alkaline rhyolites and trachyandesites. A collapsed caldera (3 km wide) with several hydrothermal vents formed by deep faults that control heat upflow and shallow water mixing processes, producing sodium-sulfate water facies. These hydrothermal saline waters flow through the El Salitre River and are mixed with rain waters in Sochagota Lake (Cifuentes et al., 2017, 2020a, 2020b).

Cifuentes et al. (2020a, 2020b) have shown that the lake waters are alkaline (pH 9.27) and characterized by high contents of Na^+ (1493 mg/L), K^+ (280 mg/L) and SO_4^{2-} (2165 mg/L), causing very high electrical conductivity (up to 127 mS/cm). Taking into account the water isotopic composition (6.4‰ for $\delta^{34}S$ and 8.1 for $\delta^{18}O$, similar to other hydrothermal fluids; see e.g., John et al., 2019; Rye et al., 1992) and the absence of evaporitic deposits, Cifuentes et al. (2020a) have proposed that the considerable salinity of the lake is caused by hydrothermal inputs of S-bearing fluids.

Fig. 1C shows the location of the 20 points of the grid where sediments from the lake were sampled. We obtained up to 50 cm-deep cores using a standard stainless Shelby tube. The top and bottom of the tubes with samples were covered with silicone and conserved at −80 °C. The redox potential, pH and electrical conductivity of the sediments were determined in situ with portable devices for soils and sediments (Hanna Instruments HI993310 and HI98168) (Table 1). Low redox potential (around −150 mV) was observed in the sediments from the lake's deepest areas (central and northern segments). Two segments were obtained from the extracted cores: samples ending with –s (Table 2) represented the 0–25 cm-deep segments, whereas samples ending with –p belonged to the 25–50 cm-deep segments.

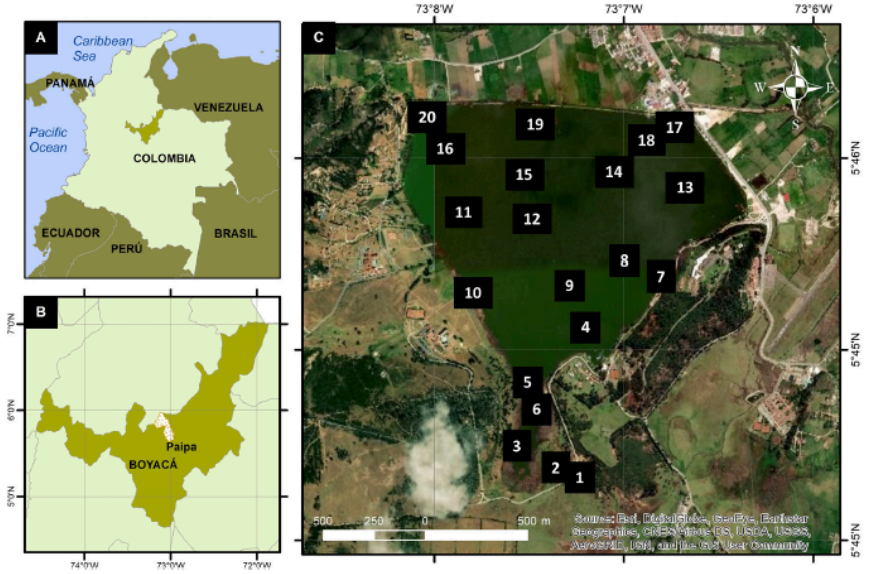

Fig. 1. Geographical setting of the study area and sampling location. A: Global context of the area; B: Local situation in Colombia; C: Locations of sampling points 1–20 at Sochagota Lake. Modified from Cifuentes et al. (2020a, 2020b).

2.2. Methods

Mineralogical characterization was carried out using X-ray diffraction (XRD), field emission scanning electron microscope (FESEM), and high-resolution transmission electron microscopy (HRTEM). XRD data were obtained from random and oriented aggregates in a PANalytical X'Pert Pro diffractometer (CICT, University of Jaén, Spain) equipped with an X'Celerator solid-state linear detector using CuKα radiation, 45 kV, 40 mA, 0.008° 2θ step increment and 10 s/step of counting time. We used ethylene glycol and heating to 550 °C treatments to identify expandable clay minerals.

FESEM studies were carried out using a Merlin Carl Zeiss microscope (CICT, University of Jaén, Spain). Back-scattered electron (BSE) images from polished sections (previously consolidated with a polyester resin) and secondary electron (SE) images were used to obtain a textural and microchemical characterization.

Two electron microscopes (FEI TITAN and Philips CM20, CIC, University of Granada) were used for the nanometric HRTEM characterization according to the experimental procedure indicated by Nieto et al. (1996). Samples were prepared using Ni grids from an alcohol or distilled water of sample particles dispersion. The nanoparticle chemical composition was obtained in scanning transmission electron microscope mode with an energy-dispersive X-ray spectroscopy (EDX) microanalysis system.

Total organic carbon (TOC) was measured in precisely weighed (2–3 mg; ± 0.01 mg) on silver capsules sediment samples using a Shimadzu TOC-V CSH Total Organic Carbon Analyzer (IRNAS, CSIC-Sevilla, Spain). Reference material (PACS-2) was run every 10 samples for analytical replication.

The chemical composition of the sediments was obtained using X-ray fluorescence spectrometry (XRF) and inductively coupled plasma-mass spectrometry (ICP-MS). A Philips Magix Pro (PW-2440) spectrometer (CIC, University of Granada) was used for the whole-sediment analyses of major elements. Sediments were finely powdered in a mill, producing a dense and homogeneous sample. In order to reduce the effect of a preferential orientation of phyllosilicates, we prepared glass beads with lithium tetraborate. The detection limit was 0.01 wt%. A set of 25 international geostandards was used for the empirical calibration. 0.5 g of powdered sediments, initially dried at 110 °C and then heated at 1000 °C for 1 h, was used to determine loss on ignition (LOI).

Trace elements were analyzed by ICP-MS with a NexION 300D (CIC, University of Granada). Sample digestion was performed with HNO_3 + HF. Certified standards (BR-N, GH, DR-N, UB-N, AGV-N, MAG-1, GS-N, and GA) were used for quantification. The detection limit was below 1 μg/kg. The standard deviation was always below 5%.

DNA extraction was carried out using a DNeasy PowerSoil Kit (Quiagen) according to the instructions of the manufacturer. The quality and the quantity of the extracted DNA were determined by QuantiFluor® ONE dsDNA system (Promega, Madison, USA). The DNA was stored at −20 °C until analysis. Regarding DNA sequencing and analysis, 16S rDNA gene amplicons were obtained following the 16S rDNA gene Metagenomic Sequencing Library Preparation Illumina protocol (Cod. 15044223 Rev. A). The gene-specific sequences used in this protocol targeted the 16S rDNA gene V3 and V4 region. Illumina adapter overhang nucleotide sequences were added to the gene-specific sequences. The primers were selected from Klindworth et al. (2013). The following 16S rDNA gene amplicon PCR primer sequences were used: forward primer, 5′TCGTCGGCAGCGTCAGATGTGTATAAGAGACAGCCTACGGGNGGCWGCAG3′; reverse primer, 5′GTCTCGTGGGCTCGGAGATGTGTATAAGAGACAGGACTACHVGGGTATCTAATCC3′. Microbial genomic DNA (5 ng/μl in 10 mM Tris pH 8.5) was used to initiate the protocol. After 16S rDNA gene amplification, the mutiplexing step was performed using a Nextera XT Index Kit (FC-131-1096). 1 μl of the PCR product was run on a Bioanalyzer DNA 1000 chip to verify the size

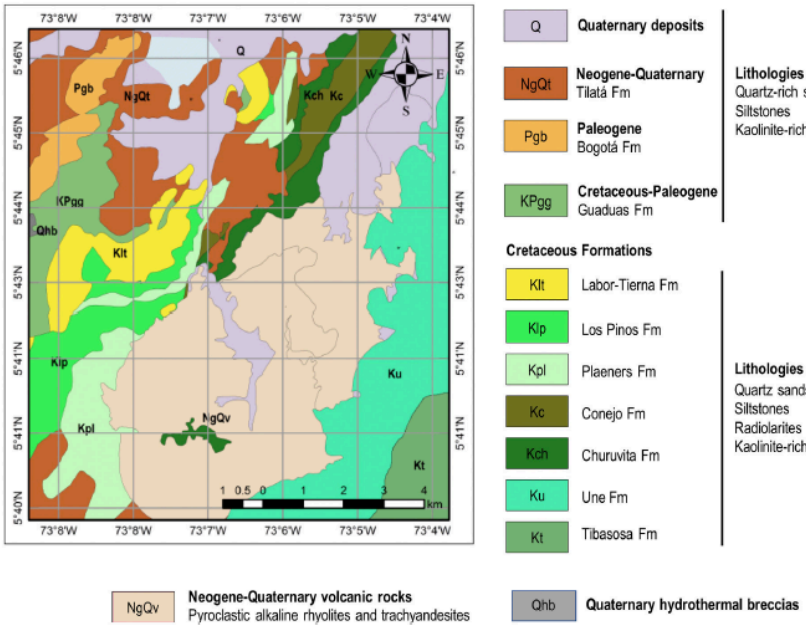

Fig. 2. Geological map of the Sochagota Lake Basin. The lake does not receive sediments from the north. Modified from Pardo et al. (2005).

(expected size ~550 bp). Following size verification, the libraries were sequenced using a 2 × 300 pb paired-end run (MiSeq Reagent kit v3 (MS-102-3001)) on a MiSeq Sequencer according to the manufacturer's instructions (Illumina). Quality assessment was performed with the use of the prinseq-lite program (Schmieder and Edwards, 2011). The sequence data were analyzed using the qiime2 pipeline (Caporaso et al., 2011). Denoising, paired-end joining, and chimera depletion were performed, starting with paired-end data using the DADA2 pipeline (Callahan et al., 2016). Taxonomic affiliations were assigned using the Naive Bayesian classifier integrated in the qiime2 plugins and the SILVA_release_132 database (Quast et al., 2013). Statistical analysis was carried out with SPSS software version 24 (IBM Corp., Foster City, CA).

3. Results

3.1. Chemical and mineralogical composition of the sediments

3.1.1. TOC, S, major element and mineral composition

Significant compositional differences between the materials sampled at the entrance of the lake (southern segment) and those from the deep areas (central and northern segments) were observed. TOC in the sediments varied from 11.1% to 0.28% (Table 2). The lowest amounts of TOC were located in sediments at the southern lake entrance with scarce vegetation, and near the El Salitre hydrothermal input. These sediments were frequently rich in SiO_2 (mean 66.67%), Al_2O_3 (up to 24.01%), Na_2O and TiO_2 (>1%) but depleted in Fe_2O_3 (<0.6%) and K_2O (mean 0.66%). The mean CaO and MgO contents were very low, commonly below 0.1% in the sediments in the southern part. The chemical composition of these sediments is caused by the presence of a matrix made of significant amounts of kaolinite, including large grains of quartz, feldspars with very altered surfaces, and microvesiculated particles of acid volcanic glass (Cifuentes et al., 2020a) (Fig. 3A).

On the other hand, the highest TOC contents were found in the microlaminated sediments from the deep zone of the lake (mean 2.74% in the central part and 3.16% in the northern segment), frequently close to sewage load discharges and vegetation-rich zones. Regarding major element composition, the sediments were enriched in Fe_2O_3 (up to 6.32% in sediments from the northern part) and K_2O (up to 2.61%) but poorer in Al_2O_3 (mean 19.89 in the northern sediments and 20.51 in the central sediments) than those in the southern part. This composition can be related with the presence of elongated rests of plants (Fig. 3B) in an abundant clay-rich matrix containing illite-dioctahedral vermiculite mixed layers (I-DV) and illite with lower amounts of kaolinite (Fig. 3C) (Cifuentes et al., 2020a). The high S contents of the sediments from the lake's deep zone (mean 19,997 mg/Kg) can also be related with the mineralogical composition of the sediments, characterized by the presence of areas rich in framboidal pyrite associated with the rest of plants (Fig. 3B). The HRTEM analyses of organic matter-rich areas revealed the crystallization of mackinawite, pyrite and S° (Fig. 4). The images suggested that

Table 1
Physicochemical properties of the Sochagota Lake sediments. R.P.: Redox potential. E.C.: Electrical conductivity.

	pH	R.P. (mV)	E.C. (μS/cm)
Southern part. El Salitre entrance ($n = 5$)	7.9	91	1977
Central part ($n = 5$)	7.8	−149	2525
Northern part ($n = 10$)	7.9	−154	2456

Table 2
Major element sediment compositions determined by XRF (SiO2, Al2O3, Fe2O3, MnO, MgO, CaO, Na2O, K2O, TiO2, P2O5) loss of ignition (LOI) and content in total organic carbon (TOC) (in weight percent). Trace element sediment compositions determined by ICP-MS (for Zr, S, Cr, Co, Ni, Cu, Zn, Ba, As, Mo, Pb, Rb, Sb, Sr) (in mg/kg). Med: Median; Max: Maximum; Min: Minimum. Up.S: mean of the unpolluted sediments from the Chicamocha Riverr (from Quevedo et al., 2020a, 2020b. E.S.: proposed guidance values for the European soils (from Gawlik and Bidoglio, 2006).

Sample	SiO_2	Al_2O_3	Fe2O3	MnO	MgO	CaO	Na_2O	K_2O	TiO_2	P_2O_5	TOC (%)	LOI	Zr	S	Cr	Co	Ni	Cu	Zn	Ba	As	Mo	Pb	Rb	Sb	Sr
Southern part																										
1p	67.01	23.20	0.87	0.00	0.05	0.01	1.23	0.71	1.20	0.08	0.28	5.50	603	662	34	–	14	30	27	129	6	–	12	43	–	32
1 s	67.02	22.98	0.71	0.00	0.07	0.11	1.03	0.70	1.27	0.08	0.37	5.72	581	367	52	–	17	31	31	133	5	–	12	43	–	42
2p	66.04	22.71	1.61	0.00	0.19	0.31	1.17	0.63	1.10	0.07	0.66	5.95	489	438	50	1	14	39	36	145	7	–	14	52	–	46
2 s	66.23	22.92	1.59	0.00	0.08	0.01	1.28	0.59	1.11	0.07	0.62	6.03	504	2001	49	1	17	37	37	123	5	–	14	51	–	39
3p	66.61	23.81	0.69	0.00	0.06	0.10	1.31	0.68	1.21	0.06	0.49	5.42	566	517	48	–	15	33	32	133	6	–	12	38	–	42
3 s	66.98	23.54	0.67	0.00	0.06	0.01	1.03	0.70	1.30	0.06	0.37	5.60	579	459	42	–	16	31	30	133	5	–	12	40	–	33
5p	66.31	22.92	1.58	0.00	0.14	0.03	1.21	0.71	1.18	0.07	0.64	5.29	502	609	48	–	16	39	41	134	7	–	14	51	–	41
5 s	66.56	24.01	0.58	0.00	0.07	0.01	1.02	0.60	1.20	0.06	0.31	5.70	574	493	42	–	15	32	29	132	5	–	12	37	–	32
6p	66.91	23.10	0.58	0.00	0.05	0.16	1.01	0.70	1.24	0.09	0.30	5.81	593	487	51	–	14	29	26	141	5	–	11	43	–	43
6 s	67.00	22.81	1.61	0.00	0.09	0.01	1.15	0.61	1.15	0.07	0.70	5.05	503	651	50	–	17	39	38	133	7	–	15	51	–	39
Mean	66.67	23.20	1.05	0.00	0.09	0.08	1.14	0.66	1.20	0.07	0.47	5.61	549	668	46	–	15	34	33	134	6	–	13	45	–	39
Med	66.67	23.10	0.87	0.00	0.07	0.03	1.15	0.68	1.20	0.07	0.47	5.61	566	517	48	–	15	33	32	133	6	–	12	43	–	39
Max	67.02	24.01	1.61	0.00	0.19	0.31	1.31	0.71	1.30	0.09	0.70	6.03	603	2001	52	1	17	39	41	145	7	–	15	52	–	46
Min	66.04	22.71	0.58	0.00	0.05	0.01	1.01	0.59	1.10	0.06	0.28	5.05	489	367	34	–	14	29	26	123	5	–	11	37	–	32
Central part																										
4p	63.09	21.01	2.22	0.01	0.27	0.12	0.88	1.28	0.94	0.07	1.00	7.34	359	4502	71	9	42	74	65	283	19	2	18	115	1	95
4 s	58.78	22.89	3.62	0.01	0.46	0.16	0.82	1.85	0.75	0.10	2.01	9.96	151	14,332	74	13	43	87	81	428	23	3	24	187	3	148
7p	58.11	18.54	6.00	0.03	0.38	0.10	0.46	2.46	0.63	0.18	9.15	12.60	143	27,432	92	25	82	180	113	487	57	5	24	245	6	113
7 s	59.86	18.85	5.07	0.02	0.41	0.10	0.50	2.44	0.65	0.17	4.11	11.77	147	26,345	91	24	82	175	111	435	54	5	23	227	5	100
8p	60.83	21.09	2.67	0.02	0.42	0.13	0.57	1.64	0.76	0.11	1.01	11.28	149	8541	71	15	45	78	89	458	38	3	24	154	3	130
8 s	58.39	21.01	4.01	0.02	0.41	0.12	0.75	2.13	0.97	0.12	2.07	9.43	278	15,737	75	17	56	100	85	451	37	4	24	193	3	123
9p	61.76	20.06	4.12	0.02	0.34	0.26	0.57	2.28	0.77	0.13	2.64	9.08	209	18,206	80	22	72	114	100	427	44	4	21	196	4	130
9 s	66.01	19.90	3.05	0.02	0.31	0.12	0.65	1.63	0.71	0.10	2.24	7.47	229	8663	61	12	41	97	74	413	32	2	18	115	2	118
9w	59.06	22.38	3.57	0.01	0.42	0.15	0.81	1.81	0.87	0.11	2.10	10.86	155	12,453	74	14	43	76	81	426	22	2	25	184	2	149
10p	65.88	20.93	2.48	0.01	0.18	0.15	0.88	1.22	0.97	0.09	1.27	6.81	427	8021	63	7	40	77	58	265	31	1	15	79	2	89
10s	66.18	18.92	3.60	0.02	0.30	0.12	0.60	1.59	0.72	0.10	2.59	7.82	228	15,390	60	12	41	90	76	426	35	2	19	111	2	121
Mean	61.63	20.51	3.67	0.02	0.35	0.14	0.68	1.85	0.79	0.12	2.74	9.49	225	14,511	74	15	53	104	85	409	36	3	21	164	3	120
Med	60.83	20.93	3.60	0.02	0.38	0.12	0.65	1.81	0.76	0.11	2.10	9.43	209	14,332	74	14	43	90	81	427	35	3	23	184	3	121
Max	66.18	22.89	6.00	0.03	0.46	0.26	0.88	2.46	0.97	0.18	9.15	12.60	427	27,432	92	25	82	180	113	487	57	5	25	245	6	149
Min	58.11	18.54	2.22	0.01	0.18	0.10	0.46	1.22	0.63	0.07	1.00	6.81	143	4502	60	7	40	74	58	265	19	1	15	79	1	89
Northern part																										
11p	61.89	20.47	4.05	0.02	0.28	0.19	0.64	2.26	0.87	0.13	2.52	9.01	238	17,446	78	20	66	103	94	397	43	4	19	195	3	136
11 s	62.28	20.23	4.07	0.02	0.30	0.19	0.61	2.28	0.85	0.13	2.57	9.00	227	17,921	80	21	66	108	94	397	43	4	19	196	3	136
12p	60.61	20.87	4.02	0.02	0.37	0.33	0.71	2.22	0.93	0.12	2.24	9.00	272	15,965	75	17	56	102	85	419	43	4	22	195	3	130
12 s	61.40	19.87	4.22	0.02	0.35	0.15	0.53	2.31	0.75	0.13	2.80	9.55	190	18,978	83	23	76	129	104	428	48	4	21	200	4	123
13p	61.54	19.84	4.25	0.02	0.51	0.15	0.52	2.32	0.74	0.14	2.88	9.64	189	19,312	85	23	76	133	104	453	50	4	24	200	4	151
13 s	60.54	21.34	3.77	0.02	0.50	0.15	0.69	1.90	0.68	0.10	1.74	9.56	151	18,321	75	13	44	84	85	443	24	3	24	188	3	149
14p	60.64	19.01	4.74	0.02	0.29	0.12	0.51	2.43	0.69	0.15	3.45	10.94	150	22,731	90	24	80	173	109	439	52	5	19	214	5	124
14 s	61.63	19.92	4.14	0.02	0.29	0.19	0.55	2.28	0.77	0.13	2.78	9.09	199	18,656	83	22	74	121	102	397	45	4	19	199	4	136
15p	61.83	19.93	4.13	0.02	0.32	0.27	0.56	2.28	0.77	0.13	2.73	9.09	204	18,262	81	22	73	116	102	430	44	4	21	196	4	134
15 s	61.26	21.06	3.75	0.01	0.48	0.14	0.84	1.88	0.67	0.08	2.51	9.25	152	15,143	75	13	44	91	83	433	22	3	24	191	2	148
16p	57.56	17.36	6.32	0.04	0.37	0.10	0.32	2.61	0.52	0.30	11.10	13.80	134	29,433	94	26	84	190	121	498	62	6	24	264	6	113
16 s	59.71	18.92	4.95	0.03	0.39	0.10	0.51	2.43	0.69	0.15	3.59	11.39	147	25,093	90	24	80	175	110	467	52	5	24	218	5	107
17p	60.45	20.73	4.05	0.01	0.35	0.42	0.68	2.26	0.88	0.13	2.41	9.30	255	17,053	76	18	56	115	85	420	43	4	22	195	3	143
17 s	60.76	20.94	4.01	0.02	0.39	0.23	0.72	2.21	0.96	0.12	2.21	9.40	274	15,909	75	17	56	101	85	418	42	4	22	194	3	117
17w	60.59	21.17	4.01	0.01	0.41	0.20	0.81	2.12	0.98	0.12	2.16	9.20	278	14,523	74	17	56	95	84	416	31	4	21	186	3	115
18 m	59.07	18.82	5.21	0.03	0.40	0.11	0.48	2.44	0.65	0.16	4.35	11.85	145	26,943	91	24	82	177	112	469	55	5	24	230	6	114
18p	61.76	19.59	4.42	0.02	0.29	0.21	0.52	2.32	0.74	0.14	2.92	9.86	184	19,929	87	23	77	134	105	401	50	4	19	201	4	137
18 s	61.64	19.29	4.44	0.02	0.24	0.18	0.52	2.35	0.72	0.14	2.96	9.99	152	20,211	88	23	78	167	106	394	51	5	19	201	5	136
18w	61.26	20.82	4.04	0.02	0.31	0.18	0.69	2.25	0.91	0.12	2.25	9.02	270	16,295	75	17	56	104	85	397	43	4	19	195	3	136
19p	59.18	19.22	4.50	0.02	0.45	0.12	0.51	2.36	0.72	0.14	3.04	10.03	151	21,170	89	24	78	168	106	434	51	5	23	207	5	124
19 s	61.89	20.20	4.08	0.02	0.36	0.25	0.59	2.28	0.79	0.13	2.59	9.00	209	17,947	80	22	67	112	97	424	43	4	21	196	4	125
20p	59.96	18.87	5.01	0.02	0.42	0.11	0.51	2.44	0.68	0.15	3.64	11.39	147	26,341	90	24	81	175	110	450	52	5	23	218	5	115
20s	58.83	19.11	4.62	0.03	0.40	0.11	0.51	2.40	0.71	0.14	3.18	10.80	150	21,276	90	24	79	170	108	458	52	5	24	210	5	111
Mean	60.71	19.89	4.38	0.02	0.37	0.18	0.59	2.29	0.77	0.14	3.16	9.96	194	19,777	83	21	69	132	99	430	45	4	22	204	4	129
Med	60.76	19.92	4.14	0.02	0.37	0.18	0.55	2.28	0.74	0.13	2.78	9.55	189	18,656	83	22	74	121	102	428	45	4	22	199	4	130
Max	62.28	21.34	6.32	0.04	0.51	0.42	0.84	2.61	0.98	0.30	11.10	13.80	278	29,433	94	26	84	190	121	498	62	6	24	264	6	151
Min	57.56	17.36	3.75	0.01	0.24	0.10	0.32	1.88	0.52	0.08	1.74	9.00	134	14,523	74	13	44	84	83	394	22	3	19	186	2	107
Up.S.	91.74	5.66	2.46	0.02	0.17	0.25	0.12	0.36	0.42	0.16	4.00	1.28			29		26	41	42				12			
E.S.															50		30	40	100				50			

bacteria were encrusted by aggregates of FeS (Fig. 4A). The nanocrystalline organization of these aggregates showed lattice fringe images with interplanar distances of around 5 Å, consistent with the (001) spacing of mackinawite (Fig. 4B). Several well-crystallized pyrite particles were characterized by the presence of Cu (Figs. 4C and D). The EDX analyses facilitated the identification of hexagonal S° nanoparticles (Figs. 4E and F).

CaO and MgO contents were slightly higher in the sediments from the deep part (central and northern segments) of the lake (up to 0.5%), associated with the presence of aggregates of <2 μm idiomorphic prismatic microcrystals of calcite cement in the sediments' micropores (Fig. 5A). A slight enrichment on the P_2O_5 content of the sediments from the northern part of the lake (up to 0.30%) can be observed.

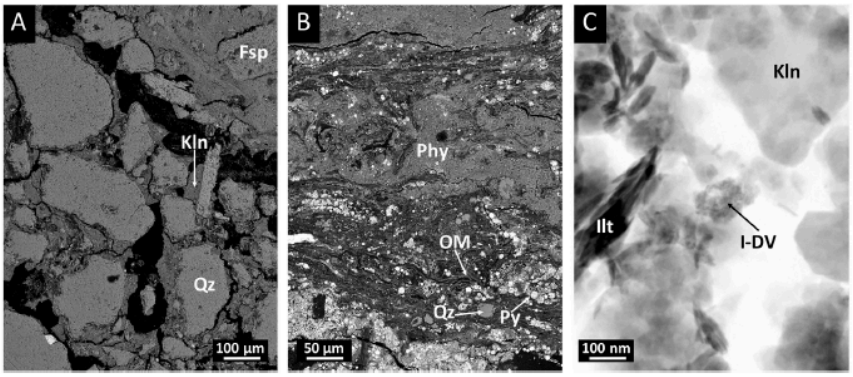

Fig. 3. Electron microscope images of sediments from the lake. A: BSE image of a sample from the southern part of the lake with crystals of quartz and feldspar in a kaolinite-rich matrix. B: BSE image of a sample from the northern part of the lake with areas rich in elongated rests of plants and framboidal pyrite in an abundant clay-rich matrix. C: HRTEM image of the clay-rich matrix of a sample from the northern part of the lake showing the presence of illite, illite-dioctahedral vermiculite mixed layers and kaolinite. Phy: phyllosilicates, Kln: kaolinite, Qz: quartz, Fsp: feldspar. Ilt: illite, I-DV: illite-dioctahedral vermiculite mixed layers. OM: organic matter.

3.1.2. Trace element composition

Trace element concentrations in sediments from Sochagota Lake also varied according to the sediment situation. Zr was enriched in the sediments from the southern part (mean 549 mg/kg), duplicating the Zr contents in the central (225 mg/kg) and northern parts of the lake (194 mg/kg) (Table 2). High concentration levels of heavy metals in the central and northern sediments can be observed (Table 2) following a decreasing order: Cu > Zn > Cr > Ni > Co > Pb > Mo. The mean values of Rb (up to 264 mg/kg), Ba (up to 498 mg/kg) and As (62 mg/kg) were also especially enriched in the northern part of the lake. Small idiomorphic crystals of barite can be observed in the sediments richer in Ba (Fig. 5B).

3.2. Bacterial populations in organic matter-rich sediments

Based on 16S rRNA gene amplicon sequencing, *Proteobacteria* was the major bacterial phylum found in the sediments (relative abundances varying from 20.7% to 30.19%; Fig. 6). *Bacteroidetes* was the second main phylum, with contents between 9.7% and 23.3%. The relative abundance of *Chloroflexi* was also important (8.6 to 19.1%). Other phylum such as *Epsilonbacteraeota, Latescibacteria, Calditrichaeota, Planctomycetes, Nitrospirae, Spirochaetes, Patescibacteria, Zixibacteria* and *Omnitrophicaeota* had lower relative abundances (2–5%).

Proteobacteria were represented by different orders of *Deltaproteobacteria* and *Gammaproteobacteria. Desulfarculales* was the most abundant *Deltaproteobacteria* order, with genus *Desulfatiglans* (Fam. *Desulfarculaceae*) being the main representative (5.4–13.6%) (Fig. 6). Microbial communities of other *Deltaproteobacteria* orders, such as *Desulfobacterales* (Fam. *Desulfobacteraceae*, G. *Sva0081 sediment group*) and Sva0485, were present in lower amounts (<2%). Genera *Thioalkalimicrobium* (up to 3.91%) and *Thiobacillus* (up to 5.33%) were the most abundant *Gammaproteobacteria* (samples 4A and 4AB).

Phylum *Bacteroidetes* microorganisms were also recognized as an important bacterial community in the organic matter-rich sediments of the lake. The order *Ignavibacteriales* was present in significant amounts (up to 7.34%), and the abundance of VadinHA17 reached up to 4.35%. Around 3% of the order *Sphingobacteriales* was present in some samples (9A and 9B).

C. Dehalococcoidia (up to 12.69%, with MSBL5 being the best-represented order) and *Anaerolineae* (up to 4.42%) were the main groups of the phylum *Chloroflexi.*

Phylum *Epsilonbacteraeota* was represented by genera *Sulfurovum, Arcobacter* and *Sulfurimonas* with amounts lower than 3.5%.

Major differences detected between samples at genus level included a higher relative abundance of genus *Desulfatiglans* and uncultured bacteria from O. MSBL5 (*Dehalococcoidia*) and Candidatus *Magasanikbacteria* (phylum *Patescibacteria*) in PS17 samples. PS9 samples showed higher relative abundances of genus *Ignavibacterium* and uncultured members of phylum *Zixibacteria*. PS4 samples (and in particular PS4B) showed higher relative abundances of the genera *Thiobacillus, Thioalkalimicrobium* and *Sulfurimonas*. Principal coordinates analysis (PCoA, Fig. 6C) indicated differences in the clustering of samples depending on sampling point.

4. Discussion

4.1. Geochemical and mineral distribution

The geochemical and mineral results revealed that two main types of sediments can be distinguished in Sochagota Lake whose distributions are associated with the flow regime of the lake. Sediments from the southern part of the lake, deposited at the entrance of the hydrothermal inputs (El Salitre) under fast-flowing conditions, were found to contain negligible organic matter (TOC 0.7%, Table 2). In this area, the deposition of organic matter is not favored by the hydrodynamic conditions, thereby promoting the oxygenation of the sediments (measured redox potential around 90 mV, Table 1). By contrast, the central and northern parts of the lake, under slower-flowing conditions, are characterized by the deposition of the finest clay-rich sediments and organic matter (TOC up to 11.10%, Cifuentes et al., 2020a) with reduced conditions (redox potential around −150 mV, Table 1).

The spatial distribution of trace elements in the sediments of Sochagota Lake seems to be associated with the distribution of organic matter content and mineral assemblages. Organic matter-poor sediments from the southern part of the lake were found to be enriched in Zr (mean 567 mg/kg) and their mineral assemblages did not contain illite, I-DV or S-bearing minerals. The Zr enrichment of sediments is commonly considered an indicator of a significant detrital contribution (e.g., Martinez-Ruiz et al., 2015). The large contents of Zr, SiO_2 and TiO_2 in these sediments can be associated with the deposition of terrigenous zircon, quartz and rutile. On the other hand, organic matter-rich

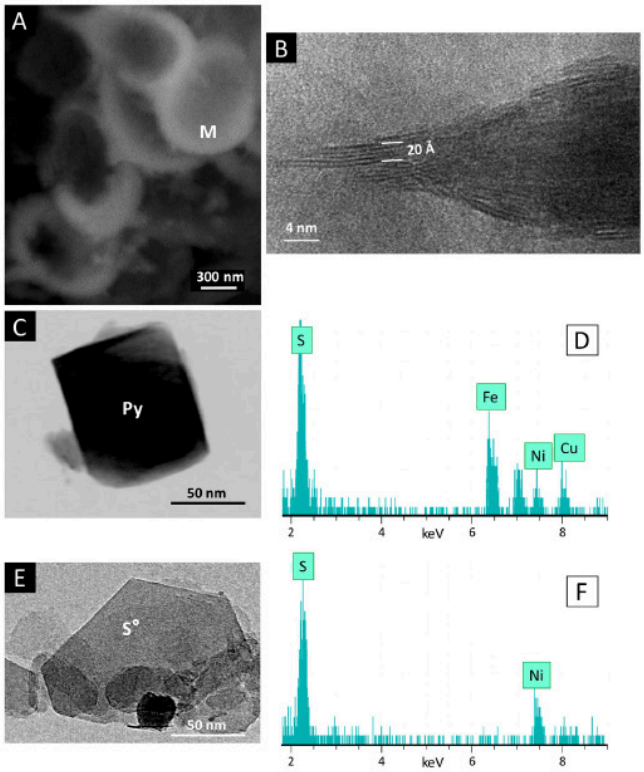

Fig. 4. HRTEM images and EDX analyses of the organic matter-rich areas of the samples from the northern part of the lake. A: Dark field HRTEM image FeS showing bacterial cell morphologies encrusted by aggregates of mackinawite. B: Lattice fringe image of the aggregates shown in A with interplanar distances of around 5 Å. C: Bright field HRTEM image of a well-crystallized Cu-bearing pyrite particle. D: EDX analysis of the particle shown in C; Ni peak is caused by the grid. E: Bright field HRTEM image of a hexagonal S° nanoparticle. F: EDX analysis of the particle shown in E; Ni peak is caused by the grid. M: mackinawite, Py: pyrite, S°: elemental sulfur.

sediments with a fine-grain sized matrix rich in illite and I-DV located in the northern and central segments of the lake were found to be enriched in heavy metals (Cu, Zn, Cr, Ni, Co, Pb, Mo), Rb, Ba and As. These sediments were characterized by the crystallization of S-bearing minerals (mackinawite, pyrite, and S°) (Cifuentes et al., 2020a). The concentrations of heavy metals in these sediments exceeded the world standard averages, and the mean level of some of these elements was clearly higher than the value of unpolluted reference sediments

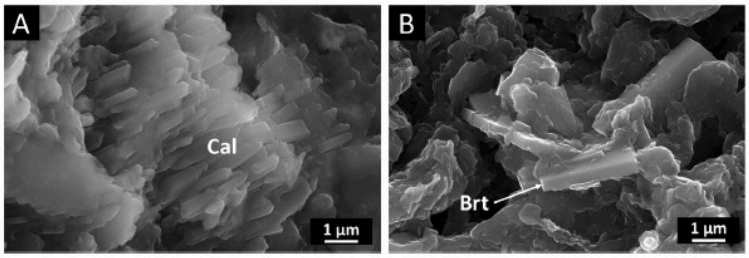

Fig. 5. A: SE image of an aggregate of calcite microcrystals in sediments from the northern part of the lake. B: Small idiomorphic crystals of barite in sediments richer in Ba. Cal: calcite, Brt: barite.

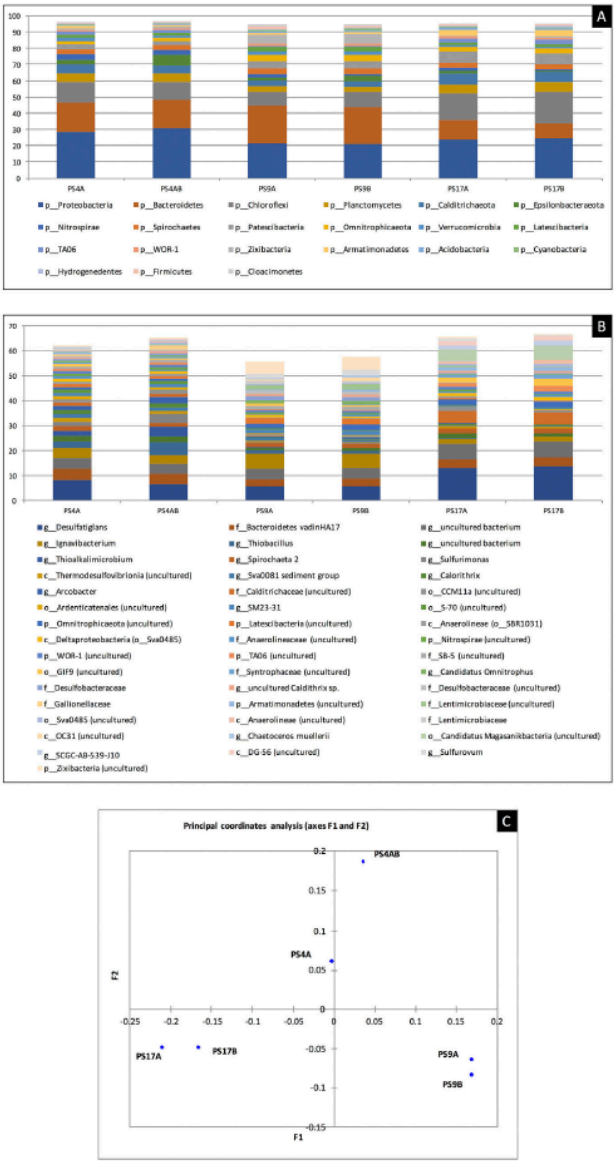

Fig. 6. Bacterial diversity in the organic matter-rich sediments from the central and northern parts of Sochagota Lake (sampling points 4, 9 and 17 in Fig. 1C). A. Phylum level. B. Genus level. Only genera with greater than 1% abundance are shown. C. Principal coordinates analysis of samples.

from the Chicamocha River area (Quevedo et al., 2020b) (Table 2). Although a regulatory framework for contaminants in sediments and soils is not available in Colombia (Martínez-Mera et al., 2019; Rueda-Saá et al., 2011), the metal contents of the northern sediments were above the background values for European soils (Gawlik and Bidoglio, 2006).

4.2. The role of the bacterial communities

The results of the 16S rRNA gene amplicon sequencing in the Sochagota Lake organic matter-rich sediments reveal the presence of a diverse bacterial community composition. Bacterial activity is associated with organic matter degradation processes, and some of the mineral processes in the C and S cycles. The main bacterial communities of the sediments of Sochagota Lake belong to fermentative genera that have previously been reported in the anoxic zones of other lakes. Several communities of *Bacteroidetes* and *Chloroflexi* were identified as important bacterial groups that could have been involved in the degradation of the sediments organic matter given that the members of these groups are frequently found in environments where complex processes of carbon degradation occur, digesting, growing on and degrading different types organic substrates (Rui et al., 2009; Zhou et al., 2016). Based on experimental research of incubated unamended and straw-amended Italian paddy soil under anaerobic conditions, Ji et al. (2018) have suggested that during the initial degradation stages of organic matter, *Sphingobacteriales* can play an important role, whereas other groups like Bacteroidetes_vadinHA17 and *Dehalococcoidia* and *Anaerolineae* are more important during the final degradation stages in sulfidic zones (Suominen et al., 2019). Wasmund et al. (2014) have classified *Dehalococcoidia* as anaerobic bacteria involved in the fermentation of plants and organosulfur compounds. Biderre-Petit et al. (2016) have described the natural occurrence of *Dehalococcoidia* bacteria in the anoxic waters of a remote meromictic lake (Lake Pavin). Němeček et al. (2018) have found the genus MSBL5 in groundwater contaminated with chlorinated solvents. These microorganisms living in anoxic environments have the ability to reductively dehalogenate organochlorides. Iino et al. (2010) have reported an *Ignavibacteriales* order with the function of CO_2 fixation.

An important SRB community was identified in the sediments of Sochagota Lake. This community was dominated by *Desulfatiglans*, although other SRB microbial communities of *Desulfobacterales* (Fam. *Desulfobacteraceae*, G. *Sva0081 sediment group*) and Sva0485 were also identified. The presence of a significant proportion of iron-reducing *Latescibacteria* (up to 2.10%) suggests that this community could have also contributed to the direct reduction of Fe^{3+}. Berg et al. (2020) have posited that fermentative bacteria can also play a relevant role in Fe^{3+} reduction indirectly. Zhang et al. (2019) have proposed that the increase in abundance and activity of IRB and SRB have direct effects on the availability of dissolved metals, which can be incorporated into the precipitated minerals (e.g., sulfides or phosphates). On the other hand, SOB communities were also found to be present in the carbonaceous sediments of Sochagota Lake. *Thioalkalimicrobium* and *Thiobacillus* were the dominant SOB belonging to the *Gammaproteobacteria* group (samples 4A and 4AB). Edwardson and Hollibaugh (2018) have also described an important *Thioalkalimicrobium* microbial community in an alkaline hypersaline lake (Mono Lake, California, USA). Other SOB such as *Sulfurovum*, *Arcobacter* and *Sulfurimonas* (*Epsilonbacteraeota*) were additionally well represented in the sediments of Sochagota Lake. Taking into account the presence of S^0 associated with areas with pyrite framboids in the studied sediments, these groups of *Gammaproteobacteria* and *Epsilonbacteraeota* were believed to be the functional SOB of this environment, producing the transformation of Fe sulfides and contributing to the possible release of metals. An et al. (2020) have indicated that these two SOB communities use diverse strategies for the oxidation of sulfur. *Epsilonbacteraeota* need a continuous supply of reduced sulfur and oxygen, but *Gammaproteobacteria* are able to adapt their energy metabolisms to different reduced environmental conditions. Yang et al. (2016) have indicated that *Thiobacillus*, *Sulfurimonas* and *Arcobacter* were involved in the autotrophic denitrification of saline sewages in Hong Kong. Moreover, Ouyang et al. (2020) and Milaković et al. (2020) have shown that *Arcobacter* can pose potential risks to the environment and human health.

4.3. The origin of the trace element enrichment

The relationship between hydrothermal inputs, carbonaceous matter content, S-bearing mineral crystallization and trace element enrichment processes in Sochagota Lake was evaluated by principal component analysis using IBM SPSS Statistics Software (Fig. 6). Two components orthogonally rotated by the Varimax method were obtained. These components were found to account for 90.38% of the variance in the system (Table 3), and may be related to possible processes occurring in the lake.

The first component was found to account for most of the system variance (84.44%) and revealed two element associations. Na, Zr, Ti, Al

Table 3
Loadings of the compositional variables in Principal Component Analysis.

	PC1	PC2
Zn	0.991	0.008
Mo	0.983	−0.043
Fe_2O_3	0.982	−0.040
Rb	0.980	0.097
Co	0.980	−0.005
S	0.977	−0.100
K_2O	0.976	0.093
Cr	0.972	0.006
Sb	0.972	−0.147
Ni	0.963	−0.101
As	0.961	−0.107
Ba	0.955	0.214
LOI	0.949	−0.056
Na_2O	−0.949	0.055
Zr	−0.949	−0.192
Cu	0.942	−0.245
MnO	0.931	−0.165
TiO_2	−0.927	−0.007
Al_2O_3	−0.907	0.250
SiO_2	−0.899	−0.149
Pb	0.885	0.280
P_2O_5	0.844	−0.387
MgO	0.841	0.396
Sr	0.831	0.479
TOC	0.771	−0.458
CaO	0.350	0.621
% Variance	84.44	5.94

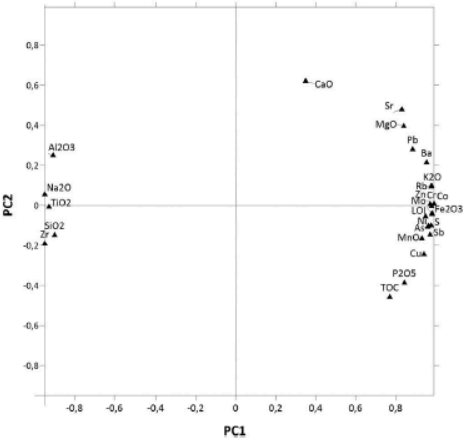

Fig. 7. Plot of the loadings of the compositional variables in principal component analysis. PC: principal component.

and Si showed high negative weights in the component (Fig. 7). Given that Al is one of major elements in the composition of kaolinite and feldspars, which could be observed in the coarser fraction of the southern lake sediments, and Zr and Ti are commonly considered to be detrital elements (Martinez-Ruiz et al., 2015), a detrital source related to the surrounding Cretaceous materials for this association is proposed.

Component 1 also grouped S, TOC, Fe, Zn, Mo, Rb, Co, K, Cr, Sb, Ni, As, Ba, LOI, Cu, Mn, Pb, P, Mg and Sr, which presented positive weights. High weights of S in this component and the water isotopic composition similar to the values of hydrothermal systems ($\delta^{34}S = 6.4‰$, $\delta^{18}O = 8.1$) (Cifuentes et al., 2020a and b) suggested that the source of the trace element with high positive weights could be associated with the hydrothermal inputs feeding the lake through the El Salitre River in its southern part. However, the high positive weights of P in the principal component 1 and its good correlations with heavy metals caused by urban wastewater and agricultural activities of the area suggest that part of the heavy metal enrichment of the central and northern sediments could also be partially attributed to anthropic activity.

Moreover, good correlations of TOC with S, Fe and trace metals in component 1 revealed that most of the trace element concentrations of the sediments could be related to the process of pyritization in a carbonaceous matter-rich environment. The importance of a decaying organic matter-rich environment for the crystallization of iron sulfides have been frequently described as important factor controlling the mineral assemblage of sediments (see e.g., Folk, 2005; Love, 1967; Love et al., 1984; MacLean et al., 2008).

The HRTEM images of mackinawite nanoparticles with (001) lattice fringes of ≈5 Å (Fig. 4 A and B) encrusting bacterial cells suggest that mackinawite precipitation was the initial step of the sedimentary uptake of the hydrothermal S in Sochagota Lake, revealing that iron monosulfide (FeS) crystallization plays an important role in the formation of pyrite (Ohfuji and Rickard, 2005; Schoonen, 2004; Wilkin and Barnes, 1997). Moreover, 16S rDNA amplicons PCR primer sequences in the central and northern sediments of the lake facilitated the identification of several bacterial communities able to reduce sulfate (*Desulfatiglans*, *Desulfobacterales* and Sva0485) and Fe^{3+} (*Latescibacteria*) in lake sediments. The textural disposition of the mackinawite nanoparticles encrusting microbial cells (Figs. 4A and B) in the carbonaceous matter-rich sediments of Sochagota Lake suggests that mackinawite precipitation is favored in the presence of sulfate-reducing microorganisms associated with the decay of plant remains (Cifuentes et al., 2020a). The monosulfide nucleation promoted by microbial cells can also enhance the accumulation of trace elements to the sediments (Hu et al., 2016). In the Sochagota Lake sediments, the presence of mackinawite inside plant fragments (Cifuentes et al., 2020a) and the identification of sulfate-reducing bacteria reveal that SO_4^{2-} hydrothermal inputs of the Sochagota Lake are reduced by sedimentary processes related to carbonaceous matter degradation to precipitate S-containing minerals in the sediments, and cause the heavy metal enrichment of the central and northern sediments. The presence of Cu-bearing pyrite crystals in these sediments suggests that the increase in trace elements is carried out during the mackinawite dissolution stage under free sulfide excess conditions, followed by a recrystallization of the pyrite framboid stage (Picard et al., 2018; Rickard et al., 2007; Rickard and Luther, 1997). Therefore, the process of metal sulfidation can take up the metals into low-solubility minerals (see e.g. Niu et al., 2018).

However, the oxidation of the reduced sulfides to S° (Fig. 4 E and F) may promote a metal release stage into the environment. The moderate positive weights of Ca, Ba and Sr in component 2 (up to 0.621), which tended to be negatively correlated with TOC content, may be associated with this oxidation step in the sediments causing the precipitation of calcite aggregates and barite (Fig. 5 and B). The SOB communities identified in the studied sediments (*Thioalkalimicrobium*, *Sulfurovum*, *Arcobacter* and *Sulfurimonas*) might have played an important role during this oxidation stage.

The concentration of the variation of K and Rb (around 0.98) in component 1 can also be related to mineral transformations occurring in the carbonaceous matter-rich sediments. The reducing conditions in the carbonaceous matter-rich sediments of Sochagota Lake could favor a low-temperature illitization. During this process, I-DV take up Fe and K through successive dissolution-precipitation reactions. Hydrothermal potassium from the organic-rich interstitial water is fixed in the neoformed illite layers, revealing that clay minerals can act as sinks for K of hydrothermal origin in geothermal regions. Reactions to form illite using I-DV as a precursor phase have previously been described by Dietel et al. (2018).

5. Conclusions

We have investigated the processes controlling the concentration and distribution of trace elements in carbonaceous matter-rich sediments from Sochagota Lake (Colombia), a lake with saline hydrothermal inputs at a tropical latitude. The southern entrance to the lake was found to be characterized by organic matter-poor sediments mainly made of quartz and kaolinite enriched in detrital elements like Na, Zr, Ti, Al and Si coming from the surrounding Cretaceous sediments. Central and northern sediments were found to be enriched in S, TOC, Fe, Zn, Mo, Rb, Co, K, Cr, Sb, Ni, As, Ba, LOI, Cu, Mn, Pb, P, Mg and Sr. The good correlations of S with these elements and the isotopic composition of the waters of the lake suggest that their origin is associated with hydrothermal inputs, although high positive correlations of P with heavy metals also imply that a source related to urban wastewater and agricultural activities cannot be discarded. The presence of bacterial groups capable of causing sulfate reduction (*Desulfatiglans*, *Desulfobacterales* and Sva0485) and Fe^{3+} (*Latescibacteria*) in the central and northern sediments of the lake, as well as the occurrence of Fe sulfide nanoparticles (some of them enriched in heavy metals) encrusting microbial cells suggest that SRB control the precipitation of the hydrothermal S and the accumulation of trace elements into the sediments. The statistical association of K and Rb with S and organic matter content indicate that the neoformation of I-DV and illite by saline reactions caused by water-sediment interactions is also associated with the reduction processes of the sediments. The presence of SOB communities (*Thioalkalimicrobium*, *Sulfurovum*, *Arcobacter* and *Sulfurimonas*), the precipitation of S°, barite and calcite crystals and the good correlations between Ca, Ba and Sr suggest that the oxidation processes of the reduced sulfide may promote the release of toxic heavy metals again into the environment.

Declaration of competing interest

The authors declare that they have no known competing financial interests or personal relationships that could have appeared to influence the work reported in this paper.

Acknowledgements

This work was financed by the Spanish research project PGC2018-094573-B-I00 from the MCIU-AEI-FEDER, and research group RNM-325 of the Junta de Andalucía (Spain). Our sincere gratitude is also extended to the Asociación Universitaria Iberoamericana de Posgrado (AUIP) and the Universidad de Boyacá. We would additionally like to thank the Colombian research groups Gestión Ambiental COL0005468 and Gestión de Recursos Hídricos COL0005477. We acknowledge the suggestions and comments from two anonymous reviewers. We acknowledge Emma Taylor (PRS) for the English edition of the paper.

References

Aiuppa, A., Dongarra, G., Capasso, G., Allard, P., 2000. Trace elements in the thermal groundwaters of Vulcano Island Sicily. J. Volcanol. Geotherm. Res. 98, 189–207.

Aiuppa, A., Federico, C., Allard, P., Gurrieri, S., Valenza, M., 2005. Trace metal modeling of groundwater-gas-rock interactions in a volcanic aquifer: Mount Vesuvius, southern Italy. Chem. Geol. 216, 289–311.

Alfaro, C., Velandia, F., Cepeda, H., 2005. Colombian geothermal resources. Proceedings World Geothermal Congress, Antalya, Turkey, April 24–29, pp. 1–11.
An, S.U., Cho, H., Jung, U.J., Kim, B., Lee, H., Hyun, J.H., 2020. Invasive Spartina anglica greatly alters the rates and pathways of organic carbon oxidation and associated microbial communities in an intertidal wetland of the Han River estuary, Yellow Sea. Front. Mar. Sci. 7, 59. https://doi.org/10.3389/fmars.2020.00059.
Andrade, G.R.P., Cuadros, J., Partiti, C.M.S., Cohen, R., Vidal-Torrado, P., 2018. Sequential mineral transformation from kaolinite to Fe-illite in two Brazilian mangrove soils. Geoderma 309, 84–99. https://doi.org/10.1016/j.geoderma.2017.08.042.
Berg, J.S., Duverger, A., Cordier, L., Laberty-Robert, C., Guyot, F., Miot, J., 2020. Rapid pyritization in the presence of a sulfur/sulfate-reducing bacterial consortium. Sci. Rep. 10, 8264. https://doi.org/10.1038/s41598-020-64990-6.
Biderre-Petit, C., Dugat-Bony, E., Mege, M., Parisot, N., Adrian, L., Moné, A., Denonfoux, J., Peyretaillade Debroas, E., Boucher, D., Peyret, P., 2016. Distribution of Dehalococcoidia in the anaerobic deep water of a remote meromictic crater lake and detection of Dehalococcoidia-derived reductive dehalogenase homologous genes. PLoS One 11, e0145558. https://doi.org/10.1371/journal.pone.0145558.
Callahan, B.J., McMurdie, P.J., Rosen, M.J., Han, A.W., Johnson, A.J., Holmes, S.P., 2016. DADA2: high-resolution sample inference from Illumina amplicon data. Nat. Methods 13, 581–583.
Caporaso, J.G., Lauber, C.L., Walters, W.A., Berg-Lyons, D., Lozupone, C.A., Turnbaugh, P.J., Fierer, N., 2011. Global patterns of 16S rRNA diversity at a depth of millions of sequences per sample. Proc. Natl. Acad. Sci. U. S. A. 108, 4516–4522.
Cifuentes, G.R., Jiménez-Espinosa, R., Quevedo, C.P., Jiménez-Millán, J., 2017. El ciclo del azufre en sedimentos de lagos con aportes hidrotermales y antrópicos: el Lago Sochagota (Boyacá - Colombia). Macla 22, 27–28.
Cifuentes, G.R., Jiménez-Millán, J., Quevedo, C.P., Jiménez-Espinosa, R., 2020a. Transformation of S-bearing minerals in organic matter-rich sediments from a saline lake with hydrothermal inputs. Minerals 10, 525. https://doi.org/10.3390/min10060525.
Cifuentes, G.R., Jiménez-Millán, J., Quevedo, C.P., Jiménez-Espinosa, R., 2020b. Isotopic evidence of the hydrothermal origin of the waters of the Sochagota Lake (Colombia). 2nd International Electronic Conference on Mineral Science.
Dietel, J., Ufer, K., Kaufhold, S., Dohrmann, R., 2018. Unusual illite–dioctahedral vermiculite interstratification with Reichweite 2 in clays from northern Hungary. Eur. J. Mineral. 30, 747–757.
Edwardson, C.F., Hollibaugh, J.T., 2018. Composition and activity of microbial communities along the redox gradient of an alkaline, hypersaline, lake. Front. Microbiol. 9, 14. https://doi.org/10.3389/fmicb.2018.00014.
Folk, R.L., 2005. Nannobacteria and the formation of framboidal pyrite: textural evidence. J. Earth Syst. Sci. 114, 369–374.
Frank, K.L., Rogers, D.R., Olins, H.C., Vidoudez, C., Girguis, P.R., 2013. Characterizing the distribution and rates of microbial sulfate reduction at Middle Valley hydrothermal vents. ISME J 7, 1391–1401. https://doi.org/10.1038/ismej.2013.17.
Gawlik, M., Bidoglio, G., 2006. Background Values in European Soils and Sewage Sludges: Results of a JRC-Coordinated Study on Background Values. Part III, Conclusions, Comments and Recommendations. EUR 22265 EN. Office for Official Publications of the European Communities, Luxembourg.
Hu, S.Y., Evans, K., Fisher, L., Rempel, K., Craw, D., Evans, N.J., Cumberland, S., Robert, A., Grice, K., 2016. Associations between sulfides, carbonaceous material, gold and other trace elements in polyframboids: implications for the source of orogenic gold deposits, Otago Schist, New Zealand. Geoch. Cosmoch. Acta 180, 197–213. https://doi.org/10.1016/j.gca.2016.02.021.
Iino, T., Mori, K., Uchino, Y., Nakagawa, T., Harayama, S., Suzuki, K., 2010. Ignavibacterium album gen. nov., sp. nov., a moderately thermophilic anaerobic bacterium isolated from microbial mats at a terrestrial hot spring and proposal of Ignavibacteria classis nov., for a novel lineage at the periphery of green sulfur bacteria. Int. J. Syst. Evol. Microbiol. 60(Pt 6), 1376–1382. doi:https://doi.org/10.1099/ijs.0.012484-0.
Ji, Y., Liu, P., Conrad, R., 2018. Response of fermenting bacterial and methanogenic archaeal communities in paddy soil to progressing rice straw degradation. Soil Biol. Biochem. 124, 70–80.
John, D.A., Lee, R.G., Breit, G.N., Dilles, J.H., Calvert, A.T., Muffler, L.J.P., Clynne, M.A., 2019. Pleistocene hydrothermal activity on Brokeoff volcano and in the Maidu volcanic center, Lassen Peak area, northeast California: evolution of magmatic-hydrothermal systems on stratovolcanoes. Geosphere 15, 946–982. https://doi.org/10.1130/GES02049.1.
Kiran, M.G., Pakshirajan, K., Das, G., 2017. Heavy metal removal from multicomponent system by sulfate reducing bacteria: mechanism and cell surface characterization. J. Hazard. Mater. 324, 62–70.
Klindworth, A., Pruesse, E., Schweer, T., Peplies, J., Quast, C., Horn, M., Glöckner, F.O., 2013. Evaluation of general 16S ribosomal RNA gene PCR primers for classical and next-generation sequencing-based diversity studies. Nucleic Acids Res. 41, e1.
Kristmannsdóttir, H., Ármannsson, H., 2003. Environmental aspects of geothermal energy utilization. Geothermics 32, 451–461.
Kühl, M., Jørgensen, B.B., 1992. Microsensor measurements of sulfate reduction and sulfide oxidation in compact microbial communities of aerobic biofilms. Appl. Environ. Microbiol. 58, 1164–1174.
Large, D., Sawlowicz, Z., Spratt, J., 1999. A cobaltite-framboidal pyrite association from the Kupferschiefer; possible implications for trace element behaviour during the earliest stages of diagenesis. Mineral. Mag. 63, 353–361.
Love, L., 1967. Early diagenetic iron sulphide in recent sediments of the Wash (England). Sedimentology 9, 327–352.
Love, L., Al-Kaisy, A.T., Brockley, H., 1984. Mineral and organic material in matrices and coatings of framboidal pyrite from Pennsylvanian sediments, England. J. Sediment. Res. 54.
MacLean, L., Tyliszczak, T., Gilbert, P., Zhou, D., Pray, T., Onstott, T., Southam, G., 2008. A high-resolution chemical and structural study of framboidal pyrite formed within a low temperature bacterial biofilm. Geobiology 6, 471–480.
Martínez-Mera, E., Torregroza, A., Crissien-Borrero, C.J., Marrugo, J., González-Márquez, L., 2019. Evaluation of contaminants in agricultural soils in an Irrigation District in Colombia. Heliyon 5, e02217. https://doi.org/10.1016/j.heliyon.2019.e02217.
Martinez-Ruiz, F., Kastner, M., Gallego-Torres, D., Rodrigo-Gámiz, M., Nieto-Moreno, V., Ortega-Huertas, M., 2015. Paleoclimate and paleoceanography over the past 20,000 yr in the Mediterranean Sea basins as indicated by sediment elemental proxies. Quat. Sci. Rev. 107, 25–46.
Milaković, M., Vestergaard, G., González-Plaza, J.J., Petrić, I., Kosić-Vukšić, J., Senta, I., Kublik, S., Schloter, M., Nikolina Udiković-Kolić, N., 2020. Effects of industrial effluents containing moderate levels of antibiotic mixtures on the abundance of antibiotic resistance genes and bacterial community composition in exposed creek sediments. Sci. Total Environ. 706.
Moreira, M., Díaz, R., Santos, H., Mendoza, U., Böttcher, M., Capilla, R., Albuquerque, A., Machado, W., 2017. Sedimentary trace element sinks in a tropical upwelling system. J. Soils Sediments https://doi.org/10.1007/s11368-017-1803-4.
Muyzer, G., Stams, A.J.M., 2008. The ecology and biotechnology of sulphate-reducing bacteria. Nat. Rev. Microbiol. 6, 441–454.
Němeček, J., Steinová, j., Špánek, R., Pluhař, T., Pokorný, P., Najmanová, P., Knytl, V., Čemík, M., 2018. Thermally enhanced in situ bioremediation of groundwater contaminated with chlorinated solvents – a field test. Sci. Total Environ. 622–623, 743–755. https://doi.org/10.1016/j.scitotenv.2017.12.047.
Nieto, F., Ortega-Huertas, M., Peacor, D.R., Arostegui, J., 1996. Evolution of illite/smectite from early diagenesis through incipient metamorphism in sediments of the Basque-Cantabrian Basin. Clay Miner. 44, 304–323.
Niu Z.S., Pan H., Guo X.P, Lu D.P, Feng, J.N. Chen, Y.R., Tou, F.Y, Liu, M., Yang, Y., 2018. Sulphate-reducing bacteria (SRB) in the Yangtze estuary sediments: abundance, distribution and implications for the bioavailibility of metals. Sci. Total Environ. 634, 296–304. doi:https://doi.org/10.1016/j.scitotenv.2018.03.345.
Noël, V., Boye, K., Kukkadapu, R.K., Bone, S., Pacheco, J.S.L., Cardarelli, E., Janot, N., Fendorf, S., Williams, K.H., Bargar, J.R., 2017. Understanding controls on redox processes in floodplain sediments of the Upper Colorado River Basin. Sci. Total Environ. 603-604, 663–675. https://doi.org/10.1016/j.scitotenv.2017.01.109.
Ohfuji, H., Rickard, D., 2005. Experimental syntheses of framboids—a review. Earth-Sci. Rev. 71, 147–170.
Ouyang, L., Chen, H., Liu, X., Wong, M.H., Xu, F., Yang, X., Xu, W., Zeng, Q., Wang, W., Li, S., 2020. Characteristics of spatial and seasonal bacterial community structures in a river under anthropogenic disturbances. Environ. Pollut. 264, 114818.
Pardo, N., Cepeda, H., Jaramillo, J.M., 2005. The Paipa volcano, eastern cordillera of Colombia, South America: volcanic stratigraphy. Earth Sci. Res. J. 9, 3–18.
Picard, A., Gartman, A., Clarke, D.R., Girguis, P.R., 2018. Sulfate-reducing bacteria influence the nucleation and growth of mackinawite and greigite. Geochim. Cosmochim. Acta 220, 367–384. https://doi.org/10.1016/j.gca.2017.10.006.
Qi, M.H., Ma, S.S., Qu, K.M., Xin, F.Y., 2004. The formation of sulfide in the marine sediments and its relationships to cultivation of shellfish. Mar. Fish. Res 25, 85–89.
Quast, C., Pruesse, E., Yilmaz, P., Gerken, J., Schweer, T., Yarza, P., Peplies, J., Glöckner, F.O., 2013. The SILVA ribosomal RNA gene database project: improved data processing and web-based tools. Nucleic Acids Res. 41, 590–596.
Quevedo, C.P., Jiménez-Millán, J., Cifuentes, G.R., Jiménez-Espinosa, R., 2020a. Clay mineral transformations in anthropic organic matter-rich sediments under saline water environment. Effect on the detrital mineral assemblages in the upper Chicamocha river basin, Colombia. Appl. Clay Sci. 196, 105576.
Quevedo, C.P., Jiménez-Millán, J., Cifuentes, G.R., Jiménez-Espinosa, R., 2020b. Electron microscopy evidence of Zn bioauthigenic sulfides formation in polluted organic matter-rich sediments from the Chicamocha River (Boyacá-Colombia). Minerals 10, 673.
Rickard, D., Luther, G.W., 1997. Kinetics of pyrite formation by the H_2S oxidation of iron (II) monosulfide in aqueous solutions between 25 and 125 C: the mechanism. Geochim. Cosmochim. Acta 61, 135–147.
Rickard, D., Grimes, S.T., Butler, I., Oldroyd, A., Davies, K.L., 2007. Botanical constraints on pyrite formation. Chem. Geol. 236, 228–246. https://doi.org/10.1016/j.chemgeo.2006.09.011.
Rueda-Saá, G., Rodríguez-Victoria, J.A., Madriñan-Molina, R., 2011. Methods for establishing baseline values for heavy metals in agricultural soils: prospects for Colombia. AcAg 60, 203–218.
Rui, J., Peng, J., Lu, Y., 2009. Succession of bacterial populations during plant residue decomposition in rice field soil. Appl. Environ. Microbiol. 75, 4879–4886.
Rye, R.O., Bethke, P.M., Wasserman, M.D., 1992. The stable isotope geochemistry of acid sulfate alteration. Econ. Geol. 87, 225–262. https://doi.org/10.2113/gsecongeo.87.2.225.
Schmieder, R., Edwards, R., 2011. Quality control and preprocessing of metagenomic datasets. Bioinform 27, 863–864.
Schoonen, M.A., 2004. Mechanisms of sedimentary pyrite formation. Geol. Soc. Am. 379, 117–134.
Suominen, S., Dombrowski, N., Sinninghe Damsté, J.S., Villanueva, L., 2019. A diverse uncultivated microbial community is responsible for organic matter degradation in the Black Sea sulphidic zone. Environ. Microbiol. https://doi.org/10.1111/1462-2920.14902.
Tarekegn, M.M., Zewdu, F., Iniyehu, A., 2020. Microbes used as a tool for bioremediation of heavy metal from the environment. Cogent. Food Agric. 6 (1). https://doi.org/10.1080/23311932.2020.1783174.
Wasmund, K., Schreiber, L., Lloyd, K.G., Petersen, D.G., Schramm, A., Stepanauskas, R., Jørgensen, B.B., Adrian, L., 2014. Genome sequencing of a single cell of the widely distributed marine subsurface Dehalococcoidia, phylum Chloroflexi. ISME J 8, 383–397.

White, C., Shaman, A.K., 1998. An integrated microbial process for the bioremediation of soil contaminated with toxic metals. Nat. Biotechnol. 16, 572–575.
Wilkin, R., Barnes, H., 1997. Formation processes of framboidal pyrite. Geochim. Cosmochim. Acta 61, 323–339.
Wolfenden, S., Charnock, J.M., Hilton, J., Livens, F.R., Vaughan, D.J., 2005. Sulfide species as a sink for mercury in lake sediments. Environ. Sci. Technol. 39, 6644–6648.
Yang, W., Lu, H., Khanal, S.K., Zhao, Q., Meng, L., Chen, G.H., 2016. Granulation of sulfur-oxidizing bacteria for autotrophic denitrification. Water Res. 104, 507–519.
Zhang, Q., Chen, H., Huang, D., Xu, C., Zhu, H., Zhu, Q., 2019. Water managements limit heavy metal accumulation in rice: dual effects of iron-plaque formation and microbial communities. Sci. Total Environ. 687, 790–799.
Zhou, G.X., Zhang, J.B., Zhang, C.Z., Feng, Y.Z., Chen, L., Yu, Z., Xin, X., Zhao, B., 2016. Effects of changes in straw chemical properties and alkaline soils on bacterial communities engaged in straw decomposition at different temperatures. Sci. Rep. 6, 22186. https://doi.org/10.1038/srep22186.

Capítulo 7.

7. Discusión

7.1 Aportes hidrotermales y efecto regulador del lago sobre la calidad de las aguas

El Lago Sochagota se recarga con aguas de la cuenca del río Salitre, que son una mezcla de alimentación superficial y endógena a lo largo del trazado del río. Con el fin de explorar más a fondo la influencia de las fuentes de agua en el agua del lago, se estudiaron los datos disponibles de la composición de las aguas subterráneas geotérmicas que contribuyen a la composición del río Salitre. Así se detectaron dos tipos principales de aguas: (i) aguas calientes ricas en SO_4^{2-}- (Cl^-) - Na^+ - K^+; y (ii) aguas frías ricas en Fe, $HCO3^-$ (Cl^-- SO_4^{2-}). Los fluidos hidrotermales asociados a los sistemas geotérmicos contienen determinadas sustancias químicas (p.ej., S, Fe, As, Pb, Zn, Mn) que pueden aparecer en concentraciones dañinas y causar una contaminación potencial de las aguas de un lago. La composición isotópica del agua del Lago Sochagota presenta valores de 6.4 ‰ para $\delta^{34}S$ y de 8.1 para $\delta^{18}O$, similar a la de fluidos hidrotermales descritos en la bibliografía (p.ej., Rye et al., 1992 y John, et al., 2019), así como la ausencia de depósitos evaporíticos en la secuencia estratigráfica (Pardo et al., 2005), hizo que se propusiera que la alta salinidad del lago fue causada por los aportes hidrotermales portadores de S de los manantiales que alimentan el río Salitre (Cifuentes et al., 2020a). Las buenas correlaciones de SO_4^{2-} con metales en las aguas del lago también sustentan un origen asociado a las entradas hidrotermales que recibe el río Salitre. La hidroquímica de las aguas frías se puede relacionar con la interacción agua-roca de un acuífero aluvial poco profundo formado por partículas volcánicas y sedimentarias y recargado por el agua de lluvia. En el lecho del río Salitre se produce una mezcla de aguas termales y salinas con aguas subterráneas más frías provocando que las aguas ricas en SO_4^{2-}- Na^+ - K^+ - Fe se acumulen en la entrada sur del lago. Esta mezcla de agua se evidencia en las muestras T19 y T20, caracterizadas por valores muy altos de salinidad, y principalmente Fe.

Los análisis hidroquímicos han revelado que en el Lago Sochagota se pueden distinguir dos tipos principales de procesos que controlan la concentración de elementos: dilución de agua y captación de determinados elementos por minerales sedimentarios. Las aguas con altos valores de CE y ricas en sulfato de la entrada sur del lago se caracterizan por contenidos más altos en Cl^-, Li, Be, Al, K, Fe, Co, Ni, Cu, Zn, As, Rb, Cs y Pb. Las concentraciones de SO_4^{2-}, Cl^-, Fe y As exceden el marco regulatorio para contaminantes en aguas (250 mg/L para SO_4^{2-} y Cl^-, 0,3 mg/L y 0,01 mg/L, respectivamente) o conductividad eléctrica (1000 µS/cm) Sin embargo, el contenido de los metales pesados remanentes se encontraba por debajo de los límites establecidos por la normativa colombiana para consumo humano y uso doméstico. La composición química de estas aguas sugiere una fuerte influencia de las entradas hidrotermales y de agua dulce que alimentan el lago a través del río Salitre. Algunos fluidos geotérmicos pueden considerarse como salmueras con un contenido excesivo de sal que pueden causar daños ambientales directos (Kristmannsdóttir, H.; *et al.,* 2003). El encharcamiento de estas salmueras puede ser una técnica eficaz para luchar contra la contaminación del agua. El Lago Sochagota es un estanque creado para preservar la calidad del agua del río Chicamocha), almacenando salmueras salinas naturales que se descargan periódicamente al río Chicamocha cuando su salinidad se reduce (Quevedo *et al*., 2020a). Estas aguas cubren sedimentos pobres en materia orgánica hechos principalmente de cuarzo y caolinita enriquecidos en elementos detríticos como Zr y Ti provenientes de los sedimentos circundantes y bajas concentraciones de metales pesados. Cifuentes *et al*. (2020b), sugiere la ausencia de procesos significativos interacción agua-sedimentos que causa la autigénesis mineral o la incorporación de elementos traza de las aguas a los sedimentos.

Por lo tanto, los datos sugieren que la composición del agua del Lago Sochagota implica interacciones entre fuentes hidrotermales, agua dulce y sedimentos. Estos procesos provocaron una fuerte disminución en muchas concentraciones de elementos, especialmente para SO_4^{2-}, Fe, Cl^-, Al, As, Cu y Co (entre 22 y 8 veces). Li, Rb, Na, K, Ni, Cs, Ba, Zn y Pb sufrieron una disminución significativa (alrededor de 3 veces) mientras que Ca, Mg y Sr se vieron menos afectados (disminución de menos de 1,5 veces). Aunque el agua dulce de la lluvia acumulada en el embalse debe jugar un papel clave en la atenuación de los metales disueltos proporcionados por los insumos hidrotermales, la disminución de la concentración es especialmente importante para los elementos involucrados en algunos de los procesos minerales que ocurren por la interacción entre agua, sedimentos y su comunidad bacteriana. Los procesos biogeoquímicos inciden en los elementos de movilidad. Los procesos de sorción y complejación en los componentes de los sedimentos, como minerales de la arcilla, óxidos, materia orgánica y la fijación y transformación biológica pueden ser factores que influyen en la distribución del contenido de elementos acuosos. Quevedo *et al*. (2020b) indicaron que en el humedal de La Playa (río Chicamocha), el depósito de sedimentos ricos en materia orgánica y la acumulación de aguas salinas generaban ambientes adecuados para procesos de reducción del agua, frecuentemente asociados a la actividad reductora de microorganismos, que promueven la producción de sulfuro, que puede formar sulfuros insolubles de metales divalentes. El alto contenido en elementos traza en los sedimentos ricos en materia orgánica del Lago Sochagota y la presencia de una importante comunidad de SRB sugieren que se promovió parte de la disminución de SO_4^{2-}, Cl^- y de elementos traza en las aguas del lago. por procesos de inmovilización debido a reacciones minerales (precipitación del S hidrotermal y acumulación de elementos traza en los sedimentos controlados por SRB). Las entradas de sulfatos

hidrotermales al Lago Sochagota se redujeron por procesos sedimentarios relacionados con la degradación de sedimentos ricos en materia carbonosa, precipitando minerales que contienen S en los sedimentos y provocando la disminución de metales en las aguas. Niu *et al*. (2018) indicaron que el proceso de sulfuración de metales puede hacer que estos metales pasan a formar parte de minerales de baja solubilidad. La atenuación de la concentración de K, Al y Rb también puede estar relacionada con las transformaciones minerales que ocurren en los sedimentos ricos en materia carbonosa. Andrade *et al.* (2018) indicaron que los minerales de la arcilla pueden transformarse rápidamente en illita a través de reacciones minerales secuenciales en ambientes hípersalinos y reductores. En estos casos, los sedimentos actúan como sumideros eficaces de potasio Andrade *et al.* (2018), Quevedo *et al.* (2020a) sugirieron que la eutrofización en un embalse más cercano (presa La Playa) creaba un ambiente en condiciones reductoras que favorecía la absorción de Fe en minerales neoformados de la arcilla (I-DV y Fe-esmectita). Cifuentes *et al.*(2020c) sugirieron que la reducción de las condiciones en los sedimentos ricos en materia carbonosa del Lago Sochagota favorecía una illitización a baja temperatura. Durante este proceso, I-DV absorbe Fe y K a través de reacciones sucesivas de disolución-precipitación. El potasio hidrotermal del agua intersticial rica en materia orgánica se fijó en las capas neoformadas de illita, revelando que los minerales de la arcilla pueden actuar como sumideros de K de origen hidrotermal en regiones geotérmicas.

Estos procesos podrían contribuir significativamente a remediar la presencia de algunos elementos en las aguas mediante procesos de atenuación natural. Recomendamos incrementar la vegetación en la entrada sur del lago para promover el depósito de sedimentos ricos en materia orgánica donde estos biogeoquímicos pueden tener lugar para intensificar

la disminución de concentración en SO_4^{2-} y As por debajo del marco regulatorio colombiano para contaminantes en aguas.

7.2 Minerales detríticos y minerales arcillosos neoformados

Los resultados de este estudio revelan que los minerales formados en el Lago Sochagota presentan diferencias significativas en el tamaño del grano, asociación mineral, y contenido de materia orgánica de acuerdo con la distancia del afluente hidrotermal (Quebrada Honda - Rio Salitre). Los datos de difracción de rayos X y microscopía electrónica sugieren que en la formación de los sedimentos del lago estuvieron implicadas diversas fuentes de aportes (detrítica, hidrotermal y órgano-antropogénica). Desde el punto de vista geomorfológico, el lago es una pequeña cuenca endorreica que se desarrolla sobre materiales neógenos y cuaternarios. El contexto geológico sugiere que la mayor parte de los minerales de los sedimentos proceden de los aportes detríticos de los materiales geológicos del entorno. El elevado tamaño de grano de los cristales de cuarzo y feldespatos sugiere que estos minerales tienen su origen en los abundantes materiales sedimentarios silíceos del cretácico al neógeno que constituyen la cuenca de drenaje. La presencia de caolinita como mineral del grupo de arcilla apunta especialmente a las areniscas neógenas de la formación Tilatá. La presencia de pequeñas cantidades de vidrio volcánico puede relacionarse con los aportes distales de la formación vulcanosedimentaria explosiva de edad neógena que constituyen el edificio volcánico de Paipa.

En los sedimentos del Lago Sochagota, la presencia de abundantes microcristales idiomorfos que cementan los poros del sedimento indica que algunas de las fases minerales tuvieron su origen en procesos autigénicos. La formación de estos minerales en sedimentos superficiales

de sistemas lacustres puede producirse como consecuencia de la saturación de la concentración de algunos iones en los fluidos intersticiales y procesos asociados a la descomposición de materia orgánica y la actividad microbiana (Vuillemin *et al*., 2013). El desarrollo de condiciones reductoras en los sedimentos y las aguas de los poros es un factor esencial que controla la formación, transformación y preservación de los minerales autigénicos. Las reacciones abióticas y el metabolismo microbiano pueden producir la formación o disolución de fases con hierro, tales como óxidos, hidróxidos, sulfuros, carbonatos o silicatos (Picard *et al*., 2018).

La combinación de situaciones en las que fluidos especialmente salinos se encuentran en contextos ricos en materia orgánica puede proporcionar ambientes especialmente adecuados para el desarrollo acelerado de reacciones que modifican la asociación mineral originalmente depositada (Andrade *et al*., 2014, 2018; Barbiero *et al*., 2016; Cuadros *et al*., 2017; Gomes *et al*., 2016). La evolución de las condiciones redox de las aguas intersticiales de los sedimentos es habitualmente considerada como uno de los principales factores que controlan la formación, transformación y preservación de los minerales autigénicos (Andrade *et al*., 2018; Vuillemin *et al*., 2013). Muchos de estos procesos se producen a través de transformaciones complejas en las que participan fases amorfas y minerales metaestables, precursores de los que finalmente se observan en la mayor parte de sedimentos (Noël *et al*., 2017). En estos casos, los elementos con capacidad de actuar como donantes o receptores de electrones, tales como el azufre y el hierro, juegan un papel esencial en el desarrollo de la asociación mineral en equilibrio. En sedimentos siliciclásticos, el hierro es comúnmente el elemento en fase sólida con actividad redox más abundante y determina la estabilidad de numerosas fases minerales (Kasina *et al*., 2017).

Las facies sulfatadas-sódico-potásicas de las aguas hidrotermales que alimentan el Lago Sochagota pueden suponer la fuente de potasio necesaria para la formación de algunas de las arcillas neoformadas. Desde la entrada sur del lago hacia el interior y la zona norte del lago, la cantidad de partículas finas de materiales arcillosos (illita e I-DV) se incrementa. Las altas condiciones hidrodinámicas en la entrada del lago y el bajo contenido de materia orgánica de esos materiales debieron evitar la formación y acumulación de las partículas finas de arcilla en la zona sur del lago (Cifuentes *et al*., 2020c). Por tanto, la formación de illita debió ocurrir durante la fuerte interacción de los sedimentos con el agua salina de los poros bajo las condiciones reductoras producidas por el alto contenido de materia orgánica (Cifuentes *et al*., 2020c). Las partículas de tamaño pequeño de grano de I-DV depositadas en esta parte del lago actuaron como los precursores apropiados para el desarrollo del proceso de illitización. Se han descrito procesos similares de illitización en otros ambientes salinos ricos en materia orgánica tales como manglares (Cuadros *et al*., 2017). Dietel *et al*. (2018) describieron el papel del interestratificado I-DV como fase intermedia precursora del proceso de illitización.

7.3 El ciclo del azufre en los materiales del Lago Sochagota

Los minerales con azufre del Lago Sochagota están concentrados en las zonas central y norte del lago en las que se encuentran materiales ricos en materia orgánica. Los sedimentos ricos en materia orgánica son capaces de mantener condiciones empobrecidas en oxígeno debido a la capacidad de dicha materia orgánica para proporcionar electrones para las reacciones de reducción. En ambientes salinos como el del Lago Sochagota, con disponibilidad de materia orgánica fácilmente degradable, los microrganismos probablemente pueden crear microambientes con

hierro reducido y sulfuros acuosos que producen la precipitación de sulfuros insolubles (Smieja-Król, *et al*., 2015).

El principal factor que controló la formación de esos minerales con azufre fue la cantidad de materia orgánica. La pirita es el mineral asociado al azufre con mayor presencia en esos materiales ricos en materia orgánica. Esto indica que la captación de hierro está asociada a la existencia de fases con azufre en los materiales con partículas finas próximos a las áreas ricas en vegetación, sugiriendo la asociación de los procesos de piritización a la abundancia de materia orgánica. La cristalización de cristales individuales de pirita y agregados framboidales asociados a la transformación de materia orgánica ha sido ampliamente descrita en sedimentos anóxicos (MacLean *et al*., 2008). Los framboides de pirita pueden formarse siguiendo moldes determinados por estructuras de materia orgánica (MacLean *et al*., 2008). Estudios experimentales previos y observaciones de campo sugieren que la formación de frambioides de pirita es promovida por la nucleación y crecimiento de monosulfuros de hierro, los cuales son posteriormente convertidos en pirita (p.ej., Wilkin *et al*., 1997; Ohfuji *et al*., 2006). De acuerdo con Hu *et al*. (2016), se cree que la mayor parte de materiales ricos en materia orgánica se transforman en tres procesos que contribuyen a la cristalización de los framboides de pirita: (a) formación y desarrollo de precursores (FeS); (b) transformación de FeS a FeS_2; y (c) crecimiento de pirita.

Las imágenes de microscopía electrónica de los sedimentos ricos en materia orgánica que contienen minerales con azufre en el Lago Sochagota muestran agregados de nanopartículas de FeS con características morfológicas ovales que sugieren una precipitación de FeS inducida biológicamente. Por ello, las SRB debieron facilitar de forma decisiva la asimilación de partículas de hierro a través de la formación de

nanopartículas de mackinawita (FeS). Las investigaciones de (Picard *et al*., 2018) confirmaron la capacidad de los microrganismos para asimilar metales (hierro) que se concentran en la superficie de los microorganismos en forma de minerales del azufre, sugiriendo que la membrana celular de los microrganismos sulfato-reductores y sus materiales extracelulares pueden actuar como estructuras para la formación y crecimiento de los minerales de azufre. Kraal *et al*. (2013) sugirieron que en sedimentos ricos en materia orgánica el rápido enterramiento bajo condiciones anóxicas previene la disolución del FeS.

La pirita y el azufre fueron seguramente producidos por la alteración de mackinawita causada por el exceso de azufre libre que genera la disolución del monosulfuro de hierro y posterior recristalización de la pirita (Rickard, *et al*., 2013, Rickard *et al*., 2007).

La transformación de sulfuro a azufre por una reacción de oxidación inorgánica se produce lentamente, lo que sugiere que la oxidación por microrganismos es el proceso prevalente para la cristalización del azufre en ambientes con baja temperatura (Luther *et al*., 2011). Sin embargo, Cosmidis *et al*. (2016) descubrieron que el H_2S puede interactuar con la materia orgánica en ambientes aerobios para formar azufre inorgánico produciendo morfologías complejas filamentosas similares a las observadas en los materiales presentes en el Lago Sochagota.

7.4 Distribución geoquímica

La distribución espacial de los elementos traza del Lago Sochagota en los sedimentos parece estar asociada con la distribución del contenido de materia orgánica y las asociaciones minerales. Los sedimentos

pobres en materia orgánica de la zona sur del Lago Sochagota están enriquecidos en circonio (media 567 mg/kg) y su asociación mineral se caracteriza por la ausencia de illita, I-DV o minerales con azufre. El enriquecimiento de los sedimentos en circonio se considera como un indicador de una contribución detrítica significativa (p. ej., Martinez-Ruiz *et al*., 2015). El elevado contenido de Zr, SiO_2 y TiO_2 en esos sedimentos puede ser asociado con el depósito de zircón terrígeno, cuarzo y rutilo. Por otro lado, los sedimentos ricos en materia orgánica illita e I-DV localizados en las zonas norte y central del lago presentan un alto contenido de metales pesados (Cu, Zn, Cr, Ni, Co, Pb, Mo), Rb, Ba y As. Esos sedimentos se caracterizaron por la cristalización de minerales con azufre (mackinawita, pirita, y S^0). (Cifuentes *et al*., 2020a).

La concentración de los metales pesados en esos sedimentos excede los valores estándar promedios mundiales y el valor promedio de algunos de esos elementos fue claramente más alto que los valores de los sedimentos no contaminados de referencia localizados en una zona cercana en el Rio Chicamocha (Quevedo *et al*., 2020b). Si bien en Colombia no se dispone de un marco regulatorio para los contaminantes presentes en sedimentos y suelos (Martínez-Mera *et al*., 2019; Rueda Saá *et al*., 2011), los contenidos de metales presentes en los sedimentos de la zona norte, se encuentran por encima de los valores de fondo de los suelos europeos. (Gawlik *et al*., 2006).

7.5 El papel de las comunidades biológicas

Los resultados del análisis de la secuencia del gen 16S rRNA en los sedimentos ricos en materia orgánica del Lago Sochagota revelan la presencia de una comunidad de bacterias con una composición diversa.

La actividad biológica está asociada a los procesos de transformación de la materia orgánica y a algunos procesos minerales que afectan a los ciclos del carbono y el azufre. Las principales comunidades de bacterias de los sedimentos del Lago Sochagota pertenecen a géneros fermentativos que han sido descritos en las zonas anóxicas de otros lagos. Diversas comunidades de *Bacteroidetes* y *Chloroflexi* fueron identificadas como un grupo importante de bacterias que pueden estar involucradas en la transformación de la materia orgánica de los sedimentos (Rui *et al*., 2009; Zhou *et al*., 2016).

Basándose en investigaciones experimentales de suelos incubados sin enmendar y suelos enmendados modificados con paja en condiciones anaerobias, Ji *et al*. (2018) han sugerido que durante las etapas iniciales de degradación de la materia orgánica, las *Sphingobacterias* pueden desempeñar un papel importante, mientras que otros grupos como *Bacteroidetes*, vadinHA17, *Dehalococcoidia* y *Anaerolineae* son más importantes durante la fase final de la degradación en las zonas sulfídicas (Suominen *et al*., 2019). Wasmund *et al*. (2014) clasificaron la *Dehalococcoidia* como una bacteria anaerobia involucrada en la fermentación de plantas y compuestos organosulfurosos. Biderre-Petit *et al*. (2016) describieron la ocurrencia natural de la bacteria *Dehalococcoidia* en las aguas anóxicas de un lago meromíctico (Lago Pavin). Němeček *et al*. (2018) también encontraron el género MSBL5 en aguas subterráneas contaminadas con solventes clorados. Estos microorganismos que viven en ambientes anóxicos tienen la capacidad para deshalogenar reductivamente compuestos organoclorados. Iino *et al*. (2010) reportaron el orden *Ignavibacteriales* con la función de fijar CO_2.

Una importante comunidad SRB fue identificada en los sedimentos del Lago Sochagota. Esta está dominada por *Desulfatiglans*.

También se identificaron otras comunidades microbiológicas de SRB como *Desulfobacterales* (Fam. *Desulfobacteraceae*, G. Sva0081) y Sva0485. La presencia de una porción significativa de *Latescibacteria* hierro-reductoras (hasta 2.10%) sugiere que esta comunidad podría también contribuir a la reducción directa de Fe^{3+}. Berg *et al*. (2020) han sugerido que las bacterias fermentativas también podrían jugar un papel importante en la abundancia de Fe^{3+} y que la actividad de las IRB y SRB tiene efectos directos sobre la disponibilidad de metales disueltos que pueden ser incorporados en los precipitados de minerales (p.ej., sulfuros o fosfatos).

También se encontraron comunidades de SOB presentes en los sedimentos carbonosos del Lago Sochagota. En estas comunidades, *Thioalkalimicrobium* y *Thiobacillus*, del grupo de las *Gammaproteobacterias* son dominantes. Edwardson y Hollibaugh (2018) también han descrito una importante comunidad microbiológica de *Thioalkalimicrobium* en un lago hipersalino (Mono Lake, California, USA). Otras SOB como *Sulfurovum, Arcobacter* y *Sulfurimonas* (Epsilonbacteraeota) se encontraron bien representadas en los sedimentos del Lago Sochagota.

Teniendo en cuenta la presencia en ciertas áreas de azufre asociado con framboides de pirita en los sedimentos estudiados, se cree que esos grupos de *Gammaproteobacteria* y *Epsilonbacteraeota* son las SOB funcionales de este ambiente que producen la transformación de sulfuros de hierro y contribuyen a la posible liberación de metales. An *et al*. (2020) indicaron que esas dos comunidades de SOB usan diversas estrategias para la oxidación de sulfuro. Las *Epsilonbacteraeota* necesitan un suministro continuo de sulfuro y oxígeno, pero las *Gammaproteobacteria* pueden adaptar su metabolismo energético en diferentes condiciones ambientales reductoras. Yang *et al*. (2016) indicaron que

los *Thiobacillus, Sulfurimonas* y *Arcobacter* estuvieron involucradas en la denitrificación autótrofa de aguas residuales salinas en Hong Kong. Ouyang *et al*. (2020) y Milaković *et al*. (2020) demostraron que las *Arcobacter* pueden ser un riesgo para el ambiente y la salud de las personas.

7.6 Origen del enriquecimiento en elementos traza e integración de procesos

La relación entre los aportes hidrotermales, la materia orgánica carbonosa, la cristalización de minerales portadores de azufre y el enriquecimiento del Lago Sochagota en elementos trazas se evaluó por análisis de componentes principales empleando el programa SPSS-IBM. Se obtuvieron dos componentes ortogonalmente rotadas por el método Varimax, responsables del 90.38% de la varianza en el sistema, y que estarían relacionadas con los posibles procesos que ocurren en el lago.

Se encontró que la primera componente es responsable de la mayor parte de la varianza del sistema (84.44%) y reveló dos asociaciones de elementos. Por un lado, Na, Zr, Ti, Al y Si presentaron elevados pesos negativos en la componente, al ser el aluminio uno de los elementos con mayor presencia en la composición de la caolinita y el feldespato, que pueden ser observados en la fracción más gruesa de los sedimentos localizados en la zona sur del lago. Además, el circonio y el titanio son constituyentes comunes en los materiales detríticos (Martinez-Ruiz *et al*., 2015). Por tanto, se propone para esta asociación una fuente detrítica asociada al aporte de los materiales cretácicos que rodean al lago.

La componente 1 también agrupó a S, COT, Fe, Zn, Mo, Rb, Co, K, Cr, Sb, Ni, As, Ba, LOI, Cu, Mn, Pb, P, Mg y Sr. Estos elementos presentan pesos positivos altos en la componente. El peso elevado del

azufre en esta componente y la composición isotópica del agua similar a los valores de los sistemas hidrotermales ($\delta^{34}S$ = 6.4‰, $\delta^{18}O$ = 8.1‰, Cifuentes *et al*., 2020a y b) sugieren que la fuente de estos elementos traza puede estar asociada a los aportes hidrotermales que se incorporan al lago por la entrada sur de la Quebrada Honda - Rio Salitre. Sin embargo, el elevado peso positivo del fósforo en la componente principal 1 y su buena correlación con los metales pesados causados por las actividades agrícolas y las aguas residuales urbanas generadas en el área sugieren que parte del enriquecimiento con metales pesados en los sedimentos de la zona central y norte puede ser parcialmente atribuido a la actividad antrópica.

Además, las buenas correlaciones del COT con azufre, hierro y los elementos traza en la componente 1 revelaron que la mayor parte de la concentración de los elementos traza en los sedimentos podría estar relacionada con los procesos de piritización en un ambiente rico en materia orgánica. La importancia de la transformación de la materia orgánica para la cristalización de sulfuros de hierro ha sido frecuentemente descrita como un factor importante que controla la asociación mineral de los sedimentos (p. ej., Folk, 2005; Love, 1967; Love *et al*., 1984; MacLean *et al*., 2008). Las imágenes HRTEM de las nanopartículas de mackinawita con franjas reticulares (001) de ≈5Å incrustando células bacterianas sugiere que la precipitación de mackinawita fue el paso inicial de la asimilación sedimentaria del azufre hidrotermal del Lago Sochagota, revelando que la cristalización de monosulfuro de hierro (FeS) es un proceso importante responsable en la formación de pirita (Ohfuji *et al*., 2005; Schoonen, 2004; Wilkin *et al*., 1997).

Adicionalmente, la secuenciación del gen 16S rDNA en los sedimentos de las zonas central y norte del Lago Sochagota permitieron la

identificación de varias comunidades de bacterias con capacidad para reducir sulfatos (*Desulfatiglans, Desulfobacterales* y Sva0485) y Fe^{3+} (*Latescibacteria*) en sedimentos de lagos. La disposición textural de las nanopartículas de mackinawita formando parte de incrustaciones sobre microorganismos en los sedimentos ricos en materia orgánica del Lago Sochagota sugieren que la precipitación de mackinawita se ve favorecida por la presencia de SRBs asociadas a la descomposición de restos de plantas.

La nucleación de monosulfuros promovida por los microrganismos también puede promover la acumulación de elementos traza en los sedimentos (Hu *et al*., 2016). En los sedimentos del Lago Sochagota, la presencia de mackinawita dentro de fragmentos de plantas y la identificación de SRBs revelan que los aportes de SO_4^{2-} hidrotermal del Lago Sochagota fueron reducidos por procesos sedimentarios relacionados con la transformación de materia orgánica, posibilitando la precipitación de minerales con azufre en los sedimentos. Esta precipitación causó el enriquecimiento en metales pesados de los sedimentos localizados en la zona centro y norte del lago. La presencia de cristales de pirita con cantidades significativas de cobre en esos sedimentos sugiere que el incremento de elementos traza se llevó a cabo durante la disolución de la mackinawita bajo condiciones de exceso de sulfuro, a la que siguió la etapa de recristalización de los frambiodes de pirita (Picard *et al*., 2018; Rickard *et al*., 2007; Rickard *et al*., 1997). Por lo tanto, los procesos de sulfuración de metales pueden captar metales en minerales con baja solubilidad (see e.g. Niu *et al*., 2018).

Sin embargo, la oxidación de los sulfuros a azufre puede promover una etapa de liberación de metales hacia el medio. Los pesos moderados positivos de Ca, Ba y Sr en la componente 2 (hasta 0.621),

los cuales tiende a estar negativamente correlacionados con el contenido en COT, pueden estar asociados con esta etapa de oxidación en los sedimentos. Está etapa causó la precipitación de agregados de calcita y barita. Las comunidades de SOB en los sedimentos estudiados (*Thioalkalimicrobium, Sulfurovum, Arcobacter y Sulfurimonas*) pueden ser importantes durante esta etapa oxidativa

Por otra parte, la concentración de la varianza del potasio y rubidio (alrededor 0.98) en la componente 1 puede relacionarse con las transformaciones minerales que ocurren en los sedimentos ricos en materia orgánica del lago. Las condiciones reductoras en los sedimentos ricos en materia orgánica del Lago Sochagota podrían favorecer un proceso de illitización de baja temperatura. Durante este proceso, el interesestratificado I-DV asimiló hierro y potasio K a través reacciones sucesivas de disolución-precipitación. El potasio hidrotermal del agua intersticial se fijó en las capas de illita neoformadas, revelando que los materiales arcillosos pueden actuar como un sumidero de potasio de origen hidrotermal en regiones geotermales.

Capítulo 8.

Conclusiones

En esta tesis se ha investigado el origen de la elevada salinidad de las aguas del Lago Sochagota (Colombia), la atenuación natural de dicha salinidad, las transformaciones minerales que ocurren en sus sedimentos ricos en materia orgánica, las comunidades bacterianas que dominan los sedimentos su influencia en las reacciones minerales que controlan la distribución geoquímica de los elementos en los sedimentos.

La composición isotópica de las aguas sugiere que el azufre disuelto es de origen hidrotermal. Los aportes hidrotermales son los responsables de la salinidad de las aguas. Las buenas correlaciones del azufre y la composición isotópica de las aguas del lago sugieren que su origen está asociado con las entradas hidrotermales, aunque alta correlación positiva del fósforo con los metales pesados también implica que existe una relación que no puede ser descartada con las descargas de aguas residuales y de las actividades agrícolas.

El Lago Sochagota puede considerarse como una estrategia efectiva para atenuar aguas de alta salinidad ricas en SO_4^{2-}, el estudio hidrogeoquímico de las aguas del Lago Sochagota y de los aportes hidrotermales conducidos al lago a través del río Salitre evidencio que la concentración de elementos mayores y menores fue alta en la entrada sur del lago y progresivamente estas concentraciones se atenuaron significativamente dentro del Lago Sochagota. Los contenidos de SO_4^{2-}, Fe, Cl^-, Al, As Cu y Co fueron los que tuvieron la mayor disminución, sin embargo, las concentraciones de SO_4^{2-} y As se mantuvieron por encima de las regulaciones colombianas. La concentración de Li, Na, K, Ni, Cs, Ba, Zn y Pb presentó una reducción moderada, pero suficiente para mostrar contenidos por debajo del marco regulatorio colombiano, mientras que Ca, Mg y Sr mostraron una escasa variación. La dilución por escorrentía de agua lluvia y la precipitación de sulfuros de hierro

mediada por bacterias reductoras de sulfato en los sedimentos ricos en materia orgánica fueron los principales procesos involucrados en la atenuación de la concentración de SO_4^{2-}, Fe, As Cu y Co en el agua del lago, así mismo el proceso de illitización, que ocurre en sedimentos podrían favorecer la disminución de K y Al.

La mayoría de los materiales depositados en el Lago Sochagota están constituidos por cuarzo detrítico y kaolinita. Se encontró que la entrada localizada en la zona sur del lago está caracterizada por la presencia de sedimentos pobres en materia orgánica constituidos principalmente por cuarzo y caolinita enriquecidos con elementos detríticos como Na, Zr, Ti, Al y Si que provienen de los sedimentos cretáceos vecinos.

Los sedimentos en las zonas norte y central del lago están enriquecidos por minerales neoformados arcillosos (illita y I-DV) generados por la interacción con las aguas del lago y el alto contenido de materia orgánica. El ambiente reductor que presenta la zona debido a la descomposición de materia orgánica favoreció los procesos de movilización e incorporación de hierro en el I-DV que actuaron como precursor mineral para una rápida illitización a baja temperatura, revelando el importante papel de los minerales arcillosos como sumideros de potasio de origen hidrotermal. en lagos de regiones geotermales

La asociación estadística del potasio y el rubidio con el azufre y el contenido de materia orgánica indica que la neofromación de I-DV y de la illita por reacciones salinas causadas por la interacción del agua de los sedimentos también está asociada con los procesos de reducción de los sedimentos.

El ciclo del azufre en el lago está relacionado con el proceso de piritización relacionado con la abundancia de materia orgánica. La neoformacion de fases portadoras de S en sedimentos ricos en materia orgánica ocurrieron mayoritariamente bajo condiciones salinas reductoras que llevaron a cabo la fijación del azufre hidrotermal enriquecido en el agua del lago.

La presencia de partículas de mackinawita en la parte interna de fragmentos de plantas de algunos núcleos ricos en materia orgánica, formando en ocasiones agregados con formas celulares, es un fuerte indicio de que el SO_4^{2-} de origen hidrotermal disuelto en las aguas del Lago Sochagota reacciona para formar minerales de azufre en los sedimentos a través de procesos de sulfato reducción asociados a la transformación de materia orgánica.

Los microorganismos favorecieron la formación y el crecimiento de mackinawita y su transformación en pirita y azufre. La presencia de una comunidad bacteriana que puede causar reducción de sulfatos (*Desulfatiglan*s, *Desulfobacterales* y Sva0485) y Fe^{3+} (*Latescibacteria*) en los sedimentos de la zona central y norte del lago, así como la aparición de nanopartículas de sulfuro de hierro (algunas de ellas enriquecidas con metales pesados) con incrustaciones de células microbiológicas sugiere que las SRB controlan la precipitación del azufre hidrotermal y la acumulación de elementos traza en los sedimentos. La pirita fue formada por la alteración de la mackinawita en un ambiente con exceso de azufre libre.

Las morfologías filamentosas complejas de azufre se formaron por la reacción del H_2S y la materia orgánica en un ambiente rico en oxígeno. La presencia de comunidades de SOB (*Thioalkalimicrobium, Sulfurovum,*

Arcobacter y Sulfurimonas), la precipitación de azufre, barita y cristales de calcita y las buenas correlaciones entre calcio, bario y estroncio sugiere que los procesos de oxidación del sulfuro reducido pueden fomentar la liberación de metales pesados tóxicos en el ambiente. Se evidencio que los sedimentos de las zonas central y norte están enriquecidos en S, COT, Fe, Zn, Mo, Rb, Co, K, Cr, Sb, Ni, As, Ba, LOI, Cu, Mn, Pb, P, Mg y Sr.

Referencias

Aiuppa, A., Federico, C., Allard, P., Gurrieri, S., Valenza, M., (2005). Trace metal modeling of groundwater-gas-rock interactions in a volcanic aquifer: Mount Vesuvius, southern Italy. Chem. Geol. 216, 289–311.

Aghasian, K., Moridi, A., Mirbagheri, A Abbaspour, M. (2019). Selective withdrawal optimization in a multipurpose water use reservoir. Int. J. Environ. Sci. Technol. 16, 5559–5568.

Alfaro, C. Geoquímica del sistema geotérmico de Paipa. Ingeominas, informe inédito. Bogotá, 2002, 88. (In Spanish)

An, S.U., Cho, H., Jung, U.J., Kim, B., Lee, H., Hyun, J.H., (2020). Invasive Spartina anglica greatly alters the rates and pathways of organic carbon oxidation and associated microbial communities in an intertidal wetland of the Han River estuary, Yellow Sea. Front. Mar. Sci. 7, 59.

Andrade Grp., Azevedo Ac., Cuadros J., Furquim Sac., Souza Junior Vs., Kiyohara Pk., Vidal-Torrado P., (2014). Transformation of kaolinite into smectite and Fe-illite in Brazilian mangrove soils. Soil Sci Soc Am J 78: 655–672.

Andrade Grp., Cuadros J., Partiti Cms., Cohen R., Vidal-Torrado P., (2018). Sequential mineral transformation from kaolinite to Fe-illite in two Brazilian mangrove soils. Geoderma 309: 84-99.

Baldermann, A., Warr, L., Letofsky-Papst, I., Mavromatis, V. (2015). Substantial iron sequestration during green-clay authigenesis in modern deep-sea sediments. Nat. Geosci.,8, 885–890.

Barco, L. M., Mendez Angarita, M. (2010). Identificación de las Caracteristicas Hidrogeologicas y Sanitarias del Lago Sochagota y de Fuentes

de Agua Termomineral en el Municipio de Paipa Boyaca. Bucaramanga, Colombia: Universidad Industrial de Santander.

Barbiero, L., Berger, G., Rezende, A., Meunier, J., Martins, E., y Furian, S. (2016). Organic control of dioctahedral and trioctahedral clay formation in an Alkaline Soil System in the Pantanal Wetland of Nhecolândia, Brazil. PloS One, 11 (7). Doi: 10.1371/journal.pone.0159972

Barnes, H.L. (1997). Solubilities of ore metals. In: Barnes, H.L. (Ed.), Geochemistry of Hydrothermal Ore Deposits, second ed. John Wiley and Sons, New York, 404–460.

Berg, J.S., Duverger, A., Cordier, L., Laberty-Robert, C., Guyot, F., Miot, J., (2020). Rapid pyritization in the presence of a sulfur/sulfate-reducing bacterial consortium. Sci. Rep. 10, 8264.

Biderre-Petit, C., Dugat-Bony, E., Mege, M., Parisot, N., Adrian, L., Moné, A., Denonfoux, J., Peyretaillade Debroas, E., Boucher, D., Peyret, P., (2016). Distribution of Dehalococcoidia in the anaerobic deep water of a remote meromictic crater lake and detection of Dehalococcoidia-derived reductive dehalogenase homologous genes. PLoS One 11, e0145558.

Björke, J.K., Stefánsson, A., Arnórsson, S., (2015). Surface water chemistry at Torfajökull, Iceland—Quantification of boiling, mixing, oxidation and water-rock interaction and reconstruction of reservoir fluid composition. Geothermics. 58, 75–86.

Chamley H. (1989). Clay Sedimentology. Springer-Verlag, Berlin.

Chamley H., Debrabant P., Candillier Am., Foulon J. (1983). Clay mineralogy and inorganic geochemical stratigraphy of Blake-Bahama Basin since the Callovian, site 534. Deep Sea Drilling Project leg 76. Initial DSDP 76 pp. 437–451

Cifuentes, G.R., Jiménez-Millán, J., Quevedo, C.P., Jiménez-Espinosa, R., (2020a). Transformation of S-bearing minerals in organic matter-rich sediments from a saline lake with hydrothermal inputs. Minerals 10, 525.

Cifuentes, G.R., Jiménez-Millán, J., Quevedo, C.P., Gálvez, A., Castellanos-Rozo, J., & Jiménez-Espinosa, R. (2020b). Trace element fixation in sediments rich in organic matter from a saline lake in tropical latitude with hydrothermal inputs (Sochagota Lake, Colombia): The role of bacterial communities. The Science of the Total Environment, 143113 .

Cifuentes, G.R., Jiménez-Millán, J., Quevedo, C.P., Nieto Fernando., Cuadros Javier., Jiménez-Espinosa, R., (2020c). Low Temperature Illitization through Illite-Dioctahedral Vermiculite Mixed-Layers in a Tropical Saline Lake rich in Hydrothermal Fluids (Sochagota Lake, Colombia). Minerals 2021, 11,523. https://doi.org/10.3390/min 11050523.

Cifuentes, G.R., Jiménez-Espinosa, R., Quevedo, C.P., Jiménez-Millán, J. (2017). El ciclo del azufre en sedimentos de lagos con aportes hidrotermales y antrópicos: el Lago Sochagota (Boyacá - Colombia). Macla 2017, 22, 27-28.

Cifuentes, G.R., Jiménez-Espinosa, R., Quevedo, C.P., Jiménez-Millán, J. (2021) Damming induced natural attenuation of hydrothermal waters by runoff freshwater dilution and sediment biogeochemical transformations (Sochagota Lake, Colombia). Submitted to Water.

Cosmidis, J., Nims, C., Diercks, D., Templeton, A.S. (2019). Formation and stabilization of elemental sulfur through organomineralization. Geochim. Cosmochim. Acta, 247, 59–82.

Cosmidis, J., Templeton, A.S. (2016). Self-assembly of biomorphic carbon/sulfur microstructures in sulfidic environments. Nat. Commun. 7, 12812.

Cuadros J., Andrade G., Ferreira To., Partiti Csm., Cohen R., Vidal Torrado P. (2017). The mangrove reactor: fast clay transformation and potassium sink. Appl Clay Sci 140: 50–58.

Deocampo, D.M. (2015) Authigenic clays in lacustrine mudstones. In: Egenhoff, S. (Ed.), Paying Attention to Mudstones: Priceless: Geological Society of America Special Paper, 515, 49–64. http://dx.doi.org/10.1130/2015.2515(03).

Deocampo D.M., Cuadros J., Wing-Dudek T., Olives J., Amouric M. (2009). Saline lake diagenesis as revealed by coupled mineralogy and geochemistry multiple ultrafine clay phases: Pliocene Olduvai Gorge, Tanzania. Am J Sci 309: 834–868.

Díaz, J., Usaquen O.L., Viasus,L.M., (2016). Modelo simplificado de calidad, hidrodinámico y de gestión para el Lago Sochagota del municipio de Paipa

Dietel, J., Ufer, K., Kaufhold, S., Dohrmann, R., (2018). Unusual illite–dioctahedral vermiculite interstratification with Reichweite 2

in clays from northern Hungary. Eur. J. Mineral. 30, 747–757.

Drief, A., Martinez-Ruiz, F., Nieto, F., Sanchez, N. (2002). Transmission electron microscopy evidence for experimental illitization of smectite in K-enriched seawater solution at 50 degrees C and basic pH. Clays and Clay Minerals, 50, 746-756.

Edwardson, C.F., Hollibaugh, J.T., (2018). Composition and activity of microbial communities along the redox gradient of an alkaline, hypersaline, lake. Front. Microbiol. 9, 14.

Ferreira, T.O., Vidal-Torrado, P., Otero, X.L., Macías, F. (2007). Are mangrove forest substrates sediments or soils? A case study in southeastern Brazil. Catena, 70, 79–91.

Findlay A., Gartman A., Turchyn S., Redeker K., Henri P., Marnocha C., Antler C., Pellerin A., Hansel C., Rose A. (2017). Coupled and cryptic cross linkages among biogeochemical cycles. Session 5K. Goldschmidt 2017.

Folk, R.L., (2005). Nannobacteria and the formation of framboidal pyrite: textural evidence. J. Earth Syst. Sci. 114, 369–374.

Frank, K.L., Rogers, D.R., Olins, H.C., Vidoudez, C., Girguis, P.R., (2013). Characterizing the distribution and rates of microbial sulfate reduction at Middle Valley hydrothermal vents. ISME J 7, 1391–1401.

Gawlik, M., Bidoglio, G., (2006). Background Values in European Soils and Sewage Sludges: Results of a JRC-Coordinated Study on Background Values. Part III, Conclusions, Comments and Recommendations. EUR 22265 EN. Office for Official Publications of the European Communities, Luxembourg.

Gomes, F., Ker, J., Ferreira, T., Moreau, A. M., y Moreau, M. (2016). Characterization and pedogenesis of mangrove soils from Ilhéus-BA, Brazil. Revista Ciência Agronômica, 47 (4). 599-608.

Griffin, J.J., Windom, H., Goldberg, E.D., (1968). The distribution of clay minerals in theWorld Ocean. Deep-Sea Res. 15, 433–459

Hu, S.Y., Evans, K., Fisher, L., Rempel, K., Craw, D., Evans, N.J., Cumberland, S., Robert, A., Grice, K., (2016). Associations between sulfides, carbonaceous material, gold and other trace elements in polyframboids: implications for the source of orogenic gold deposits, Otago Schist, New Zealand. Geoch. Cosmoch. Acta 180, 197–213.

Huggett J., Cuadros J., Gale As., Wray D., Adetunji J. (2016). Low temperature, authigenic illite and carbonates in a mixed dolomite-clastic lagoonal and pedogenic setting, Spanish Central System, Spain. Appl Clay Sci 132–133: 296–312.

Ideam. (S.F). Carácterísticas Climatológicas De Ciudades Principales. Obtenido de http://www.ideam.gov.co/documents/21021/418894/Caracter%C3%ADsticas+de+Ciudades+Principales+y+Municipios+Tur%C3%ADsticos.pdf/c3ca90c8-1072-434a-a235-91baee8c73fc

Iino, T., Mori, K., Uchino, Y., Nakagawa, T., Harayama, S., Suzuki, K., (2010). Ignavibacterium album gen. nov., sp. nov., a moderately thermophilic anaerobic bacterium isolated from microbial mats at a terrestrial hot spring and proposal of Ignavibacteria classis nov., for a novel lineage at the periphery of green sulfur bacteria. Int. J. Syst. Evol. Microbiol. 60(Pt 6), 1376–1382.

Ji, Y., Liu, P., Conrad, R., (2018). Response of fermenting bacterial and methanogenic archaeal communities in paddy soil to progressing rice straw degradation. Soil Biol. Biochem. 124, 70–80.

John, D.A., Lee, R.G., Breit, G.N., Dilles, J.H., Calvert, A.T., Mu Er, L.J.P., Clynne, M.A. (2019). Pleistocene hydrothermal activity on Brokeo_ volcano and in the Maidu volcanic center, Lassen Peak area, northeast California: Evolution of magmatic-hydrothermal systems on stratovolcanoes. Geosphere, 15, 946–982.

Kaasalainen, H., Stefánsson, A. (2011). Sulfur speciation in natural hydrothermal waters, Iceland. Geochim. Cosmochim. Acta 2011, 75, 2777–2791.

Kaasalainen, H., Stefánsson, A., Giroud, N., Arnórsson, S. (2015). The geochemistry of trace elements in geothermal fluids, Iceland. App. Geochem. 2015, 62, 207–223.

Kasina, M., Bock, S., Wurdemann, H., Pudlo, D., Picard, A., Lichtschlag, A., Marz, C., Wagenknecht, L., Wehrmann, Lm., Vogt, C., Meister, P. (2017). Mineralogical and geochemical analysis of Fe-phases in drill-cores from the Triassic Stuttgart Formation at Ketzin CO_2 storage site before CO arrival. Environ Earth Sci 76: 161.

Khadse, G.K.; Meshram, D.B.; Deshmukh, P.; Labhasetwar, P.K. Water quality of Tehri dam reservoir and contributing riv-ers in the Himalayan region. India. 2019, Sustain. Water Resour. Manag. 5, 1951–1961.

Kiran, M.G., Pakshirajan, K., Das, G., (2017). Heavy metal removal from multicomponent system by sulfate reducing bacteria: mechanism and cell surface characterization. J. Hazard. Mater. 324, 62–70.

Kraal, P., Burton, E.D., Bush, R.T. (2013). Iron monosulfide accumulation and pyrite formation in eutrophic estuarine sediments. Geochim. Cosmochim. Acta 2013, 122, 75–88.

Kristmannsdóttir, H., Ármannsson, H., (2003). Environmental aspects of geothermal energy utilization. Geothermics 32, 451–461.

Kühl, M., Jørgensen, B.B., (1992). Microsensor measurements of sulfate reduction and sulfide oxidation in compact microbial communities of aerobic biofilms. Appl. Environ. Microbiol. 58, 1164–1174.

Lanson, B., Beaufort, D., Berger, G., Bauer, A., Cassagnabere, A., Meunier, A. (2002). Authigenic kaolin and illitic minerals during burial diagenesis of sandstones: a review. Clay Miner. 37, 1–22. doi: 10.1180/0009855023710014

Large, D., Sawlowicz, Z., Spratt, J., (1999). A cobaltite-framboidal pyrite association from the Kupferschiefer; possible implications for trace element behaviour during the earliest stages of diagenesis. Mineral. Mag. 63, 353–361.

Love, L., (1967). Early diagenetic iron sulphide in recent sediments of theWash (England). Sedimentology 9, 327–352.

Love, L., Al-Kaisy, A.T., Brockley, H., (1984). Mineral and organic material in matrices and coatings of framboidal pyrite from Pennsylvanian sediments, England. J. Sediment. Res. 54.

Luther, G.W., Findlay, A., Macdonald, D.J., Owings, S.M., Hanson, T.E., Beinart, R.A., Girguis, P.R. (2011). Thermodynamics and kinetics of sulfide oxidation by oxygen: A look at inorganically controlled reactions and biologically mediated processes in the environment. Front. Microbiol. 2, 62.

Maclean, L.C.W., Tyliszczak, T., Gilbert, P.U.P.A., Zhou, D., Pray, T.J., Onstott, T.C., Southam, G. A (2008). Highresolution chemical and structural study of framboidal pyrite formed within a low temperature bacterial biofilm. Geobiology 6, 471–480.

Martínez-Mera, E., Torregroza, A., Crissien-Borrero, C.J., Marrugo, J., González-Márquez, L., (2019). Evaluation of contaminants in agricultural soils in an Irrigation District in Colombia. Heliyon 5, e02217.

Martinez-Ruiz, F., Kastner, M., Gallego-Torres, D., Rodrigo-Gámiz, M., Nieto-Moreno, V., Ortega-Huertas, M., (2015). Paleoclimate and paleoceanography over the past 20,000 yr in the Mediterranean Sea basins as indicated by sediment elemental proxies. Quat. Sci. Rev. 107, 25–46.

Milaković, M., Vestergaard, G., González-Plaza, J.J., Petrić, I., Kosić-Vukšić, J., Senta, I., Kublik, S., Schloter,M., Nikolina Udiković-Kolić, N., (2020). Effects of industrial effluents containing moderate levels of antibiotic mixtures on the abundance of antibiotic resistance genes and bacterial community composition in exposed creek sediments. Sci.Total Environ. 706.

Moreira, M., Díaz, R., Santos, H., Mendoza, U., Böttcher, M., Capilla, R., Albuquerque, A., Machado, W., (2017). Sedimentary trace element sinks in a tropical upwelling system. J. Soils Sediments.

Muyzer, G., Stams, A.J.M., (2008). The ecology and biotechnology of sulphate-reducing bacteria. Nat. Rev. Microbiol. 6, 441–454.

Němeček, J., Steinová, J., Špánek, R., Pluhař, T., Pokorný, P., Najmanová, P., Knytl, V., Černík, M., (2018). Thermally enhanced

in situ bioremediation of groundwater contaminated with chlorinated solvents – a field test. Sci. Total Environ. 622–623, 743–755.

Niu Z.S., Pan H., Guo X.P, Lu D.P, Feng, J.N. Chen, Y.R., Tou, F.Y, Liu, M., Yang, Y., (2018). Sulphate-reducing bacteria (SRB) in the Yangtze estuary sediments: abundance, distribution and implications for the bioavailibility of metals. Sci. Total Environ. 634, 296–304.

Noël, V., Boye, K., Kukkadapu, R.K., Bone, S., Pacheco, J.S.L., Cardarelli, E., Janot, N., Fendorf, S., Williams, K.H., Bargar, J.R., (2017). Understanding controls on redox processes in floodplain sediments of the Upper Colorado River Basin. Sci. Total Environ. 603- 604, 663–675.

Nordstrom, D.K., Mccleskey, R.B., Ball, J.W. (2009). Sulfur geochemistry of hydrothermal waters in Yellowstone National Park: IV Acid-sulfate waters. App. Geochem. 24, 191–207.

Ohfuji, H., Rickard, D., (2005). Experimental syntheses of framboids—a review. Earth-Sci. Rev. 71, 147–170.

Ohfuji, H., Rickard, D. (2006). High resolution transmission electron microscopic study of synthetic nanocrystalline mackinawite. Earth Planet. Sci. Lett. 241, 227–233.

Ouyang, L., Chen, H., Liu, X.,Wong, M.H., Xu, F., Yang, X., Xu,W., Zeng, Q.,Wang, W., Li, S., (2020). Characteristics of spatial and seasonal bacterial community structures in a river under anthropogenic disturbances. Environ. Pollut. 264, 114818.

Pardo, N., Cepeda, H., Jaramillo, Jm. (2005). The Paipa volcano, Eastern Cordillera of Colombia, South America: volcanic stratigraphy. Earth Sci Res J 9: 3-18.

Picard, A., Gartman, A., Clarke, D.R., Girguis, P.R. (2018). Sulfate-reducing bacteria influence the nucleation and growth of mackinawite and greigite. Geochim. Cosmochim., 220, 367–384.

Qi, M.H., Ma, S.S., Qu, K.M., Xin, F.Y., (2004). The formation of sulfide in the marine sediments and its relationships to cultivation of shellfish. Mar. Fish. Res 25, 85–89.

Quevedo, C.P., Jiménez-Millán, J., Cifuentes, G.P., Jiménez-Espinosa, R., Nieto, F. (2018). Efecto de los procesos redox en embalses de regulación sobre la asociación de minerales de la arcilla de los sedimentos aluviales del Río Chicamocha (Colombia). SEA 2018

Quevedo, C.P., Jiménez-Millán, J., Cifuentes, G.R., Jiménez-Espinosa, R., (2020b). Electron microscopy evidence of Zn bioauthigenic sulfides formation in polluted organic matter-rich sediments from the Chicamocha River (Boyacá-Colombia). Minerals 10, 673.

Quevedo, C.P.; Jiménez-Millán, J.; Cifuentes, G.R.; Jiménez-Espinosa, R., (2020a) Clay mineral transformations in anthropic organic matter-rich sediments. under saline water environment. Effect on the detrital mineral assemblages in the Upper Chicamocha River Basin, Colombia. Applied Clay Sci., 196, 105776.

Rickard, D., Luther, G.W. (2007). Chemistry of Iron Sulfides. Chem. Rev. 107, 514–562.

Rickard, D. (2012). Microbial sulfate reduction in sediments. In Developments in Sedimentology: Sulfidic Sediments and Sedimentary Rocks; van Loon, A.J., Ed.; Elsevier: Oxford, UK; pp. 319–351.

Rye, R.O., Bethke, P.M., Wasserman, M.D.(1992). The stable isotope geochemistry of acid sulfate alteration. Econ. Geol., 87, 225–262.

Rueda-Saá, G., Rodríguez-Victoria, J.A., Madriñan-Molina, R., (2011). Methods for establishing baseline values for heavy metals in agricultural soils: prospects for Colombia. AcAg 60, 203–218.

Rui, J., Peng, J., Lu, Y., (2009). Succession of bacterial populations during plant residue decomposition in rice field soil. Appl. Environ. Microbiol. 75, 4879–4886.

Schoonen, M.A., (2004). Mechanisms of sedimentary pyrite formation. Geol. Soc. Am. 379, 117–134.

Sheng, Y., Sun, Q., Bottrell, S.H., Mortimer, R.J. (2015): Reduced inorganic sulfur in surface sediment and its impact on benthic environments in offshore areas of NE China. Environ. Sci. Process Impacts, 17, 1689-1697.

Smieja-Król, B., Janeczek, J., Bauerek, A., Thorseth, I.H. (2015). The role of authigenic sulfides in immobilization of potentially toxic metals in the Bagno Bory wetland, southern Poland. Environ. Sci. Pollut. Res.22, 15495–15505.

Suominen, S., Dombrowski, N., Sinninghe Damsté, J.S., Villanueva, L., (2019). A diverse uncultivated microbial community is responsible for organic matter degradation in the Black Sea sulphidic zone. Environ. Microbiol. https://doi.org/10.1111/1462-2920.14902.

Tarekegn,M.M., Zewdu, F., Iniyehu, A., (2020). Microbes used as a tool for bioremediation of heavy metal from the environment. Cogent. Food Agric. 6 (1).

Vuillemin, A., Ariztegui, D., De Coninck, A.S., Lücke, A., Mayr, C., C, J. Schubert Cj. (2013). The PASADO Scientific Team Origin and significance of diagenetic concretions in sediments of Laguna Potrok Aike, southern Argentina. J Paleolimnol 50: 275–291.

Wang, W., Z. Zhang, G. Tian, and A. Wang (2015), From nanorods of palygorskite to

nanosheets of smectite via a one-step hydrothermal process, RSC Adv., 5, 58107–

58115, doi:10.1039/C5RA05187H.

Wasmund, K., Schreiber, L., Lloyd, K.G., Petersen, D.G., Schramm, A., Stepanauskas, R., Jørgensen, B.B., Adrian, L., (2014). Genome sequencing of a single cell of the widely distributed marine subsurface Dehalococcoidia, phylum Chloroflexi. ISME J 8, 383–397.

White, C., Shaman, A.K., (1998). An integrated microbial process for the bioremediation of soil contaminated with toxic metals. Nat. Biotechnol. 16, 572–575.

Wilkin, Rt., Arthur, Ma., Dean We. (1997). History of water-column anoxia in the Black Sea indicated by pyrite framboid size distributions. Earth Planet Sci Lett 148: 517– 525.

Wilkin, R., Barnes, H., (1997). Formation processes of framboidal pyrite. Geochim. Cosmochim. Acta 61, 323–339.

Willis, C.M., Griggs, G.B. (2003). Reductions in Fluvial Sediment Discharge by Coastal Dams in California and Implications for Beach Sustainability. J. Geol., 111, 167–182.

Wolfenden, S., Charnock, J.M., Hilton, J., Livens, F.R., Vaughan, D.J., (2005). Sulfide species as a sink for mercury in lake sediments. Environ. Sci. Technol. 39, 6644–6648.

Xu, J., Murayama, M., Roco, C.M., Veeramani, H., Michel, F.M., Rimstidt, J.D.;Winkler, C., Hochella, M.F.J. (2016). Highly-defective nanocrystals of ZnS formed via dissimilatory bacterial sulfate reduction: A comparative study with their abiogenic analogues. Geochim. Cosmochim. Acta, 180, 1–14.

Yang, W., Lu, H., Khanal, S.K., Zhao, Q., Meng, L., Chen, G.H., (2016). Granulation of sulfuroxidizing bacteria for autotrophic denitrification. Water Res. 104, 507–519.

Zelibor, J.L., Senftle, F.E., Reinhardt, J.L. (1988). A proposed mechanism for the formation of spherical vivianite crystal aggregates in sediments. Sedimentary Geology, 59, 125–142

Zhang, Y., Liao, J., Pei, Z., Lu, X., Xu, S.,Wang, X. (2019). Effect of dam construction on nutrient deposition from a small agricultural karst catchment. Ecol. Indic., 107.

Zhang, Q., Chen, H., Huang, D., Xu, C., Zhu, H., Zhu, Q., (2019). Water managements limit heavy metal accumulation in rice: dual effects of iron-plaque formation and microbial communities. Sci. Total Environ. 687, 790–799.

Zhou, G.X., Zhang, J.B., Zhang, C.Z., Feng, Y.Z., Chen, L., Yu, Z., Xin, X., Zhao, B., 2016. Effects of changes in straw chemical properties and alkaline soils on bacterial communities engaged in straw decomposition at different temperatures. Sci. Rep. 6, 22186.

UNIVERSIDAD DE JAÉN

Centro de Estudios Avanzados en Ciencias de la Tierra, Energía y Medio Ambiente
Facultad de Ciencias Experimentales
Departamento de Geología